รายงานวิจัยฉบับสมบูรณ์ ประจำปีงบประมาณ 2559

ชื่อโครงการ การใช้เนียร์อินฟราเรดสเปกโทรสโกปีแทนวิธีเทอร์โมกราวิเมทรี และบอมบ์แคลอริเมทรีในการวิเคราะห์สมรรถนะการแยกสลายด้วยความร้อน การเผาไหม้ พารามิเตอร์เชิงจลน์ และค่าความร้อนสูงของชิ้นไม้ไผ่สับ

ชื่อโครงการ Near infrared spectroscopy as an alternative for thermogravimetry and bomb calorimetry in evaluation of pyrolysis, combustion performance, kinetics parameter and higher heating value of bamboo wood chips

ชื่อหัวหน้าโครงการวิจัยผู้รับทุน/ผู้วิจัย
รองศาสตราจารย์ ดร. ปานมนัส ศิริสมบูรณ์
สถาบันเทคโนโลยีพระจอมเกล้าเจ้าคุณทหารลาดกระบัง

กันยายน 2559

รหัสโครงการ 2559A11862003

รายงานวิจัยฉบับสมบูรณ์ ประจำปีงบประมาณ 2559

ชื่อโครงการ

การใช้เนียร์อินฟราเรดสเปกโทรสโกปีแทนวิธีเทอร์โมกราวิเมทรี และบอมบ์แคลอริเมทรี
ในการวิเคราะห์สมรรถนะการแยกสลายด้วยความร้อน
การเผาไหม้ พารามิเตอร์เชิงจลน์ และค่าความร้อนสูงของชิ้นไม้ไผ่สับ

ชื่อหัวหน้าโครงการวิจัยผู้รับทุน/ผู้วิจัย
รองศาสตราจารย์ ดร. ปานมนัส ศิริสมบูรณ์

หน่วยงานต้นสังกัด
หลักสูตรวิศวกรรมเกษตร ภาควิชาวิศวกรรมเครื่องกล
คณะวิศวกรรมศาสตร์
สถาบันเทคโนโลยีพระจอมเกล้าเจ้าคุณทหารลาดกระบัง

สนับสนุนโดย สำนักบริหารโครงการวิจัยส่งเสริมการวิจัย
ในอุดมศึกษาและพัฒนามหาวิทยาลัยวิจัยแห่งชาติ

สำนักงานคณะกรรมการการอุดมศึกษา

Table of Content

List of Table

List of Figures

กิตติกรรมประกาศ

คณะผู้วิจัย (รศ.ดร. ปานมนัส ศิริสมบูรณ์ หัวหน้าโครงการ, ดร. วันพุทธ แซ่ฉั่ว ผู้ร่วมวิจัย และ Mr. Amrit Shrestha นักศึกษาปริญญาโท และนายเจษฎา โพธิ์สม นักศึกษาปริญญาเอก) ขอขอบคุณที่การวิจัยครั้งนี้ได้รับทุนสนับสนุนการวิจัยจากสำนักบริหารโครงการส่งเสริมการวิจัยในอุดมศึกษาและพัฒนามหาวิทยาลัยวิจัยแห่งชาติ สำนักงานคณะกรรมการการอุดมศึกษา ประจำปีงบประมาณ พ.ศ. 2559

รองศาสตราจารย์ ดร. ปานมนัส ศิริสมบูรณ์ (หัวหน้าโครงการวิจัยผู้รับทุน)

ดร. วันพุทธ แซ่ฉั่ว ผู้ร่วมวิจัย

ชื่อโครงการ การใช้เนียร์อินฟราเรดสเปกโทรสโกปีแทนวิธีเทอร์โมกราวิเมทรี และบอมบ์แคลอริเมทรีในการวิเคราะห์สมรรถนะการแยกสลายด้วยความร้อน การเผาไหม้ พารามิเตอร์เชิงจลน์ และค่าความร้อนสูงของชิ้นไม้ไผ่สับ
แหล่งเงิน// สำนักบริหารโครงการส่งเสริมการวิจัยในอุดมศึกษาและพัฒนามหาวิทยาลัยวิจัยแห่งชาติ สำนักงานคณะกรรมการการอุดมศึกษา ประจำปีงบประมาณ
ประจำปีงบประมาณ .....พ.ศ. 2559..... จำนวนเงินที่ได้รับการสนับสนุน 350,000 บาท
ระยะเวลาทำการวิจัย 1 ปี ตั้งแต่วันที่ 1 เดือน.ตุลาคม. พ.ศ. 2558 ถึงวันที่ 30 เดือน กันยายน พ.ศ. 2559
ชื่อ-สกุล หัวหน้าโครงการ และผู้ร่วมโครงการวิจัย
รองศาสตราจารย์ ดร. ปานมนัส ศิริสมบูรณ์ (หัวหน้าโครงการวิจัยผู้รับทุน) และดร. วันพุทธ แซ่ฉั่ว ผู้ร่วมวิจัย
หน่วยงานต้นสังกัด หลักสูตรวิศวกรรมเกษตร ภาควิชาวิศวกรรมเครื่องกล คณะวิศวกรรมศาสตร์ สถาบันเทคโนโลยีพระจอมเกล้าเจ้าคุณทหารลาดกระบัง

บทคัดย่อ

ไม้ไผ่สับเป็นพืชเชื้อเพลิงสีเขียวสำหรับประเทศไทย ใช้ประโยชน์ทั้งทางด้านเศรษฐศาสตร์และสิ่งแวดล้อม โดยมีการกำหนดกฎและหลักเกณฑ์ที่ดีสำหรับการปลูกสร้างสวนป่าโดยปราศจากการทำลายห่วงโซ่อาหาร ก่อนการจำหน่ายเชื้อเพลิงชีวมวลในเชิงพานิชย์ ค่าความร้อน คุณลักษณะทางไพโรไลซิสและการเผาไหม้ และจลนพลศาสตร์พารามิเตอร์จะต้องถูกยอมรับก่อน เพื่อจะได้ราคาที่แท้จริงแทนที่จะเป็นราคาที่ได้จากการสุ่มต่อกิโลกรัม ดังนั้นเพื่อที่จะวัดสมบัติของเชื้อเพลิงชีวมวลโดยไม่ต้องใช้เวลานานมาก เช่น การวิเคราะห์เทอร์โมเกรวิเมตริก (TGA) (16-24 ชั่วโมงต่อตัวอย่าง) และบอมบ์แคลอริมิเตอร์ (50 นาทีต่อตัวอย่าง) กระบวนการเหล่านี้เป็นกระบวนที่ใช้เวลามาก การทดสอบแบบไม่ทำลายเนียร์อินฟาเรดสเปกโทรสโกปี (2-3 นาทีต่อตัวอย่างสำหรับทุกๆ พารามิเตอร์) จึงถูกนำมาใช้ในงานวิจัยนี้ นอกจากนี้ความรู้ทางจลนพลศาสตร์ของกลไกการย่อยสลายของเชื้อเพลิงชีวมวลช่วยในการตรวจสอบค่า พลังงานกระตุ้น พรีเอกซ์โปเนลเชียลแฟคเตอร์ และลำดับปฏิกริยา ซึ่งค่าต่างๆเหล่านี้เป็นพารามิเตอร์สำคัญสำหรับการออกแบบของเครื่องปฏิกรณ์ และการหาค่าองค์ประกอบที่เหมาะสมของผลิตภัณฑ์ เนียร์อินฟาเรดสเปกโทรสโกปีได้ถูกรายงานสำหรับการประเมินผลของจลนพลศาสตร์พารามิเตอร์เช่นกัน

คำสำคัญ : เนียร์อินฟราเรดสเปกโทรสโกปี เทอร์โมกราวิเมทรี บอมบ์แคลอริเมทรี การแยกสลายด้วยความร้อน การเผาไหม้ พารามิเตอร์เชิงจลน์ ค่าความร้อนสูง ชิ้นไม้ไผ่สับ

Research Title: Near infrared spectroscopy as an alternative for thermogravimetry and bomb calorimetry in evaluation of pyrolysis, combustion performance, kinetics parameter and higher heating value of bamboo wood chips

Researcher: Assoc. Prof. Dr. Panmanas Sirisomboon and Dr. Wanphut Saechua

Faculty: Engineering **Department:** Mechanical Engineering **University:** King Mongkut's Institute of Technology Ladkrabang

ABSTRACT

Bamboo wood chips could be a superior green fuel for Thailand to take advantage of economical and environmental benefits by establishing good rule and regulation toward afforestation of energy crops without altering the food chain. Before selling the biomass commercially, the heating value, pyrolysis and combustion characteristics, and kinetic parameters must be recognized in advance so that it will get its actual monetary value instead of random cost per kilogram. In order to measure its properties without consuming more time as thermogravimetric analysis (TGA) (16-24 hrs/sample) and bomb calorimeter (50 min/sample) are lengthy processes, a non-destructive near infrared (NIR) spectroscopy (2-3 minutes/sample for every parameters) is used for this research. In addition, knowledge of kinetics of biomass decomposition mechanism helps to determine the activation energy, pre-exponential factor and reaction order, which are essential parameters for the design of a reactor and optimized composition of products. NIR spectroscopy is reported for evaluation of kinetics parameters as well.

Keywords: near infrared spectroscopy, thermogravimetry, bomb calorimetry, pyrolysis, combustion performance, kinetics parameter, higher heating value, bamboo wood chips

CHAPTER 1

INTRODUCTION

1.1. Importance and Significance of Research

Current fossil fuel crisis, increasing cost of fuel and rising environmental air pollution concerns has fostered the development of biomass resources as an alternative energy source [1, 2]. Biomasses in term of agricultural resources supply energy in two forms from energy crops and residue of crops [3, 4]. So, a fast growing energy crops are needed which can mitigate the current energy crisis having less impact on environmental pollution. In such case, bamboo can be a crucial plant as it is one of the most fast growing, productive and versatile multi-purpose tree which can be grown in wide range of soil.

In 2013 A.D, the total energy consumed in Thailand was 75,214 ktoe; where, the highest energy, 47.79% of the total, was derived from the petroleum products. On the other hand, the consumption of renewable energy other than biomass was 5,278 ktoe which was in similar figure to coal and natural gas consumption, 5,947 and 5,339 ktoe respectively [5]. However, the consumption of biomass in forms of fuel wood, paddy husk, char coal, agricultural wastes was 8,076 ktoe which was higher than the consumption of coal and natural gas products [5]. These figures indicate that the biomass has potential to substitute the fossil fuels.

The energy plays a vital role in a country economy [6] and, also, one of the most essential needs for human being. Thailand falls under tropical zone where the average temperature is 27 °C and annual rain fall of 1,200-1,600 mm/year [7]. Bamboo is found naturalized in most tropical and subtropical areas of the world [8]. It is advantageous for both energy and environment because biomass is considered as CO_2 neutral [9]. In general, pelletization of biomass produce the pellet which has higher density and enhance in heating value in compare to raw of same kind [10]. Meanwhile, it is easier and safe to transport and has greater economic value in the share market. Therefore, Thailand government can take advantage of such economic and environmental benefit energy crops by establishing good rule and regulation toward afforestation of energy crops without altering the food chain. It is not necessary to be only leading exporter of biomass energy but must be able to supply the demanded energy to its own market. This activity will lead to a first zero

emission country by also creating a new job opportunities. Furthermore, the ash can use as an agricultural fertilizer, neutralizing agent, calcination or additives in building materials according to their composition [11].

Before selling the biomass or its pellet, commercially, its moisture content and combustion characteristics "Combustion performance index, Burnout index and Ignition index" must be recognized in advance so that it will get its actual monetary value instead of random cost per kilogram. The moisture content and combustion characteristics of the single batch of wood pellets produced in a factory may not be similar with all the batches as they are derive from different source and age. These properties are equally important for biomass or its pellet production plant and the combustion plants. So, in order to measure its properties without consuming more time as thermogravimetric analysis (TGA) and oven drying method are lengthy process, so a new method should be implemented. To mitigate this problem, near infrared (NIR) spectroscopy has found a scope for its application.

The thermogravimetric and oven dry procedure are destructive and takes approximately 3-24 hours for thermogravimetric analysis and more than 12 hours for oven dry method which also requires a skilled manpower. NIR spectroscopy is based on the absorption of electromagnetic radiation in the region from 780 to 2500 nm (12820-4000 cm-1) [12]. The fundamental absorptions occurring in the infrared region extend down to lower wavelengths as overtones and combinations. The NIR spectroscopy technique can provide rapid results in seconds or continuously on-line, rather than in hours or days, with an accuracy and reproducibility equivalent to most reference methods. Other advantages of NIR include its low cost per test, low labor costs, no required chemicals to purchase or dispose great flexibility in sample presentation and the capability of testing many constituents simultaneously. This method is environment friendly because it requires no chemicals. The instrument is simple to install and operate, does not produce any emissions which need to be removed by drainage or exhaust and easy to prepare sample. Many instruments are of the stand-alone type and their durability allows them to work well for more than ten years. Instruments can be networked to use the same calibration, with their performance controlled from a single control center. NIR spectroscopy has been applied for the evaluation of moisture content of rice straw by Jin et al [13], solid biofuels by Jensen et al [14], Jatropha curcas kernels by Posom and Sirisomboon [15], compost by Suehara et al [16], Miscanthus x giganteus and short rotational coppice willow by

Fagan et al [17] and many other authors. Furthermore, NIR spectroscopy has been applied for the evaluation of lignocellulosic compound content of sugarcane biomass [18] straw content of straw-coal blends [19] heating value of straw [20], Miscanthus and coppice willow [21]. However, there has been none of works that relate combustion parameters of biomass with NIR spectroscopy. Therefore, we propose a research on "Near infrared spectroscopy as an alternative for the measurement of in evaluation of pyrolysis, combustion performance, kinetics parameter and higher heating value of bamboo wood chips" to solve the problem of delay in measurement.

1.2. Objective

The overall objective of this study is to develop the model that correlate the NIR spectral characteristic of the wood chips of bamboo (*Dendrocalamus sericeus* cl. Phamon) with its TGA pyrolysis and combustion performance, kinetics parameters by kinetics analysis and heating value obtained by bomb calorimeter and to prove the possibility of NIR spectroscopy to be an alternative and rapid method for evaluation of the properties.

The specific objective are to:- evaluate the Volatiles Matter, Fixed Carbon, Ash, Heating value, Combustion performance index, Burnout index, Ignition index, Kinetics parameters such as Activation energy, Pre-exponential factor, Order of reaction, Pyrolysis performance such as Onset temperature, Peak temperature, Maximum mass loss rate and offset temperature) of bamboo wood chips from different culm circumferences.

1.3. Expected result

11.1 ได้แบบจำลองในการวิเคราะห์สมรรถนะการแยกสลายด้วยความร้อน การเผาไหม้ พารามิเตอร์เชิงจลน์ และค่าความร้อนสูงของชิ้นไม้ไผ่สับโดยตรงด้วยวิธีไม่ทำลายโดยใช้เทคนิคเนียร์อินฟราเรดสเปกโทรสโกปี โดยสามารถนำแบบจำลองที่ได้ไปใช้จริงในห้องปฏิบัติการแผนกตรวจสอบคุณภาพและแผนกควบคุมการผลิตของชิ้นไม้ไผ่สับเป็นชีวมวลเพื่อการผลิตพลังงานของโรงงานหรือหน่วยงานวิจัยที่เกี่ยวข้องเพื่อลดเวลา การใช้สารเคมี และแรงงานในการตรวจสอบซึ่งหมายถึงการลดต้นทุนในการผลิต

11.2 ได้องค์ความรู้ใหม่ในการประยุกต์ใช้เทคนิคเนียร์อินฟราเรดสเปกโทรสโกปีในการวิเคราะห์สมรรถนะการแยกสลายด้วยความร้อน การเผาไหม้ พารามิเตอร์เชิงจลน์ และค่าความร้อนสูงของชิ้นไม้ไผ่สับ

11.3 สามารถเพิ่มศักยภาพของการปรับปรุงและประกันคุณภาพของการผลิตชิ้นไม้ไผ่สับเป็นชีวมวลเพื่อการผลิตพลังงานทั้งเพื่อการส่งออกและขายภายในประเทศได้ ทำให้โรงงานสามารถมั่นใจในคุณภาพของวัตถุดิบ

11.4 สามารถเพิ่มศักยภาพของการควบคุมกระบวนการผลิตชิ้นไม้ไผ่สับเป็นชีวมวลเพื่อการผลิตพลังงานเนื่องจากวัดสมบัติดังกล่าวได้ทุกล็อตการผลิตและมีกระบวนการผลิตที่แน่นอน

11.5 ผลงานสามารถจดสิทธิบัตร และหรือเผยแพร่ในวารสารระดับชาติและระดับนานาชาติได้ เช่น J. Near Infrared Spectroscopy (IF1.480) Bioresource Technology (IF 4.494) Biomass & Bioenergy (IF 3.394)
*บทความวิจัยที่คาดว่าจะได้รับการตีพิมพ์:

1. The pyrolysis and combustion performance of bamboo (*Dendrocalamus sericeus* cl. Phamon) wood chips.
2. Thermal kinetics parameters of bamboo (*Dendrocalamus sericeus* cl. Phamon) wood chips.
3. Evaluation of pyrolysis characteristics of bamboo (*Dendrocalamus sericeus* cl. Phamon) wood chips using near infrared spectroscopy.
4. Evaluation of combustion characteristics of bamboo (*Dendrocalamus sericeus* cl. Phamon) wood chips using near infrared spectroscopy.
5. Evaluation of higher heating value of Leucaena leucocephala pellets using near infrared spectroscopy.
6. Evaluation of thermal kinetics parameters of bamboo (*Dendrocalamus sericeus* cl. Phamon) wood chips using near infrared spectroscopy.

1.4.Reference

[1]. López-González D., Fernandez-Lopez M., Valverde J.L. and Sanchez-Silva L. "Thermogravimetric-mass spectrometric analysis on combustion of lignocellulosic biomass." Bioresource Technol., vol. 143, 2013. Pp. 562-574

[2]. Sivasangar S., Taufiq-Yap Y.H., Zainal Z. and Kitagawa K. "Thermal behavior of lignocellulosic materials under aerobic/anaerobic environments.", Int. J. Hydrogen Energ., vol. 38, 2013. Pp. 16011-16019

[3]. Liu T., McConkey B., Huffman T., Smith S., MacGregor B., Yemshanov D. and Kulshreshtha S. "Potential and impacts of renewable energy production from agricultural biomass in Canada.", Appl Energ., vol. 130, 2014. Pp. 222-229

[4]. Stern N. "The economics of climate change: the stern review" Cambridge University Press; 2007. p. 118–315.

[5]. Prasad J.V.N.S., Korwar G.R., Rao K.V., Mandal U.K., Rao G.R., Srinivas I., Venkateswarlu B., Rao S.N. and Kulkarni H.D. "Optimum stand density of *Leucaena leucocephala* for wood production in Andhra Pradesh, Southern India.", Biomass Bioenerg., vol. 35, 2011. Pp. 227-235

[6]. Gutteridge, R.C., 1998. The potential of nitrogen fixing trees in livestock production system. In: Daniel, J.N., Roshetko, J.M. (Eds.), Nitrogen Fixing Trees for FodderProduction: Proceedings of an International Workshop. Forest, Farm, and Community Tree Research Reports. Winrock International Institute, pp. 1–16 (SpecialIssue, 20–25 March 1995).

[7]. Alternative Energy and Efficiency Information Center. "Energy in Thailand: Facts and Figures 2013." Department of Alternative Energy Development and Efficiency, Ministry of Energy, Thailand. (2013)

[8]. Ramage J, Scurlock J. "Biomass.", In: Boyle G, editor. Renewable energy-power for a sustainable future. Oxford: Oxford University Press; 1996.

[9]. Thai Meteorological Department. "Thailand weather, Meteorological knowledge.", [Online]. Available: http://www.tmd.go.th/info/info.php?FileID=22. 2014.

[10]. Lim T.K. 2012. Edible Medicinal and Non-Medicinal Plants: Volume 2, Fruits. Springer, New York.

[11]. Demirbas A. "Potential applications of renewable energy sources, biomass combustion problems in boiler power systems and combustion related environmental issues.", Prog. Energ. Combust. , vol. 31, 2005. Pp. 171-192

[12]. Poddar S., Kamruzzaman M., Sujan S.M.A., Hossain M., Jamal M.S., Gafur M.A. and Khanam M.. "Effect of compression pressure on lignocellulosic biomass pellet to improve fuel properties: Higher heating value.", Fuel, vol.131, 2014. Pp. 43-48

[13]. Molino A., Nanna F. and Villone A. "Characterization of biomasses in the southern Italy regions for their use in thermal processes.", Appl. Energ., vol. 131, 2014. Pp. 180-188

[14]. Sirisomboon P., Kaewkuptong A. and Williams P. " Feasibility study on the evaluation of the dry rubber content of field and concentrated latex of Para rubber by diffuse reflectance near infrared spectroscopy.", J. Near Infrared Spec., vol. 21, 2013. Pp. 81–88

[15]. Sabatier D., Thuries L., Bastianelli D. and Dardenne P. "Rapid prediction of the lignocellulosic compounds of sugarcane biomass by near infrared reflectance spectroscopy: comparing classical and independent cross-validation.", J. Near Infrared Spec., vol. 20, 2012. Pp.371-385

[16]. He C., Chen L., Yang Z., Hang G., Liao N. and Han L. "A rapid and accurate method for on-line measurement of straw-coal blends using near infrared spectroscopy. ", Bioresource Technol., vol. 110, 2012. Pp. 314-320

[17]. Jin S., Chen H. "Near-infrared analysis of the chemical composition of rice straw.", Ind. Crop Prod., vol. 26, 2007. Pp. 207-211

[18]. Huang C., Han L., Yang Z., Liu X. "Ultimate analysis and heating value prediction of straw by near infrared spectroscopy.", Waste Manage., vol. 29, 2009. Pp. 1793-1797

[19]. Everard C.D., McDonnell K.P. and Fagan C.C. "Prediction of biomass gross calorific values using visible and near infrared spectroscopy.", Biomass Bioenergy., vol. 45, 2012. Pp. 203-211

[20]. Panwar N.L., Kaushik S.C. and Kothari S. "Role of renewable energy sources in environmental protection: A review.", Renew Sust Energ Rev, vol. 15, 2011. Pp 1513-1524

[21]. Demirbas A. "Recent advance in biomass conversion technologies.", Energy Educ. Sci. Tech., vol. 6, 2000. Pp 19-40

CHAPTER 2

LITERATURE REVIEW

2.1. Biomass

The energy resources have been split into three categories: fossil fuels, renewable resources and nuclear resources [13, 14]. Renewable energy sources, often named as alternative energy resources, are those resources which can be used to produce energy again and again: e.g. solar energy, wind energy, biomass energy, geothermal energy, etc. [15]. Energy crops and residue of crops are the two major sources of energy that is supplied by agricultural product. Bioenergy production can replace fossil fuels contributing to the reduction of greenhouse gas (GHG) emissions by direct burning of biomass to generate electricity [2, 3]. Combustion of biomass does not contribute to net increase in CO_2 during its combustion because biomass consumes the same amount of CO_2 from the atmosphere during its growth as it release during combustion [6, 16, and 17]. Biomass, also, plays the great role in the world economy. Although, much of the rural population in developing countries, which represents about 50% of the world's population, relies on biomass as energy but in industrialized country biomass represent only 3% of primary energy consumption [4]. The components of biomass include hemicelluloses, cellulose, lignin, extractives, lipids, proteins, simple sugars, starch, water, hydrocarbon, ash, and other compounds where cellulose, hemicelluloses and lignin plays a vital role during biomass combustion [6].

2.2. Bamboo

Bamboo is the vernacular or common term for members of a particular taxonomic group of large woody grasses (subfamily Bambusoideae, family Andropogoneae/Poaceae). Bamboos are distributed mostly in tropical region; occur naturally in subtropical and temperate zones of all continents except Europe, at latitudes from 46°N to 47°S and from sea level to 4000m elevation. Bamboos are use as construction and reinforcing fibers, paper, textile, food, combustion and other bioenergy applications [5]. The salient features of Dendrocalamus sericeus cl. Phamon commonly name as phai sang mon in Thailand [18]:-

- Height >15 m
- Culm diameter:- 10 cm
- Dark green culms and foliage, thick-wall culms

- Easy growing, moisture-retentive soil, full sun, somewhat drought-resistant
- Culms for house construction and furniture, mainly planted in Thailand for producing chop-sticks and tooth-picks

Identification not yet verified

2.3. Near infrared spectroscopy

Fagan et al[9] predicted moisture content of Miscanthus x giganteus and short rotational coppice willow with a root mean square error of cross validation of 0.90% (R2=0.99). Jin et al. [7] predicted moisture content of rice straw with standard error of prediction 1.01 % (R2=0.8871). In addition, NIR spectroscopy has been investigated for determination of chemical content in biomass. Via et al. [19] characterized the changes in biomass (sweet gum, loblolly pine, and switch grass) with torrefaction for near infrared reflectance (NIR) and attenuated total reflectance Fourier transform infrared (ATR-FTIR) spectroscopy. Calibration models were built for the prediction of proximate analysis after torrefaction. It was concluded that both systems could be used for rapid monitoring, NIR performed better than FTIR. He et al. [11] used NIR spectroscopy for qualitative analysis of straw, blend1 (straw content from 70-99% and coal), blend2 (straw content from 1-30%and coal) and coal where correct classification percentage were 89.87, 79.66, 94.92 and 100%, respectively. Sabatier et al. [10] evaluated the lignocellulosic compounds including hemicelluloses, cellulose and lignin in sugarcane biomass and obtained correlation of determination (R2) of 0.45-0.77 and standard error of prediction (SEP) of 1.16-1.37% dry matter.

However, to this date, there is no any research reported on the evaluation of combustion performance including combustion index, ignition index and burn out index of biomass and or its pellets by NIR spectroscopy.

2.4. Bomb calorimeter

It is a device used to measure the heat of combustion of particular reaction; the higher heating value. The higher heating value includes the energy released by the condensation of water present in the biomass initially and the water formed from the hydrogen in the fuel. In order to determine the higher heating value, Podder et a.l[8] used the oxygen bomb calorimeter in their research on effect of compression pressure on eight different species of lignocellulosic biomass pellet (Gurjan Balsam (*Dipterocarpus turbinatus* Gaertn.), Teak (*Tectona grandis* L.f.), Burmese Teak (*T. grandis*), Champak (*Michelia champaca*), Scots Pine (*Pinus sylvestris*), Mahogany (*Sweitenia macrophylla*),

Jackfruit (*Artocarpus heterophyllus*) and Burma Ironwood (*Xylia kerrii*)) to improve the higher heating value.

2.5. Thermogravimetric analysis (TGA)

The present definition of thermal analysis formulated by the International Confederation for Thermal Analysis and Calorimetry (ICTAC) reads as follows: Thermal Analysis (TA): A group of techniques in which a property of the sample is monitored against time or temperature while the temperature of the sample, in a specified atmosphere, is programmed [21]. TGA helps us to study the thermal behavior of a sample, biomass, under inert and reactive atmosphere. Taking the advantage of TGA, various researchers performed research on pyrolysis and combustion characteristic of biomass deploying thermogravimetric analyzer as described below:

Luo et al [22] performed "experimental study on the oxygen-enriched combustion of biomass micro fuel" and concluded that the oxygen enriched atmosphere improves the combustion, however volatile releasing temperature, ignition temperature and burnout temperature decreases which was also proved by Qing et al.[23] .From the experiment of Yang et al. [24], it was concluded that particle size of 250μm to 2mm has insignificant influence on pyrolysis process. Also, pyrolysis process can be categorized into four zones: initially, in the temperature range of below 220, moisture evaporation takes place around 100°C, hemicellulose decomposes around 220-300 °C, cellulose around 300-340°C and lignin decomposition manly occur above 340°C. Barneto et al., [25] studied the pyrolysis characteristic and combustion behavior of *Leucaena leucocephala* biomass and its compost with the help of TG and DTG along with the biomass component i.e. hemicellulose, cellulose and lignin. Sivasangar et al., [1] .studied the thermal behavior of lignocellulosic materials under aerobic/anaerobic environments comparing raw and demineralize empty palm fruit's bunch (EFB) and conclude that the mineral contents in raw EFB act as a catalyst which enhance the decomposition of raw biomass at lower temperature as compared to demineralize EFB. Also, hemicellulose shows the early decomposition followed by the cellulose and lignin. Furthermore, the reactive environment favors complete decomposition than inert atmosphere.

2.6. Kinetic analysis

The fundamentally kinetic model obeys the famous Arrhenius equation and the rate of reaction (k) [26] is given by:

$$K(t) = Aexp\left[\frac{-E}{RT}\right], \quad (1)$$

$$\frac{d\alpha}{dt} = Ae^{-\frac{E}{RT}}(1-\alpha)^n, \quad (2)$$

where A is the frequency or pre-exponential factor, E is the activation energy of the reaction, R is the universal gas constant, T is the absolute temperature, n is the order of reaction, t is the time, and α is the fraction of reactant decomposed at time t (min).

The extent of reaction, α is defined in terms of mass change in the sample or the mass of volatile generated

$$\alpha = \frac{W_0 - W}{W_0 - W_f}, \quad (3)$$

Where, W_O, W and W_f are the initial, actual and final weights of the sample, respectively

In order to simplify the calculations, the order of the reaction, n is assumed to be unity, and hence Eq. (2) can be derived [26] and presented as follows:

$$ln\left[-\frac{\ln(1-\alpha)}{T^2}\right] = ln\left[\frac{AR}{\beta E}\right] - \frac{E}{RT}, \quad (4)$$

where β is heating rate. Above Eq. (4) will result in a straight line with slope $-E/R$ and an intercept of ln $[AR/\beta E]$. This was done by plotting graph between following:

$$ln\left[-\frac{1-(1-\alpha)}{T^2(1-n)}\right] versus \frac{1}{T} (for\ n \neq 1), \quad (5)$$

Or

$$ln\left[-\frac{ln(1-\alpha)}{T^2}\right] versus \frac{1}{T} (for\ n = 1), \quad (6)$$

The values of α and T would be obtained from the TG analysis. The criterion used for the acceptable values of E and A is that the final value of n should yield the values of E whose linear correlation coefficient are best fitted. The apparent activation energies were obtained from the slope and pre-exponential factors from the intercept of regression line.

The parameter of kinetic analysis such as activation energy, pre-exponential factor, and order of the reaction of samples are determined by using modified form of Arrhenius equation. Activation energy helps to find out the minimum amount of energy needed to initiate a chemical change, whereas pre-exponential factor and the order of the reaction helps in calculating the reaction rate [27]. Many researchers have been studied kinetic analysis using thermogravimetric data for biomass such as sugarcane bagasse and cotton stalks powders [28], wood, pellets [29], saw dust and wheat husk [27] woody biomass[30], lignocellulosic biomass[31] and date palm[26].

2.7.Combustion performance

Combustion performance is the combustion ability of a fuel. The performance is indicated by combustion performance index (S), ignition index (D_i) and burnout index (D_f) which could be calculated by the following equations:

$$S = \frac{(dW/dt)^c_{max} \times (dW/dt)^c_{mean}}{T_i^2 \times T_h}$$

$$D_i = \frac{(dW/dt)_{max}}{t_p t_e}$$

$$D_f = \frac{(dW/dt)_{max}}{\Delta t_{\frac{1}{2}} t_p t_f}$$

where $(dW/dt)^c_{max}$ is the maximum mass loss rate, $(dW/dt)^c_{mean}$ is the average of mass loss, T_i is ignition temperature, T_h is burnt out temperature, t_p is time at maximum mass loss, t_e is ignition time, t_f is burnt out time, and $t_{1/2}$ is time at $(dW/dt)/(dW/dt)^c_{max}$ = 1/2
The higher the indices indicate that the fuel has higher combustion performance.

2.8. Possibility of applying NIR spectroscopy on evaluation of pyrolysis and combustion performance and kinetics parameters

Due to the pyrolysis and combustion performance and kinetics parameters are physical parameters which have no NIR absorption bands, they should correlate with chemical constituents that have the absorption bands. The pyrolysis and combustion performance are related to the lignocellulosic compound, i.e. hemicelluloses, cellulose and lignin [26,27,28] ,where there is NIR absorption bands at 1218, 1360, 1492, 1584, 1728, 1830, 2110, 2186, 2262, 2314 nm are for hemicelluloses [32] and at 1780, 1820, 2270, 2336, 2488 nm are for cellulose [33]. For lignin, the wavelength range at 2449-1287 nm (4083-7773 cm^{-1}) was used successfully for lignin prediction in corn stalk [34]. Jin and Chen [12], Liu and Chen [34] and Sabatier et al [18] proved that NIR spectroscopy is suitable for the analysis of compounds (hemicellulose, cellulose and lignin) in lignocellulosic material. These reviews indicate that there is a possibility to evaluate the pyrolysis, combustion performance and kinetics parameters which are derived from the thermogravimetric analysis based on combustion and pyrolysis. However, to apply NIR spectroscopy, due to broad band of vibration, it is needed chemometric in multivariate analysis such as partial least square regression to develop calibration model. NIR spectroscopy has been successful in determination of some physical characteristics such as rubber latex viscosity with R^2 of 0.95 [35], refractive index of vegetable oil with R^2 of 0.94[36]. Wood density with R^2 of 0.96[37] and higher heating value of torrefied biomass with R^2 of 0.92[20].

2.9. Reference

[1]. Sivasangar S., Taufiq-Yap Y.H., Zainal Z. and Kitagawa K. "Thermal behavior of lignocellulosic materials under aerobic/anaerobic environments.", Int. J. Hydrogen Energ., vol. 38, 2013. Pp. 16011-16019

[2]. Liu T., McConkey B., Huffman T., Smith S., MacGregor B., Yemshanov D. and Kulshreshtha S. "Potential and impacts of renewable energy production from agricultural biomass in Canada.", Appl Energ., vol. 130, 2014. Pp. 222-229

[3]. 4Stern N. The economics of climate change: the stern review. Cambridge University Press; 2007. p. 118–315.

[4]. Meelu O.P. and Morris R.A. "Green manuring research in the Philippines e a review.", Philipp. J. Crop Sci., vol. 11, 1989. Pp. 153-159

[5]. Shelton H.M., Jones R.J. Opportunities and limitations in *Leucaena*. In: Shelton H.M., Piggin C.M., Brewbaker JL, Editors. Leucaena opportunities and limitations: proceedings of a workshop held in Bangor, Indonesia. Canberra: ACIAR Proceedings; 1995. p. 16-23.

[6]. Gutteridge, R.C., 1998. The potential of nitrogen fixing trees in livestock production system. In: Daniel, J.N., Roshetko, J.M. (Eds.), Nitrogen Fixing Trees for FodderProduction: Proceedings of an International Workshop. Forest, Farm, and Com-munity Tree Research Reports. Winrock International Institute, pp. 1–16 (SpecialIssue, 20–25 March 1995).

[7]. Lim T.K. 2012. Edible Medicinal and Non-Medicinal Plants: Volume 2, Fruits. Springer, New York.

[8]. Poddar S., Kamruzzaman M., Sujan S.M.A., Hossain M., Jamal M.S., Gafur M.A. and Khanam M.. "Effect of compression pressure on lignocellulosic biomass pellet to improve fuel properties: Higher heating value.", Fuel, vol.131, 2014. Pp. 43-48

[9]. Sirisomboon P., Kaewkuptong A. and Williams P. " Feasibility study on the evaluation of the dry rubber content of field and concentrated latex of Para rubber by diffuse reflectance near infrared spectroscopy.", J. Near Infrared Spec., vol. 21, 2013. Pp. 81–88

[10]. Sabatier D., Thuries L., Bastianelli D. and Dardenne P. "Rapid prediction of the lignocellulosic compounds of sugarcane biomass by near infrared reflectance spectroscopy: comparing classical and independent cross-validation.", J. Near Infrared Spec., vol. 20, 2012. Pp.371-385

[11]. He C., Chen L., Yang Z., Hang G., Liao N. and Han L. "A rapid and accurate method for on-line measurement of straw-coal blends using near infrared spectroscopy. ", Bioresource Technol., vol. 110, 2012. Pp. 314-320

[12]. Jin S., Chen H. "Near-infrared analysis of the chemical composition of rice straw.", Ind. Crop Prod., vol. 26, 2007. Pp. 207-211

[13]. Everard C.D., McDonnell K.P. and Fagan C.C. "Prediction of biomass gross calorific values using visible and near infrared spectroscopy.", Biomass Bioenergy., vol. 45, 2012. Pp. 203-211

[14]. Panwar N.L., Kaushik S.C. and Kothari S. "Role of renewable energy sources in environmental protection: A review.", Renew Sust Energ Rev, vol. 15, 2011. Pp 1513-1524

[15]. Demirbas A. "Recent advance in biomass conversion technologies.", Energy Educ. Sci. Tech., vol. 6, 2000. Pp 19-40

[16]. Rathore N.S., Panwar N.L. Renewable energy sources for sustainable development. New Delhi, India: New India Publishing Agency; 2007

[17]. Hein K.R.G., Bemtgen J.M. "EU clean coal technology, co combustion of coal and biomass.", Fuel Process. Technol., vol. 54, 1998. Pp. 159-169

[18]. Spliethoff H. and Hein K.R.G. "Effect of co-combustion of biomass on emissions in pulverized fuel furnaces.", Fuel Process. Technol., vol. 54, 1998. Pp. 189-205

[19]. Rao Y.V. " Leucaena plantations-a-farming experience.", Leucaena Res. Rep., vol. 5, 1984. Pp. 48-49

[20]. Via B.K., Adhakari S. and Taylor S. "Modeling for proximate analysis and heating value of torrefied biomass with vibration spectroscopy.", Bioresource Technol., vol. 133, 2013. Pp. 1-8

[21]. Hemminger W. and Sargev S.M. "Definitions, nomenclature, terms and literature.", In: Brown M. E. editor. Handbook of thermal analysis and calorimetry. Vol.1, Principles and practice. Elsevier; 1998

[22]. Luo S.Y., Xiao B., Hu Z.Q., Liu S.M. and Guan Y.W. "Experimental study on oxygen-enriched combustion of biomass micro fuel.", Energy, vol. 34, 2009. Pp. 1880–1884

[23]. Qing W., Hao X., Hongpeng L., Chunxia J. and Jingru B. "Thermogravimetric analysis of the combustion characteristic of oil shale semi-coke/biomass blends.", Oil Shale, vol. 28, 2011. Pp. 284-295

[24]. Yang H., Yan R., Chin T., Liang D. T., Chen H., and Zheng C. "Thermogravimetric Analysis-Fourier Transform Infrared Analysis of Palm Oil Waste Pyrolysis.", Energ. Fuel., Vol. 18, 2004. Pp. 1814-1821

[25]. Barneto A.G., Carmona J.A., Ferrer J.A.C. and Balanco M.J.D. "Kinetic study on the thermal degradation of a biomass and its compost: Composting effect on hydrogen production.", Fuel, vol. 89, 2010. Pp. 462-473

[26]. Sait H.H., Hussain A., Salema A.A. and Ani F.N. "Pyrolysis and combustion kinetics of date palm biomass using thermogravimetric analysis.", Bioresource Technol., vol. 118, 2012. Pp. 382-389

[27]. Parthasarathy P., Narayanan K.S. and Arockiam L. "Study on kinetic parameters of different biomass samples using thermo-gravimetric analysis.", Biomass and Bioenergy., vol. 58, 2013. Pp. 58-66

[28]. El-Sayed S.A. and Mostafa M.E. "Pyrolysis characteristics and kinetic parameters determination of biomass fuel powders by differential thermal gravimetric analysis (TGA/DTG).", Energ. Convers. Manage., vol. 85 ,2014, Pp.165-172

[29]. Reschmeier R., Roveda D., Müller D. and Karl J. "Pyrolysis kinetics of wood pellets in fluidized beds", J. Anal. App. Pyrol., vol.108, 2014, Pp. 117–129

[30]. Ren S., Lei H., Wang L., Bu Q., Chen S., Wu J. "Thermal behavior and kinetic study for woody biomass torrefaction and torrefied biomass pyrolysis by TGA. ", Biomass and Bioenergy., vol. 116, 2013, Pp. 420 -426

[31]. López-González D., Fernandez-Lopez M., Valverde J.L. and Sanchez-Silva L. "Thermogravimetric-mass spectrometric analysis on combustion of lignocellulosic biomass", Bioresource Technol., vol. 143 , 2013, Pp. 562–574

[32]. Osborne B., Fearn T. and Hindle P.H. "Practical NIR Spectroscopy with Applications in Food and Beverage Analysis.", Longman Scientific and Technical, Harlow, UK (1993)

[33]. Workman J., Jr. and Weyer L. "Practical Guide to Interpretive Near-Infrared Spectroscopy." CRC Press, Taylor & Francis group, New York, USA (2008).

[34]. Liu L. and Chen H. "Prediction of maize stover components with near infrared reflectance spectroscopy (NIRS).", Spectrosc. Spect. Anal. vol. 27(2), 2007, Pp. 275-278

[35]. Sirisomboon P. and Chowbankrang R., Williams P. "Evaluation of apparent viscosity of Para rubber latex by diffuse reflection near infrared spectroscopy.", Applied Spect., vol. 66, 2012, Pp. 595-599

[36]. Pereira A.F.C., Pontes M.J.C., Neto F.F.G., Santos S.R.B., Galvão R.K.H. and Araújo M.C.U. "NIR spectrometric determination of quality parameters in vegetable oils using *i*PLS and variable selection.", Food Res. Internal., vol. 41, 2008, Pp. 341-348

[37]. Riggio M., Sandak J., Sandak A., Pauliny D. and Babiński L. "Analysis and prediction of selected mechanical/dynamic properties of wood after short and long-term waterlogging.", Construct. Building Mat., vol. 68, 2014, Pp. 444-454

CHAPTER 3

NON-DESTRUCTIVE EVALUATION OF HIGHER HEATING VALUE, VOLATILE MATTER, FIXED CARBON AND ASH CONTENT OF BAMBOO USING NEAR INFRARED SPECTROSCOPY

3.1. Abstract

This research aimed to determine the higher heating value (HHV), volatile matter (VM), fixed carbon (FC) and ash content (A) of ground bamboo using Fourier transform near-infrared spectroscopy as an alternative for bomb calorimetry and thermogravimetry. The different circumference of the culm have a range approximately of 16-18, 18-20, 20-22, 22-24, 24-26, 26-28, 28-30, 30-32, 32-34, 34-36, 36-38 and 38-40 cm. Model development was optimized using partial least squares regression. The HHV, VM, FC and A were predicted with coefficient of determination (R^2) of 0.924, 0.944, 0.850 and 0.508; root mean square error of prediction (RMSEP) of 122 Jg^{-1}, 0.653%, 1.21% and 0.768%; ratio of the standard deviation to standard error of validation (RPD) of 3.66, 4.53, 3.10 and 1.44; bias of 14.4 Jg^{-1}, 0.229%, -0.668% and -0.108%, respectively.

The report shows that the NIR spectroscopy is fairly successful in determination of HHV and VM, and is usable with caution for most applications for determination of FC. For A, the method was not recommended. In addition, the models for HHV, VM and FC were influenced by lignin, cellulose and lignin and cellulose respectively.

Keywords: Fourier transform near infrared spectroscopy; volatile matter; fixed carbon; ash content; higher heating value; partial least squares regression

3.2. Introduction

Bamboo is a kind of biomass which has many advantages such as fast-growing, high strength, and a high yielding natural source [1, 2]. Bamboos are large woody grasses that include 1250 species within 75 genera. It produces rapid growth and attains stand maturity within five years [3]. Some species can grow up to a foot a day under the right condition..[4] In the south of Asia, bamboo is used for building walls, floor, roof, apparatus, and handicrafts. In addition, bamboo also has great potential as a renewable energy [5,6] Scurlock et al.[3]reported that bamboo has potential to provide bioenergy due to low ash content (A) (1% or less) and higher heating value (HHV) that ranged

from 19090-19570 Jg^{-1}. Darabant et al.[7] reported that bamboo *B. beecheyana* and *D. membranaceus* species were attractive options as bioenergy feedstock with high volatile mater (VM), low A and high HHV of 74.08 and 74.17%; 1.92 and 1.97%; and 19347 and 19513 Jg^{-1}, respectively. Meanwhile, Cheng et al. [6] reported HHV of the two bamboo species were in the range of 19.4–19.9 $MJkg^{-1}$ In addition, age difference of bamboo biomass can make a significant influence on yield and properties of the fast pyrolysis products.[6] It is possible that the chemical composition of biomass also changes with either age or external factors such as location, harvest age, soil properties and so on. Darabant et.al [7] Biomass yield from bamboo depends on the location where it is produced. For bamboo biomass, the cellulose content decreased, lignin content increased and ash content increased when the age of bamboo increased from one year to three years. [6] These factors affected on the thermal processing characteristic.

Understanding of the characteristic of biomass helps in designing the optimum thermal conversion system. [8] The HHV and proximate analysis data are important in thermal processing. [9,10] The HHV is the one of the thermal characteristics that expresses how much energy can be obtained from biomass material. [11] When biomass is used in thermal conversion process and power plant, the knowledge of HHV is required. It is an important parameter for power plants planning using biomass fuel. [12, 13] Meanwhile, VM and fixed carbon (FC) help to know the combustion behavior and the plant design. [9] In fast pyrolysis processing, VM is a substance that vaporizes such as gas or vapor. It was used to evaluate the performance of the biomass pyrolysis and gasifier by the rate of gas production. [14] In addition, it also helps to evaluate the bio-oil condensation. In slow pyrolysis, the knowledge of FC helps to evaluate the weight of bio-char or solid product. On the other hand, A is the solid residue after the fuel is burned. It is negative to heat consumption and this knowledge is important for the design of the storage bins in thermal conversion processing, [15] besides, the high A effects there is problem for transportation system.[9]

In the trade of biomass, a random cost per kilogram is used for biomass price and it is not fair. Therefore, the price of biomass should be set by considering the HHV and proximate analysis data. Normally, HHV can be determined by bomb calorimeter. The proximate analysis data can be determined using thermogravimetric (TG) analysis by direct measure of weight changes on each sample's TG chart. [9] Both parameters need a high skilled technician. Then, workers are uncomfortable in these methods because the time consumption is taken at approximately 3-24 hrs

per sample for TG analysis and 50 min for bomb calorimeter. Hence, the new method that can be used to rapidly check the properties for setting the price of biomass instead of the old methods is essential.

Near infrared (NIR) spectroscopy is the technique which there were many advantages such as non-destructive (sample can be returned to population), rapid (usually time consumption was 2-3 minute), environment friendly (no or few chemical) and low labor cost. There were some application of NIR spectroscopy on biomass such as moisture content and HHV of *Jatropha cucas* L.[16], thermal properties of *Jatropha cucas* L.[17], hemicellulose, cellulose and lignin in sorghum [18], HHV of biomass from dedicated Irish bioenergy crops, i.e. *Miscanthus* and two varieties of short rotational coppice willow (SRCW)[19], moisture, calorific value, ash and carbon content of harvested *Miscanthus* and SRCW[20], and moisture content, total carbon content, A and HHV of a multi-variety biomass pellet sample set.[21]

In addition, determining characteristic (thermal properties and proximate analysis data) of biomass by rapid non-destructive means is important in determining the theoretical yield from a biochemical conversion.[19] It can be used to monitor biological or thermochemical conversion processes of bamboo as a quality evaluation method and to design thermal chemical conversion methods such as gasification and pyrolysis processes of bio-energy. Thus, this study aimed to apply NIR spectroscopy on the determination of HHV, VM, FC and A of ground bamboo.

3.3. Material and methods

3.3.1. Sample preparation

Bamboo of Phamon variety of 12 different groups of culm circumference (approximately 16-18, 18-20, 20-22, 22-24, 24-26, 26-28, 28-30, 30-32, 32-34, 34-36, 36-38 and 38-40 cm) measured from 10 cm above the ground was collected which is planted in Uttaradit province of Thailand. The bamboo trunk was cut 10 cm above the ground to avoid the soil and root attached to the trunk. The bamboo samples were collected of different culm circumferences because the assumption was made that, "the bamboo of different culm sizes would provide different thermal properties and energy properties". A total of 80 samples were obtained. Ten kg bamboo of each sample were chopped by the chopping machine (P5508, Patipong, Thailand) and dried under the sun until the

moisture reached around 5% wb, ground pass through the sieve diameter of 3 mm (60201, QC, UK) and kept in the aluminum bag before experiment. The 5% moisture content of the dried bamboo wood chips was obtained by randomly selected samples for determination of moisture content by hot air oven method is used at the temperature of 105°C until constant weight.

3.3.2. Near infrared spectral scanning

The experiment was done at the laboratory of Near Infrared Spectroscopy Research Center for Agricultural Product and Food (www.nirsresearch.com) at the Curriculum of Agricultural Engineering, Department of Mechanical Engineering, Faculty of Engineering at King Mongkut's Institute of Technology Ladkrabang. The scanning of the sample was done using FT-NIR Spectrometer (MPA, Bruker, Germany) with diffuse reflectance mode at the wavenumber range of 12500-3600 cm^{-1} with resolution of 8 cm^{-1} through the quartz bottom of sample cup of 43 mm in diameter and 50 mm in height, containing the ground samples of height, which there was no light leak. Before each sample was scanned, the gold plate was scanned as reference. The samples were scanned and number of spectra for each sample is noted.

3.3.3. Biomass characterization

Higher heating value (HHV) of biomass was measured with a bomb calorimeter (C200, IKA, Germany) and evaluated using *isoperibol* method. Before the measurement, bomb calorimeter was calibrated using two of 0.5 g Benzoic acid pellet (C723, IKA, Germany). And then, the 0.5-1 g sample was weighed using electronic balance (ARC 140 Adventure, OHAUSS, 0.0001 g resolution), pelletized and subjected into the bomb calorimeter.

Biomass characteristic including volatile matter, ash, and fixed carbon were determined using thermogravimetric analysis. In analysis, for monitoring mass loss and mass loss rate, thermogravimetric analyser (TG 209 F3 Tarsus, Netzsch, Germany, 0.1 µg resolution; 6.8 mm diameter aluminum oxide (AL_2O_3) crucible) was used for ground bamboo sample of 6.0±0.5 mg. Thermal program started from maintaining temperature at 30°C in 20 ml/min N_2 flushed environment for 1 hour to ensure the zero O_2 environment, then increase the temperature to 700°C with the heat rate of 10°C/min for pyrolysis, keep the temperature at 700°C for 1 hour to ensure completing pyrolysis process, and then fed with 20 ml/min O_2 for 1 hour for combustion. The mass loss at different time and temperature were recorded. The thermogravimetric (TG) profile and differential thermogravimetric (DTG) profile was obtained using Proteus 6.0.0. (NETZSCH Software,

Germany). TG and DTG curve showed the typical of degradation such as moisture release, devolatilization and char degradation which can be used for approximation of the composition of biomass. The biomass characteristic was determined by direct measure of weight changes on each sample's TG chart. The volatile matter and ash content were determined from sample's DTG chart. The ash content is the mass residue after burned. After that, fixed carbon can be calculated as follows:

$$FC\% = 100 - (VM\% + Ash\%) \quad (1)$$

Where, VM%, FC% and Ash% were the volatile matter, fixed carbon and ash content of ground bamboo, respectively.

When HHV and proximate analysis data were determined, the outlier of reference data were also determined using the following equation:

$$\frac{(X_i - \overline{X})}{SD} \geq \pm 3 \quad (2)$$

Where X_i is the measured value of sample i. $\overline{X}$ and SD are the average and standard deviation of the measured values of all samples, respectively. If the equation was satisfied, the sample was outlier and it was then removed from reference data set.

3.3.4. Repeatability, reproducibility and maximum coefficient of determination (R^2_{Max})

Before the model was developed, the spectral data and the measured reference data were checked for the repeatability and reproducibility. The reproducibility of spectral data is the standard deviation of absorbance values, when the sample was re-loaded and re-scanned for 10 times (Phil Williams, personal communication). The 10th loading was left in the cell and re-scanned 9 more times, to achieve 10 scans with the sample in the same position within the cell. The standard deviation of the obtained absorbance values was the repeatability of the instrument. The absorbance value at wavenumber of 5176 cm^{-1} (1932 nm) was used for the calculation. The absorption at any wavenumber could be selected for determination of the repeatability and reproducibility of NIR scanning. The wavenumber of 5176 cm^{-1} (1932 nm) was the absorption band of water in the ground bamboo spectrum. The NIR absorption band of water was the obvious highest peak in the spectrum. The peak was easily changed when the scanning conditions were varied. The repeatability of measured value was the standard deviation of the different between duplicates. On the other hand, the reproducibility of measured value was the standard deviation of the different between duplicates, but it was obtained from blind samples. Then the repeatability of

measured value was used to determine the maximum coefficient of determination (R^2_{Max}), which was calculated using following formula [22]:

$$R^2_{Max} = \frac{SD_y^2 - Rep^2}{SD_y^2} \quad (3)$$

where SD_y is the standard deviation of data of measured value in calibration set. R^2_{Max} is possible only when there are no errors in the spectra or the model.

3.3.5. Spectrum pre-processing and NIR spectroscopy modeling

The NIR spectroscopy models for predicting the HHV, VM, FC and A from ground bamboo obtained from bamboo trunks with different circumferences of the culms was established using Partial Least Squares regression (PLS). The software program (OPUS, v. 7.0.129, Germany) was used for multivariate analysis for spectrum preprocessing and model development. The spectra without pre-processing or with pre-processing by the following methods: constant offset elimination, straight line subtraction, vector normalization, min-max normalization, multiplicative scatter correction (MSC), first derivatives, second derivatives, first derivatives + straight line subtraction, first derivatives+ vector normalization and first derivatives + MSC was used for model development. The samples was then subdivided into 80% of the calibration sample set and 20% of the validation sample set by using random division automatically by the software, however, the maximum value and minimum value were set to be in the calibration set. The optimal model was selected by lowest of root mean square error of prediction. The outlier was calculated by Mahalanobis distance limit.

The regression coefficient and X-loading weight of each PLS factor was determined by the software program and plotted. The coefficients of determination (R^2), root mean square error of prediction (RMSEP), ratio of prediction to deviation (the standard deviation to standard error of prediction, RPD) and bias were used to assess the performance of the PLS model. According to Williams (2007), the model with R^2 between 0.66-0.81 could be used for screening and some other "approximate" calibration. Therefore R^2 below 0.66 should be considered as low R^2 which the model could not be applied for quantitative analysis.

3.4. Results and discussion

3.4.1. *Repeatability, reproducibility and* R^2_{max}

Table 3: 1 Repeatability, reproducibility and R_Max^2 of higher heating value, volatile matter, fixed carbon, ash and absorption at 5176 cm-1 (1932 nm) of ground bamboo.

Paramerter	**Repeatability**		
	SD of the difference of Duplicate	SD of the difference of Blind Duplicate	R^2 Max
Higher Heating Value	68.34	64.46	0.955
Volatile matter	0.593	0.916	0.960
Fixed Carbon	1.087	0.845	0.862
Ash Content	0.829	0.552	0.561
Absorption value at 5176cm $^{-1}$1932 nm of Sample number 28	0.00467	0.01816	-

Repeatability, reproducibility and R^2_{max} of HHV, VM, FC, A and absorption at 5176 cm^{-1} (1932 nm) of ground bamboo were shown in Table 3:1. They were the precision of reference laboratory and NIR spectrometer. The values of R^2_{max} of higher heating value (0.955), volatile matter (0.960) and fixed carbon (0.862) were high indicated that the NIR model was reasonable for development. Though the value for ash content was too low (0.561) indicated that it is not reasonable to develop NIR model. The repeatability of the reference laboratory for ash content was also high (21% of mean). The ratio of the repeatability of absorbance value per its mean (0.004668/0.408386) was approximately 1.14%. Meanwhile, the ratio of the reproducibility of absorbance value per its mean (0.01816/0.401406) also was approximately 4.50%. These meant that the error of 1.14% occurred due to NIR spectrometer and the error approximately of 3.36%

(4.5-1.14%) occurred due to sample. They were the unexplained variance of the scanning system. R^2_{Max} is possible only when there are no error in the spectra.[26]

3.1.1 Measured values

Table 3: 2 Higher heating value, volatile matter, fixed carbon and ash content of ground bamboo obtained from bamboo trunks with different circumferences of the culms.

Diameter range (mm)	N	Higher heating value (J g^{-1})	Volatile matter (%)	Fixed carbon (%)	Ash content (%)
16<L≤18	8	17706.75±342a	59.52±1.81bc	30.49±2.59bcd	4.18±1.26a
18<L≤20	6	17780.33±120a	62.22±2.27a	28.62±3.11d	3.61±0.65a
20<L≤22	6	17775.16±317a	60.75±2.84ab	29.76±3.36cd	4.06±1.32a
22<L≤24	7	17730.92±357a	58.44±2.09bcd	31.52±1.53abc	4.25±0.87a
24<L≤26	6	17892.41±142a	57.28±1.10cd	33.08±1.10ab	3.96±0.73a
26<L≤28	6	17846.33±449a	56.82±1.66cd	33.74±0.73a	3.47±1.01a
28<L≤30	8	17653.93±524a	57.39±1.71cd	32.24±2.12abc	3.89±1.21a
30<L≤32	8	17773.06±385a	57.69±2.90cd	32.32±2.13abc	3.67±0.95a
32<L≤34	7	17875.92±550a	57.17±1.17cd	33.15±1.71ab	4.06±0.72a
34<L≤36	7	17896.92±341a	56.75±2.52d	33.12±1.82ab	3.56±1.16a
36<L≤38	5	17966.70±226a	58.69±2.22bcd	32.28±2.06abc	3.08±0.36a
38<L≤40	6	17997.66±203a	58.06±2.21cd	32.68±1.33ab	3.93±0.57a

Different letters in the same column indicates the different means that are significantly at p>0.05 by the Duncan multiple range test. N is number of samples. L is circumference of the culm.

Table3:2 shows the HHV, VM, FC and A of ground bamboo. As expected, the HHV and A were not different between the different circumferences of the culms. For VM and FC, there were 4 different levels but they were also not obviously seen. Hisham et al.[23] and Scurlock et al.[3] reported that the thermal and chemical characteristic of bamboo changed with the different age such as HHV, hemicellulose and cellulose. Thus, it could be concluded that there also was no relationship between size of circumference and age of bamboo.

3.4.2. Sample spectra

The mean NIR spectra of ground bamboo can be observed in Figure 3:1. There were obvious peaks at 6,792, 5176, 4725, 4413, 4305 and 3988 cm^{-1} (1472, 1932, 2116, 2266, 2323 and 2508 nm). The wavebands of 1471 nm are N-H stretching first overtone of CONHR[24], 1930 nm is O-H stretching + H-O-H bending combination of polysaccharides[33], 2110 and 2262 nm are hemicellulose, 2323 nm is C-H stretching + C-H deformation of CH_2, 2500 nm is C-H stretching + C-C stretching of starch.[24] Polysaccharide were the starch and cellulose structure, they consists of many monosaccharide. Cellulose is a linear polysaccharide polymer. It was the primary component in the cell wall, and starch also was the source of energy of plant cells. Meanwhile, the structure of CH_2 appears on lignocellulosic such as hemicelluloses, cellulose and lignin.

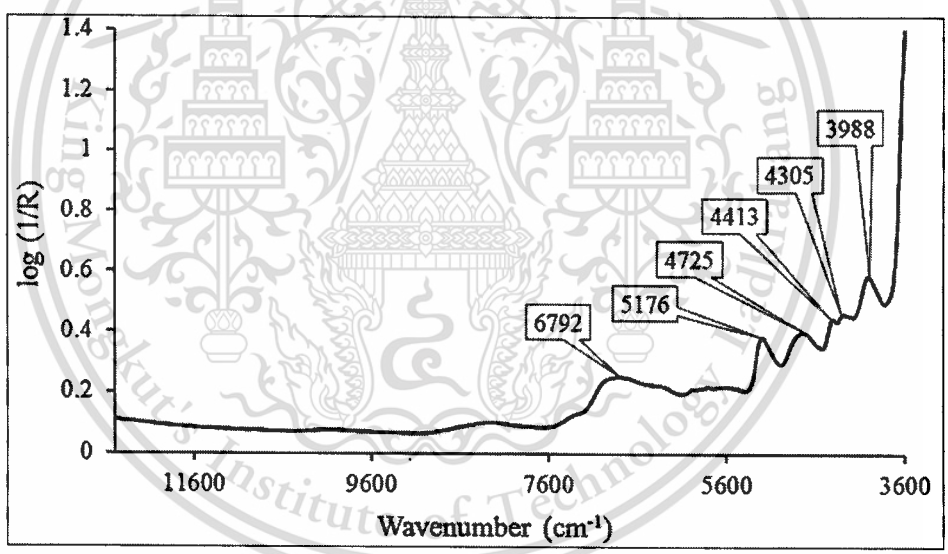

Figure 3: 1 Average NIR spectra of ground bamboo.

3.4.3. Model and validation

The statistical data used for model development are shown in Table 3:3. Table 3:4 shows the results of the optimum PLS models for the properties studied.

Table 3: 3 Statistical data of higher heating value, volatile matter, fixed carbon and ash content of ground bamboo used in model development.

Parameters	Calibration set					Validation set				
	N	Max	Min	Mean	SD	N	Max	Min	Mean	SD
Higher heating value (Jg^{-1})	64	18357.0	16534.5	17842.9	323.3	16	18319.5	16898.5	17701.9	456.5
Volatile matter (%)	64	65.015	54.510	58.371	2.259	16	62.905	53.56	58.223	2.859
Fixed carbon (%)	64	36.28	26.525	32.294	1.9601	16	35.47	25.76	30.893	3.227
Ash content (%)	64	6.65	1.72	3.868	0.957	16	6.13	1.84	3.726	1.130

Table 3: 4 Results of partial least squares regression models for higher heating value, volatile matter, fixed carbon and ash content of ground bamboo.

Parameter	wavenumber range (cm^{-1})	Pre-processing	Calibration set			Validation set			
			PLS factor	R^2	RMSEE	R^2	RMSEP	RPD	Bias
Higher heating value	6102-4597.7	Min-Max normalization	7	0.87	124	0.924	122	3.66	14.4
Volatile matter	6102-5446.3	First derivative	8	0.827	1.01	0.944	0.653	4.53	0.229

	4424.2-4246.7								
Fixed carbon	7502.2-6800.2 5450.2-4246.7	First derivative + vector normalization	8	0.803	0.932	0.850	1.21	3.10	-0.668
Ash content	9828-8933.2 8046-5376.9	First derivative +straight line substation	8	0.673	0.587	0.508	0.768	1.44	-0.108

3.4.4. Higher heating value

The best model for prediction of HHV was developed using wavenumber range of 6102-4597.7 cm^{-1}, spectrum pre-processing of min-max normalization and PLS factor number of 7. It was selected by the lowest of RMSEP. The R^2, RMSEP, RPD and bias of validation set were 0.924, 122 J g^{-1}, 3.66 and 14.4 J g^{-1}. Williams[29] indicated that the model provided R^2 between 0.92 and 0.96 could be used for most applications, including quality assurance and RPD in the range of 3.1-4.9 could be used for screening. The ratio between bias and mean of reference value (14.4 J g^{-1}/17701.9 Jg^{-1}) was approximately 0.0813%. Therefore, the model should be acceptable.

The R^2_{max} and R^2 for HHV were 0.955 and 0.924, respectively. Normally, R^2_{max} is the coefficient of determination of the prediction model when there are no errors in the spectra. This means that 4.5% of the total variation was the unexplained variance due to reference method. While, R^2 equal to 0.924, accordingly, 7.6% of the total variation was the total unexplained variance. It included unexplained variance due to spectra and sample. Thus, 3.1% (7.6-4.5%) was the unexplained variance due to either NIR spectra error or sample. According to the above explanation, the ratio of the repeatability and reproducibility of absorbance value per its mean were in a range of 1.14 to 4.5%. Thus, it can be seen that 1.96% (3.10-1.14%) was the unexplained variance of sample. Moreover, it can be seen that R^2 can be approximated by the ratio of the repeatability and reproducibility of absorbance value per its mean subtract from R^2_{max} or $R^2 \approx 0.955$ - (approximately 1.14 to 4.5%). Therefore, the error of higher heating value prediction of 4.5%, 1.14% and 1.96% was due to reference method, NIR instrument and sample, respectively.

Therefore, the model can be improved by increasing the replicate number of reference value, checking the accuracy of NIR instrument or always scanning the reference material before each sample scan, and improving the homogeneity of particle size.

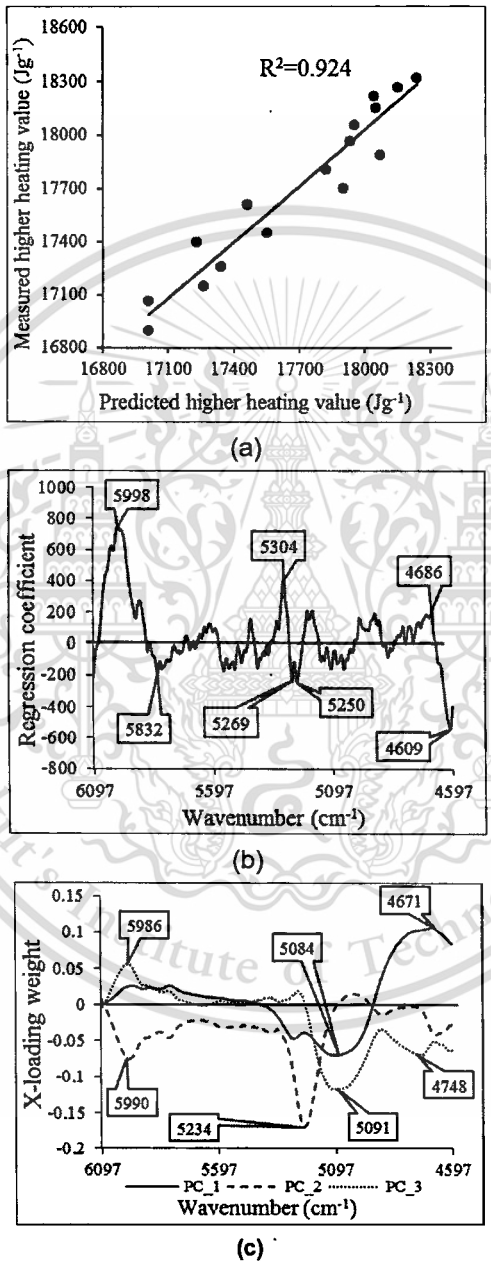

Figure 3: 2 a) Measured vs NIR spectroscopy predicted higher heating value of ground bamboo of validation set b) Regression coefficient plots c) X-loading plots. PC_1, PC_2 and PC_3 are PLS factor 1, 2 and 3.

Figure 3:2 shows the scatter plots of measured value by reference laboratory technique (Y axis) and predicted value by NIR spectroscopy (X axis) of validation, regression coefficient plot and X-loading plot for the higher heating value of ground bamboo. The regression coefficient plot and X-loading weight plots of the first three PLS factors used in model development are used to interpret the effect of absorbance at a peak wavenumber (X variable) on the prediction of the constituent or properties (Y variable) on the molecular level. The high value at any wavenumber indicates that the vibration of the particular bonds at the wavenumber strongly influences the model prediction.

The absorbance region of 5998 cm^{-1}(1667 nm), 4609 cm^{-1}(2170 nm) and 5304 cm^{-1} (1885 nm) in regression coefficient plots were important in the prediction of higher heating value. They correspond to C-H first overtone of vinyl group, C-H stretching and C-H deformation combination of C-H alkenes (HC=CH) and O-H stretching + 2×C-O stretching of water and polyvinyl alcohol OH.[33] The X-loading weight plot showed high peaks at 5234 cm^{-1} (1911 nm) related with O-H stretching first overtone of POH[24], at 4671 cm^{-1} (2141 nm) related with =C-H stretching + C=C stretching of HC-CH[24] and at 5091 cm^{-1} (1964 nm) related O-H and CH combination from methanol (CH_3OH).[33] These results agrees with the results of Guimarães et al.[22], they reported that the peaks are at about 5940 cm^{-1} (first overtone of aromatic C-H stretching), 5230 cm^{-1} (first overtone of aromatic O-H stretching), 4415 cm^{-1} (combination band of O-H and C-O stretching) was dependent to lignin. In addition, the molecule of HC-HC, alkenes (HC=CH), methanol (CH_3OH), vinyl group (C_2H_3) and polyvinyl alcohol OH also appeared on lignin structure (Figure 6 (3:3)).[34] They were the hydrocarbon which are a primary energy source.

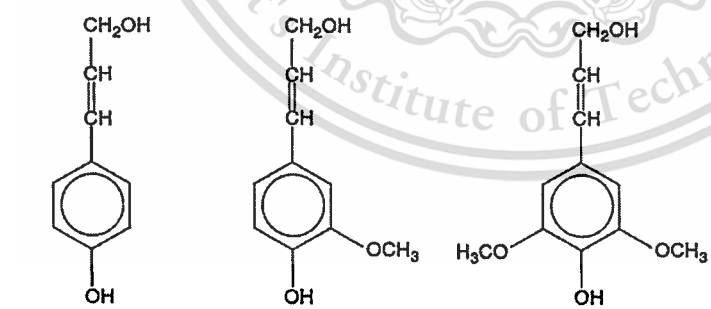

p-Coumaryl alcohol Coniferyl alcohol Sinapyl alcohol

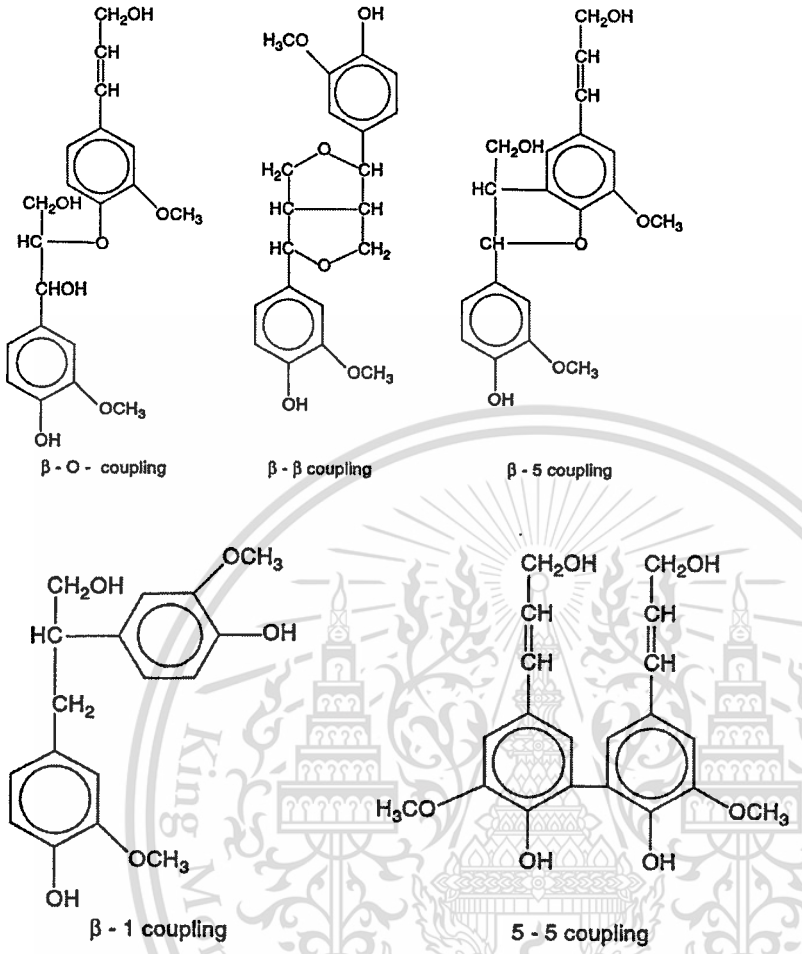

Figure 3: 3 a Structure of monomer precursors for the enzymatic synthesis of lignin (p-coumaryl alcohol, coniferyl alcohol and sinapyl alcohol) and main intermonomeric couplings (β-O-4, α-O-4, β-β, β-5, 5-5, 4-O-5, β-1) [34]

Meanwhile, lignin content was mainly related to HHV of biomass.[26,27] Posom and Sirisomboon[16] reported that vibration bands of fiber and cellulose had important effect on the prediction of HHV of *Jatropha curcas* L. This agreed with the results of Fagan et at.[20], which was shown that vibration band at 1148 nm and 1524 nm which were wave bond of C-H second overtone of CH_3 and O-H stretching first overtone of starch, which was important in the prediction of calorific value of *Miscanthus* and Short Rotational Coppice Willow (SRCW). Thus, determination of HHV was effected by the vibration of C-H bond of lignocellulosic compound.

Volatile matter

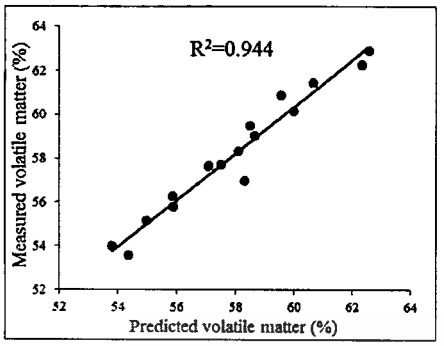

(a)

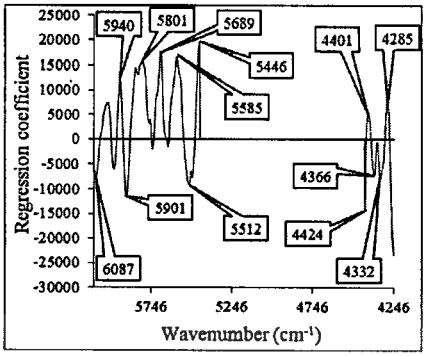

(b)

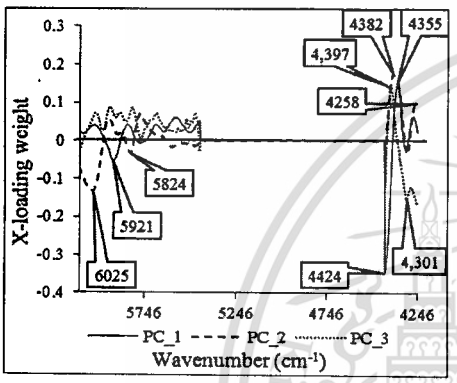

(c)

Figure 3: 4 a) Measured vs NIR spectroscopy predicted volatile matter of ground bamboo of validation set b) Regression coefficient plots c) X-loading plots. PC_1, PC_2 and PC_3 are PLS factor 1, 2 and 3.

Scatter plots of measured value by reference laboratory technique (Y axis) and predicted value by NIR spectroscopy (X axis) of validation; regression coefficient plot and X-loading plot of the optimum model for the volatile matter of ground bamboo were shown in Figure 3:4.

Table 4 shows the characteristic and performance of the best model for prediction of volatile matter. The model was developed using wavenumber range of 6102-5446.3 and 4424.2-4246.7, spectrum pre-processing of first derivative and PLS factor number of 8. The R^2, RMSEP, RPD and bias of validation model were 0.944, 0.653%, 4.53 and 0.229%. The ratio of bias per mean measured value was approximately 0.393% (0.229% of 58.223%). For volatile matter, R^2_{max} and R^2 were 0.960 and 0.944, respectively. This means that 4.0% of the unexplained variance was due to reference method. The different of unexplained variance between R^2_{max} and R^2 was 1.6%. Then, the error of 0.46% (1.6-1.14%) was due to samples. In addition, R^2 equal to 0.960 - (approximately 1.14% to 4.5%). R^2 was 0.944, this mean that 5.6% was the total unexplained variance and 94.4% was the explained variance where NIR information was accounted for by

volatile matter content. Hence, the total error (unexplained variance) of 5.6% (100-94.4%) was 4.0% from reference method, 1.14% from NIR instrument and 0.46% from samples. Therefore, there were three factors that influenced the error of prediction, especially the reference method.

The absorbance region of 5446 cm^{-1} (1836 nm), 5689 cm^{-1} (1758 nm) and 5585 cm^{-1} (1791 nm) nm in regression coefficient plots were important in the prediction of volatile matter. They were the bond vibration of O-H stretching +2×C-O stretching of cellulose, sucrose structure, C-H stretching first overtone of cellulose, respectively. While X-loading plots also show the important peak at 4424 cm^{-1} (4424 nm), 4382 cm^{-1} (2282 nm), 4301 cm^{-1} (2325 nm) which are O-H stretching + O-H deformation of starch, C-H stretching +C-H deformation of CH_3 and C-H stretching +C-H deformation of CH_2, respectively. Thus, the wave band of O-H stretching and C-H stretching of cellulose effected to volatile matter prediction, which are similar to those reported by Lv et al.[28] and Burhenne et al.[29] where it was noticed that gas yield of biomass pyrolysis increased with increase of cellulose content, but bio-char yield decreased. Guimarães et al.[18] reported that cellulose related to peak of 4415 cm^{-1} (O-H and C-O stretching combination band) and 4290 cm^{-1} (combination of C-H stretching and CH_2 deformation). While Wannapeera et al.[30] reported that biomass (rice husk, rice straw and corncob) contains the highest cellulose content, gave the highest total gas yield. In addition, sucrose also affects volatile matter prediction whereas sucrose is made up from glucose and fructose; cellulose also is a glucose polymer.[31]

3.4.5. Fixed carbon

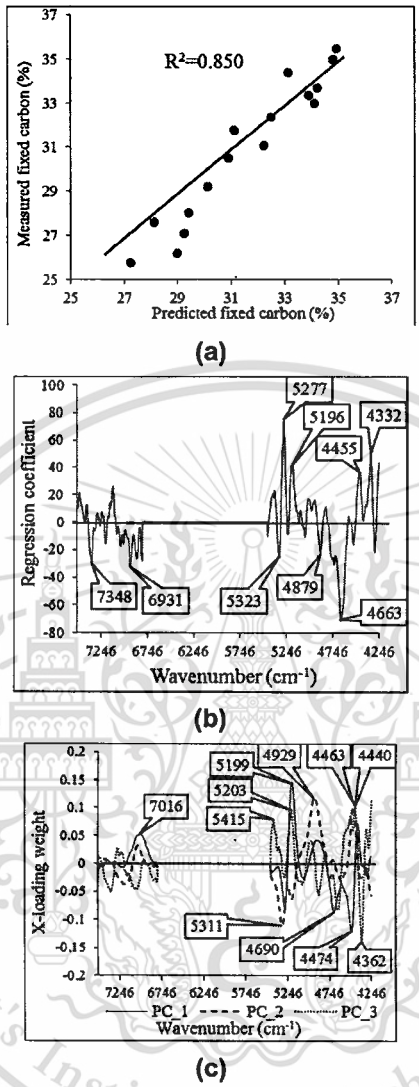

Figure 3: 5 a) Measured vs NIR spectroscopy predicted fixed carbon of ground bamboo of validation set b) Regression coefficient plots c) X-loading plots. PC_1, PC_2 and PC_3 are PLS factor 1, 2 and 3.

Figure 3:5 shows scatter plots of measured value by reference laboratory technique (Y axis) and predicted value by NIR spectroscopy (X axis) of validation; regression coefficient plot and X-loading plot of the optimum model for fixed carbon of ground bamboo.

The best model for prediction of fixed carbon was developed using wavenumber range of 7502.2-6800.2 cm^{-1} and 5450.2-4246.7 cm^{-1}, spectrum pre-processing of first derivative + vector normalization and PLS factor number of 8 (Table 3:4). The R^2, RMSEP, RPD and bias of

validation model were 0.850, 1.21%, 3.1 and -0.668% (Table 3:4). The model that provided R^2 between 0.83 and 0.90 could be used with caution for most applications, including research and RPD in the range of 3.1-4.9 could be used for screening.[29] The ratio between bias and mean measured value was approximately 2.16% (-0.668% of 30.893%), the model may be accepted by user before model operation.

The R^2_{max} and R^2 were 0.862 and 0.850, respectively. These meant that the 86.2% of the total variance was the explained variance. The other 13.8% of the total variation was the unexplained variance which was the error of reference data. The different between R^2_{max} and R^2 was 0.012 or 1.2%. Then, the unexplained variance of 0.06% (1.2-1.14%) was from samples. Hence, R^2 could be estimated by 0.862 - (approximately 1.14% to 4.5%). Hence, the total unexplained variance of fixed carbon prediction was 15% (100-85.0%). It was the summation of unexplained variance due to 13.8% from reference method, 1.14% from NIR instrument and 0.06% from samples.

The absorbance region at 5277 cm^{-1} (1895 nm), 4663 cm^{-1} (2145 nm) and 4332 cm^{-1} (2308 nm) in regression coefficient plots were important in the prediction of fixed carbon. These wavelengths were primarily associated with O-H hydrogen bonding between water and expose polyvinyl alcohol OH of alcohol OH; sucrose; and C-H stretching + C-H deformation of CH_2, respectively. While X-loading plots also show the important peak at 5199 cm^{-1} (1923 nm), 4362 cm^{-1} (2293 nm), 4474 cm^{-1} (2235 nm) which are the absorption of O-H assigned to molecular water [O-H stretching and HOH deformation combination of O-H molecular, N-H stretching + C=O stretching of amino acid, and C-H stretching and CH_2 deformation combination of polysaccharides.

These results are similar to those reported by Fagan et al.[24] that C-H stretching and/or deformation of CH, CH_2, CH_3, aromatics, -CHO and cellulose (1215, 1360, 1395, 1400, 1685, 1725, 2200 and 2336 nm); O-H stretching and deformation of ROH at 1410 and 2080 nm respectively; C=O stretching (2nd overtone) of $-CO_2H$, CONH, and CONH (1900, 1920 and 2030 nm); N-H stretching (1st overtone) of $CONH_2$ (1430 nm); and finally S–H stretching (1st overtone) of -SH (1740 nm) related to prediction carbon content of *Miscanthus* and Short Rotational Coppice Willow (SRCW).

The main peaks were the peaks of alcohol OH and CH_2, both are in the lignocellulosic structure, either lignin or cellulose. Especially, OH was the one bond of lignin structure. Burhenne et al. [33]

reported that biomass containing high lignin content can produce the high bio-char. In addition, there was a peak of polysaccharides. According to Floch et al. [32], fibrous polysaccharides were either starch or cellulose. It is a good source of energy. Therefore, the model for fixed carbon was depended on lignin and cellulose.

3.4.6. Ash content

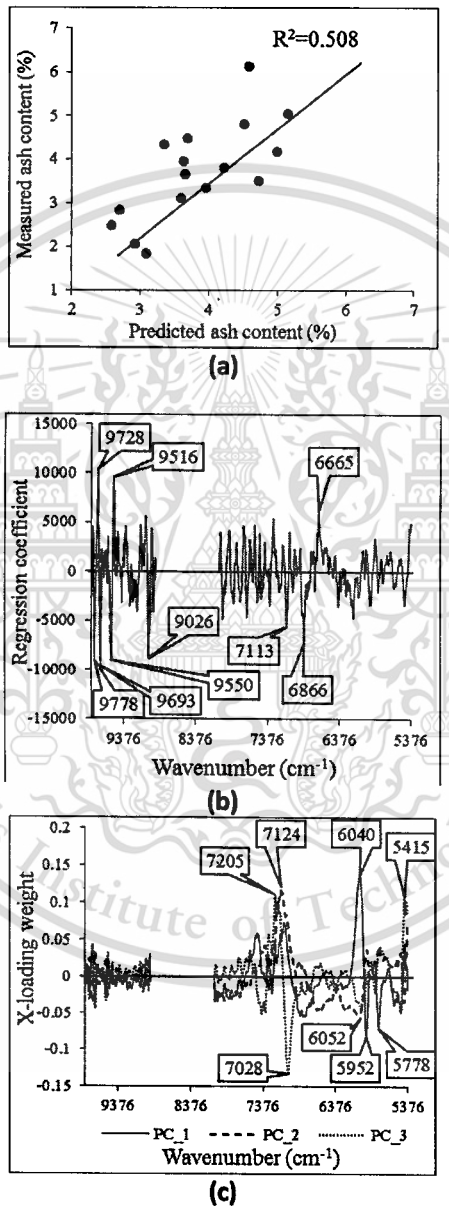

Figure 3: 6 a) Measured vs NIR spectroscopy predicted ash content of ground bamboo of validation set c) Regression coefficient plots c) X-loading plots. PC_1, PC_2 and PC_3 are PLS factor 1, 2 and 3.

Scatter plots of measured value by reference laboratory technique (Y axis) and predicted value by NIR spectroscopy (X axis) of validation, regression coefficient plot and X-loading plot for the optimum model for ash content of ground bamboo were shown in Figure 3:6. The best model for prediction of ash content were developed using wavenumber range of 9828-8933.2 cm^{-1} and 8046-5376.9 cm^{-1}, spectrum preprocessing of first derivative + straight line substation and PLS factor number of 8 (Table 3:4). The R^2, RMSEP, RPD and bias of validation model were 0.508, 0.768%, 1.44 and -0.108% (Table 3:4). The ratio of bias per mean measured value was approximately 2.89% (-0.108% of 3.726%). The result had a low of R^2, this mean that only 50.8% of the variance in absorbance value can be accounted for by variance in ash content. Therefore, 49.2% was the unexplained variance. R^2_{max} For ash content prediction was 0.561, which was the coefficient of determination of the prediction when there was no error of spectra. The RPD also was low because the range of ash content is so narrow or no different of ash content in different circumference bamboo. Consequently, the model analysis was not necessary. [25] Because the ratio of the repeatability and reproducibility of absorbance value per its mean were in a range of 1.14% to 4.5%. Therefore, R^2 can be approximated as $R^2 \approx$ 0.561 - (approximately 1.14% to 4.5%). However, the different between R^2_{max} and R^2 was equal to 0.053 or 5.3%. Therefore, the total of unexplained variance of ash content model was 49.2% which were 43.9% from reference method, 1.14% from NIR instrument and 4.16% from samples.

3.5.Conclusion

The PLS model development for evaluation of the higher heating value, volatile matter and fix carbon of ground bamboo was feasible. However, it was not possible for evaluation of ash content in these samples, largely because the range in ash was low. The peak for C-H stretching of phenolic ring structures, from which lignin is formed, affected tthe prediction of HHV. The prediction of volatile matter was primarily influenced by O-H stretching +2×C-O stretching of cellulose structure. Prediction of fixed carbon was primarily associated with O-H hydrogen bonding between water and polyvinyl alcohol OH of alcohol OH, which may be a lignin structure. Moreover, the result showed that the reference method had the highest influence on error of prediction. Thus, NIR spectroscopy could be used as a nondestructive technique for most applications, including quality assurance for prediction of higher heating value and volatile matter, and could be used for prediction of fixed carbon with caution for most applications, including research. These properties can be used to design thermal chemical conversion methods such as

gasification and pyrolysis processes of biomass as well as to monitor biological or thermochemical conversion processes of bamboo. In trading, the properties can be used to set the price alternatively to the old method.

3.6. Acknowledgements

The authors thank the Near Infrared Spectroscopy Research Center for Agricutultural Product and Food (www.nirsresearch.com) at King Mongkut's Institute of technology Ladkrabang, Bangkok, Thailand, for instrument. We also acknowledge the financial support from the Royal Golden Jubilee PhD scholarship (PHD/0070/2557) of Thailand research fund (TRF).

3.7. References

[1] E. Villar-Cociña, E.V. Morales, S.F. Santos, H.S. Jr.b and M. Frías, "Pozzolanic behavior of bamboo leaf ash: Characterization and determination of the kinetic parameters", *Cem. Concr. Compos.* **33,** 68–73(2011).

[2] Z. Jiang, Z. Liu, B. Fei, Z. Cai, Y. Yu and X. Liu, "The pyrolysis characteristics of moso bamboo", J. Anal Appl Pyrol 94. 48–52. (2012)

[3] J.M.O. Scurlock, D.C. Dayton and B. Hames, "Bamboo: an overlooked biomass resource?", *Biomass Bioenergy* **19,** 229-244(2000).

[4] A.O. Oyedun, T. Gebreegziabher and C.W. Hui, "Mechanism and modelling of bamboo pyrolysis", *Fuel Process. Technol.* **106,** 595–604(2013).

[5] P. Peng and D. She, "Isolation, structural characterization, and potential applications of hemicelluloses from bamboo: A review", *Carbohydr. Polym.* **112,** 701–720(2014).

[6] L. Cheng, S. Adhikari, Z. Wang and Y. Ding, "Characterization of bamboo species at different ages and bio-oil production", *J. Anal. Appl. Pyrol* **116,** 215–222(2015).

[7] A. Darabant, M. Haruthaithanasana, W. Atklaa, T. Phudphonga and E. Thanavata, "Bamboo biomass yield and feedstock characteristics of energy plantations in Thailand", *Energy Procedia* **59,** 134 – 141(2014).

[8] K-Y. Chiang, K-L. Chien and C-H. Lu, "Characterization and comparison of biomass produced from various sources: suggestions for selection of pretreatment technologies in biomass-to-energy", *Appl. Energy* **100,** 164–171(2012).

[9] R. García, C. Pizarro, A.G. Lavín and J.L. Bueno, "Biomass proximate analysis using thermogravimetry", *Bioresour. Technol.* **139,** 1–4(2013).

[10] R. García, C. Pizarro, A.G. Lavín and L.J. Bueno, "Characterization of Spanish biomass wastes for energy use", *Bioresour. Technol.* **103,** 249–258 (2012).

[11] C. Huang, L. Han, Z. Yang and X. Liu, "Prediction of heating value of straw by proximate data, and near infrared spectroscopy", *Energ Convers Manage* **49,** 3433–3438(2008).

[12] D.R. Nhuchhen and P.A. Salam, "Estimation of higher heating value of biomass from proximate analysis: A new approach". *Fuel* **99,** 55–63(2012).

[13] E.P. Friedl, H. Rotter and K. Varmuza, "Prediction of heating values of biomass fuel from elemental composition". *Analytica Chimica Acta* **544,** 191–198(2005).

[14] P.N. Sheth and B.V. Babu, "Production of hydrogen energy through biomass (waste wood) gasification". *Int. J. Hydrogen Energy* **35,** 10803 -10810(2010).

[15] C. Lanzerstorfer, "Chemical composition and physical properties of filter fly ashes from eight grate-fired biomass combustion plants", *J. Environ. Sci.* **1,** 191–197(2015).

[16] J. Posom and P. Sirisomboon, "Evaluation of the moisture content of *Jatropha curcas* kernels and the heating value of the oil extracted residue using near-infrared spectroscopy", ***Biosystem Eng* 130,** 52-59(2015).

[17] J. Posom and P. Sirisomboon, "Evaluation of the thermal properties of Jatropha curcas L. kernels using near-infrared spectroscopy". ***Biosystem Eng* 125,** 45-53(2014).

[18] C.C. Guimarães, M.L. Simeone, R.A.C. Parrella and M.M. Sena, "Use of NIRS to predict composition and bioethanol yield from cell wall structure components of sweet sorghum biomass", *Microchem. J.* **117,** 194-201(2014).

[19] C.D. Everard, K.P. McDonnell and C.C. Fagan, "Prediction of biomass gross calorific values using visible and near infrared spectroscopy". *Biomass Bioenerg.* **45,** 203-211(2012).

[20] C.C. Fagan, C.D. Everard and K.McDonnell, "Prediction of moisture, calorific value, ash and carbon content of two dedicated bioenergy crops using near-infrared spectroscopy". *Bioresour. Technol.***102,** 5200–5206(2011).

[21] G.D. Gillespie, C.D. Everard and K.P. McDonnell, "Prediction of biomass pellet quality indices using near infrared spectroscopy". Energy. 80, 582-588. , 2015

[22] P. Dardenne, "Some considerations about NIR spectroscopy: Closing speech at NIR-2009" (2009)

[23] H.N. Hisham, S. Othman, H. Rokiah, M. A. Latif, S. Ani and M.M. Tamizi, "Characterization of bamboo *gigantochloa Scortechinii* at different ages", *J. Trop For Sci* **18(4),** 236–242(2006).

[24] B.G. Osborne and T. Fearn, *Near Infrared Spectroscopy in Food Analysis*. Longman Science & Technical, London (1986).

[25] P. Williams, *Near-Infrared Technology—Getting the Best Out of Light Edition 5.0. A Short Course in the Practical Implementation of Near-Infrared Spectroscopy for the User*. PDK Grain, Nanaimo, Canada (2007).

[26] A. Álvarez, C. Pizarro, R. García, JL. Bueno. "Spanish biofuels heating value estimation based on structural analysis", *Ind Crop Prod* **77,** 983–991(2015).

[27] G. Dorez, L. Ferry, R. Sonnier, A. Taguet, J.-M. Lopez-Cuesta, "Effect of cellulose, hemicellulose and lignin contents on pyrolysis and combustion of natural fibers", *J. Anal. Appl. Pyrol* **107,** 323–331(2014).

[28] D. Lv, M. Xu, X. Liu, Z. Zhan, Z. Li and H. Yao, "Effect of cellulose, lignin, alkali and alkaline earth metallic species on biomass pyrolysis and gasification", *Fuel Process. Technol.* **91,** 903--909(2010).

[29] L. Burhenne, J. Messmer, T. Aicher and M-P. Laborie, "The effect of the biomass components lignin, cellulose and hemicellulose on TGA and fixed bed pyrolysis", *J. Anal. Appl. Pyrol* **101,** 177–184(2013).

[30] J. Wannapeera, N. Worasuwannarak and S. Pipatmanomai, "Product yields and characteristics of rice husk, rice straw and corncob during fast pyrolysis in a drop-tube/fixed-bed reactor. *Songklanakarin J. Sci. Technol.* **30(3),** 393-404(2008).

[31] P. McKendry, "Energy production from biomass (part 1): overview of biomass", *Bioresour. Technol.* **83,** 37-46(2002).

[32] A.L. Floch, M. Jourdes, P-L. Teissedre, "Polysaccharides and lignin from oak wood used in cooperage: Composition, interest, assays: A review". *Carbohydr. Res.* **417,** 94-102(2015).

[33] J. Workman and J.R.L. Weyer. *Practical Guide to Interpretive Near-Infrared Spectroscopy*. Taylor & Francis, Boca Raton, FL, pp. 240–262 (2007).

[34] H. Pereira. *The chemical composition of cork. Cork: Biology, Production and Uses*. Elsevier's science & Technology, Nederland, pp. 71(2007).

CHAPTER 4

NONDESTRUCTIVE EVALUATION OF COMBUSTION PERFORMANCE INDEX, BURNOUT INDEX, IGNITION INDEX OF BAMBOO USING NEAR INFRARED SPECTROSCOPY

4.1.ABSTRACT

The combustion performance parameter of the bamboo chips including ignition index, burnout index and combustion performance index were found to be 88.33E-04, 0.16E-03and 3.95E-07, On the other hand, the two diode array NIR-instruments (NIR-Gun and Micro-NIR) and Fourier transform near infrared (FT-NIR) instrument were used to make model of combustion performance parameter i.e. ignition index, burnout index and combustion performance index using the same partial least squares regression technique. The total number of the sample used for making the model was 80 for both types of instruments. The samples were grounded to 2 mm size. The diffuse NIR-instruments models of combustion performance parameter used 13-20 PLS factors for the making the model. However, the diffuse NIR-instruments were unable to predict the combustion performance parameter of the grounded bamboo chips with any accuracy. The spectra were suffered from the noise, and the variability of the calibration set samples used for making the models (for combustion index 4.613-2.794E-07, ignition index 11.907-6.994E-03, and burnout index 2.04-1.23E-04) was low. This may be the reason why the diffuse NIR-instrument failed to predict. In contrast, the FT-NIR was able to predict the ignition index and burnout index but with very low accuracy. The coefficient of determination of prediction set, bias and RPD of optimum model of ignition index are 0.432, 3.960E-05 and 1.33, with the number of PLS factors of the model 4, and the coefficient of determination of prediction set, bias and RPD of optimum model of burnout index are 0.513, -2.210E-07, and 1.43, with the number of PLS factors of the model 7.

4.2.Intoduction

Before selling the biomass commercially, its combustion performance parameters i.e. combustion performance index, burnout index and ignition index must be recognized in advance because combustion characteristics may be varied with different source and age so that it will get its actual monetary value instead of random cost per kilogram. These properties are equally important for biomass or its pellet production plant and the combustion plants. So, in order to measure its

properties without consuming more time as thermogravimetric analysis (TGA) a new method should be implemented. To mitigate this problem, near infrared (NIR) spectroscopy has found a scope for its application.

The thermogravimetric procedures are time consuming process, approximately 3-24 hours for thermogravimetric analysis, which also requires a skilled manpower. NIR spectroscopy covers the electromagnetic radiation in the region from 780 to 2500 nm (12820-4000 cm^{-1}) [1]. The NIR spectroscopy technique can provide rapid results in seconds or continuously on-line, rather than in hours or days, with an accuracy and reproducibility equivalent to most reference methods. Other advantages of NIR include its low cost per test, low labor costs, no required chemicals to purchase or dispose of, great flexibility in sample presentation and the capability of testing many constituents simultaneously. This method is environmentally friendly because it requires no chemicals. The instrument is simple to install and operate, does not produce any emissions which need to be removed by drainage or exhaust and easy to prepare sample. Many instruments are of the stand-alone type and their durability allows them to work well for more than ten years. Instruments can be networked to use the same calibration with their performance controlled from a single control center [2].

Furthermore, NIR spectroscopy has been applied for the evaluation of lignocellulosic compound content of sugarcane biomass[3], straw content of straw-coal blends[4], heating value of straw [5], *Miscanthus* and coppice willow [6]. However, till this date there are no works that relate combustion parameters of biomass with NIR spectroscopy. The objectives of this study were: to develop the model that correlates the NIR spectral characteristic of the bamboo chip (Dendrocalamus sericeus cl. Phamon) with its combustion performance parameters i.e. ignition index, burnout index and combustion performance index and to prove the possibility of NIR spectroscopy as an alternative, rapid and accurate method for evaluation of those properties.

4.3. Material and Methods

4.3.1. Sample preparation

The bamboo samples, *Dendrocalamus sericeus* cl. Phamon, were procured from Uttaradit, Thailand. The bamboo trees were cut about 10 cm from the ground level, and about 1 m from the base of bamboos was selected for the study. The bamboos were then chopped by the chopping

machine (P5508, Patipong, Thailand). The total number of bamboo trees were 90 consisting of various circumference ranging from 16-39 cm.

4.3.2. Near infrared (NIR) scanning for combustion performance parameters

The chopped bamboo chips were dried under sun and were grounded to pass through 2 mm diameter sieve (SM100, Retsch, Germany). The grounded samples were then scanned by three NIR instruments: NIR-Gun (FQA, Fantec, Japan) in reflectance mode (over the short wavelength range from 600-1100 nm at 2 nm intervals, Micro-NIR (JDSU, USA) in reflectance mode (operating in the long wavelength range between 1150-2150 nm) at 7 nm intervals and FT-NIR (12500-3600 cm^{-1} at 8 cm^{-1} resolution). The total numbers of samples used for making NIR-model were 80. Each sample was scanned two times. The samples were scanned in air conditioning room, 25±2 °C. The reflectance (R) spectrum were transformed into absorbance, log(1/R), spectra using CA maker software (Fantec, Japan) and The Unscrambler X 10.3 (Camo, Norway) for spectra obtained by NIR-Gun and Micro-NIR respectively, while, OPUS version 7.0.129 (Bruker, Germany) for making the FT-NIR model. The part of spectra that contain noise or unusual characteristics was erased and was not used for model development.

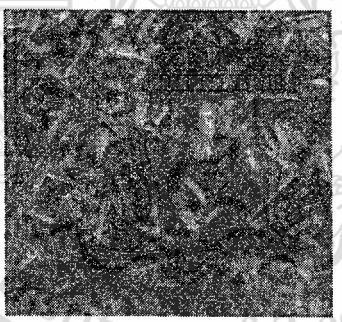

(a)

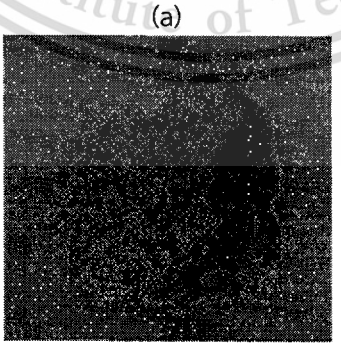

(b)

Figure 4: 1 (a) Dried bamboo chips (b) Grounded bamboo chips

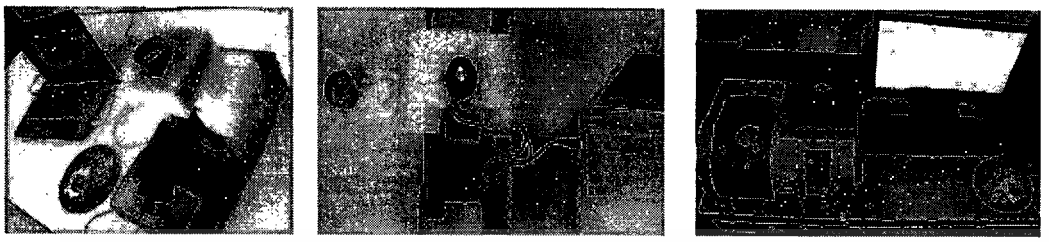

(a) (b) (c)

Figure 4: 2 Near infrared scanning for combustion performance parameters performed by (a) NIR-gun and (b) Micro-NIR and (c) FT-NIR

4.3.3. Thermogravimetric analysis

The grounded samples after scanned by the NIR-instruments were subjected for thermogravimatric analysis for the combustion performance which was performed by the thermogravimetric analyzer (TG 209 F3 Tarsus, Netzsch, Germany, 0.1 µg resolution, heating rate ranges from 0.001 to 100 $Kmin^{-1}$, 6.8 mm diameter aluminum oxide (AL2O3) crucible) in an air conditioning room temperature of 25±2°C and the thermogravimetric (TG) profile and differential thermogravimetric (DTG) profile were analyzed using Proteus 6.0.0. (Netzsch Software, Germany). At the heating rate of $10°Cmin^{-1}$, the temperature of furnace was increased from 33°C to 900°C in an air flux (O_2) of 20 $mLmin^{-1}$. The samples were kept isothermal at 33°C for 10 minutes. The mass of the sample was monitored continuously as a function of temperature and time. The sample size was kept constant at around 6 mg. And, from the thermogravimetric curve Ignition index (D_i), Burnout index (D_f), Combustion performance index (S) were calculated as discussed in Chapter 2.

4.3.4. Spectra pretreatment and mathematical modelling

The spectrum pre-treatments and model development were performed on The Unscramble X 10.3 software (Camo, Norway) for the spectra scanned by the NIR-Gun and Micro-NIR, and OPUS version 7.0.129 (Bruker, Germany) was used for FT-NIR. After the wet-test, the reference data were merged with corresponding spectral data. The data were then arranged in descending order, and data were separated into calibration and prediction set. The highest and lowest reference values were included in calibration set. By Unscrambler X, various pre-treatments on calibration data set were performed before model development which includes no pre-treatment, Savitzky-

Golay (S-G) smoothing (2^{nd}order polynomial with 11 and 21 points), mean normalization, maximum normalization, range normalization, 1^{st} derivative (2^{nd} order polynomial with 11 and 21 points), 2^{nd} derivative (2^{2n} order polynomial with 11 and 21 points), baseline offset, linear baseline correction, standard normal variate (SNV), de-trending, SNV plus de-trending and multiple scatter correction (MSC). Similarly, for OPUS, various pretreatment includes: no pretreatment, constant offset elimination, straight line subtraction, vector normalization, SNV, min-max normalization, MSC, 1^{st} derivatives, 2^{nd} derivatives, 1^{st} derivatives + straight line subtraction, 1^{st} derivatives + SNV and 1^{st} derivatives + MSC.

Partial least square regression technique was used to develop the NIR models. The models were checked by test set validation method, and the optimum model was selected for lowest number of factor, highest coefficient of determination of prediction, and low value of standard error of cross validation, standard error of prediction and bias.

4.4. Result and Discussion

4.4.1. Measurement of combustion performance parameters by diode array instruments

The raw spectra, log (1/R), of the grounded bamboo samples scanned from NIR-Gun is shown in Figure 4.3. The raw spectra obtained from the NIR-Gun scanning show unusual characteristics to each other, so the scanning that shows similar characteristics/features were selected and second derivative (second order polynomial with 5 points) was performed in order to study the spectral characteristics, Figure 4.4 and 4.5, respectively. The raw spectra show the absorption in the region 620-680 nm, 720-840 nm and in 960-1000 nm. The region 600-700 nm is associated with the visible range which is normally associated with chlorophyll absorption [3]. The region 960-1000 nm is associated with the third overtone of O—H stretching and hydrocarbon. The second derivative shows the several peaks in the region 620-680 nm, 720-840 nm, and independent peak at 973 nm is associated with the second overtone of O—H stretching, principally water, and the overlapping peaks are associated with C—H stretch third overtone [9,10]. The several peaks in 720-840 nm region are observed with the noticeable peaks at 733 nm, 760 nm (O—H str., third overtone, water) [7], 788 nm (N—H str., third overtone, ArNH2) [7].

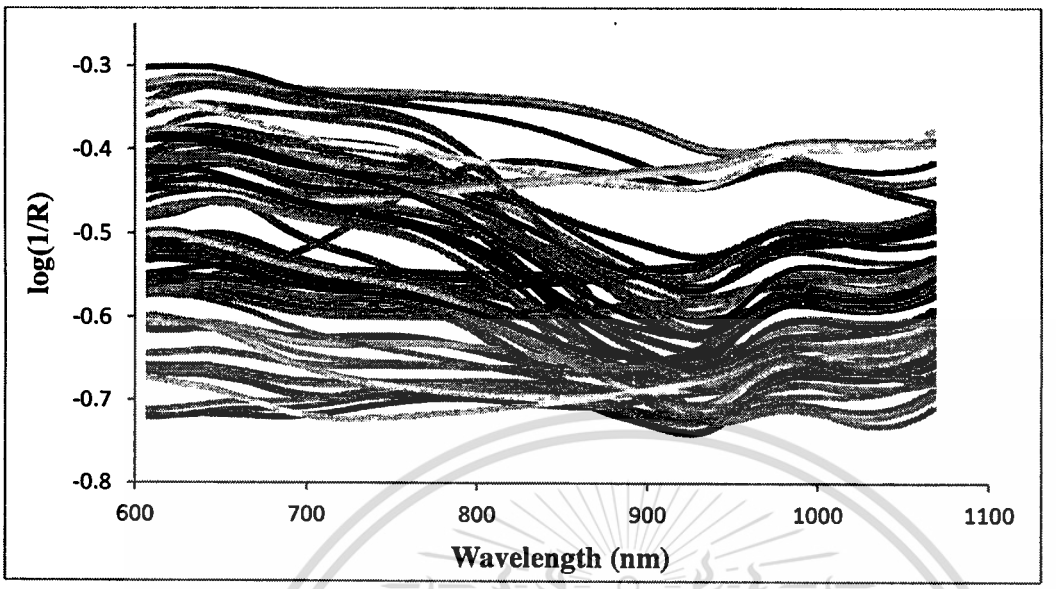

Figure 4: 3 Raw spectra of the grounded bamboo chips scanned by NIR-Gun spectrometer.

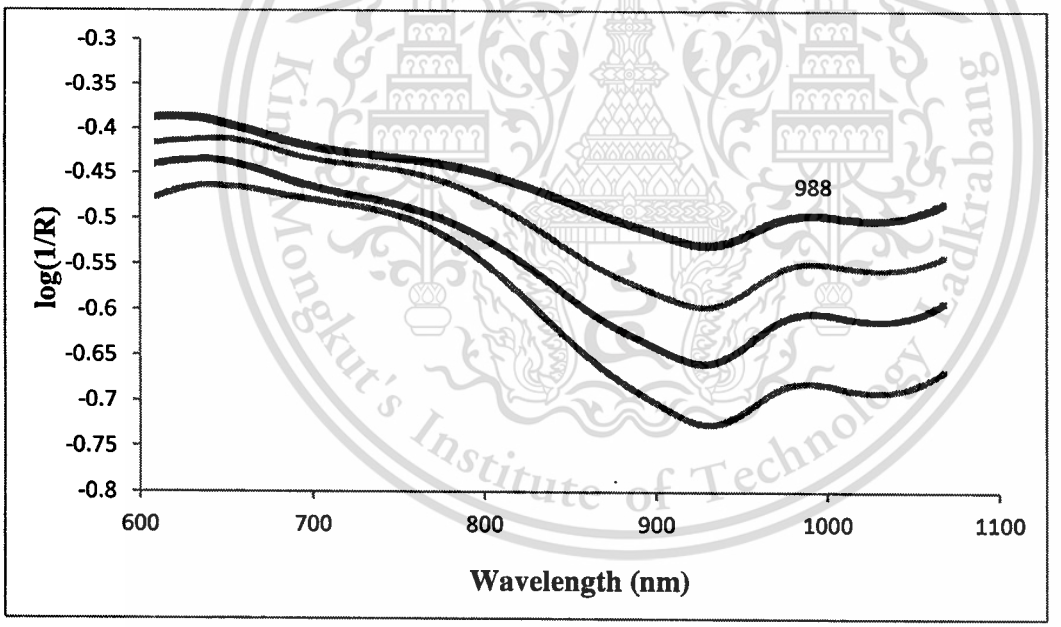

Figure 4: 4 Selected raw spectra of the grounded bamboo chips scanned by NIR-Gun spectrometer.

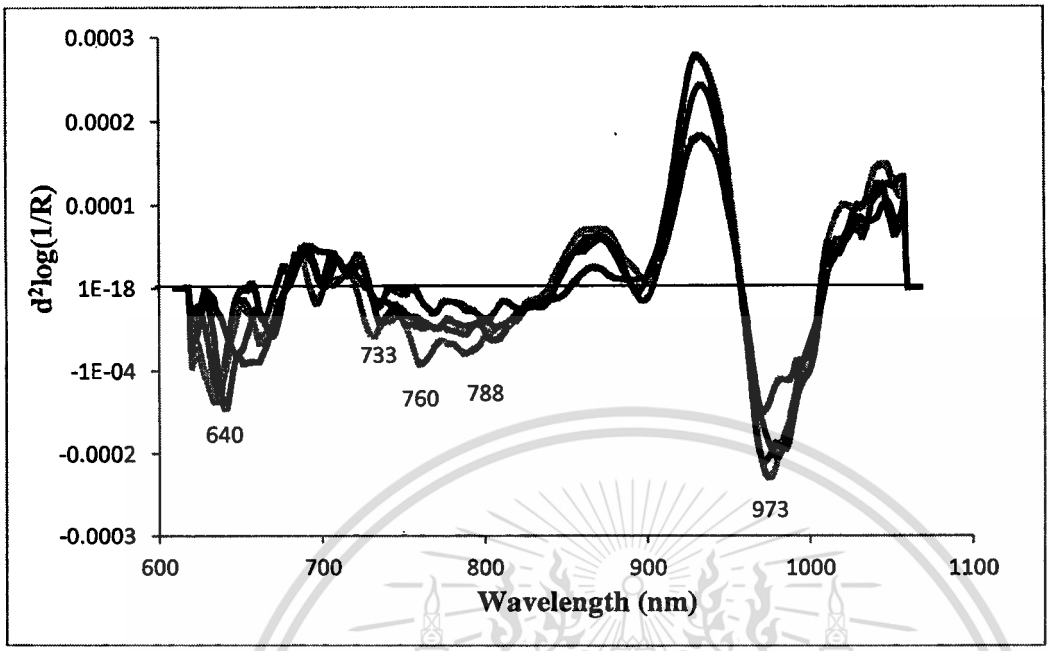

Figure 4: 5 Second derivative (second order polynomial with 5 points) of the selected raw spectra of the grounded bamboo chips scanned by NIR-Gun spectrometer.

The raw spectra of the Micro-NIR, Figure 4.6, scanning show the similar characteristics unlike NIR-Gun scanning, however, the spectra seem noisy. In order to study the spectral characteristics, Savitzky-Golay (S-G) smoothing (second order polynomial with 11 points) and second derivative (second order polynomial with 5 points) of the spectra, Figure 4.7 and 4.8 respectively, were performed. Since the raw spectra contained noise, the S-G smoothing of the raw spectra was taken into consideration which shows the absorption in the region 1380-1580 nm, 1800-1900 nm and 2020-2060 nm. The region 1380-1580 nm is assigned as first overtone of O—H stretching, 1800-1900 nm third overtone of CH deformation, and 2020-2060 nm is assigned as second overtone of —C=H— stretch [8]. The second derivative shows the several peaks in the region 1180-2050 nm. The noticeable peaks are at 1285 nm, 1358 nm (2×C—H str. + C—H def., CH3), 1440 nm (O—H str. first overtone, sucrose, starch), 1506 nm (N—H str. first overtone, protein), 1572 nm (N—H str., first overtone, -CONH-), 1669 nm (C-H aromatic C-H (aryl)), 1780 nm (C—H str., first overtone, cellulose), 1860 nm (C—Cl chlorinated organics, chlorinate hydrocarbons), 1898 nm (O—H str. + 2×C—O str., starch), 1979 nm (N—H asym. Str. + amide 2, protein), 2038 nm (N—H combination band from urea (NH2—C=O—NH2, urea) [1,7]

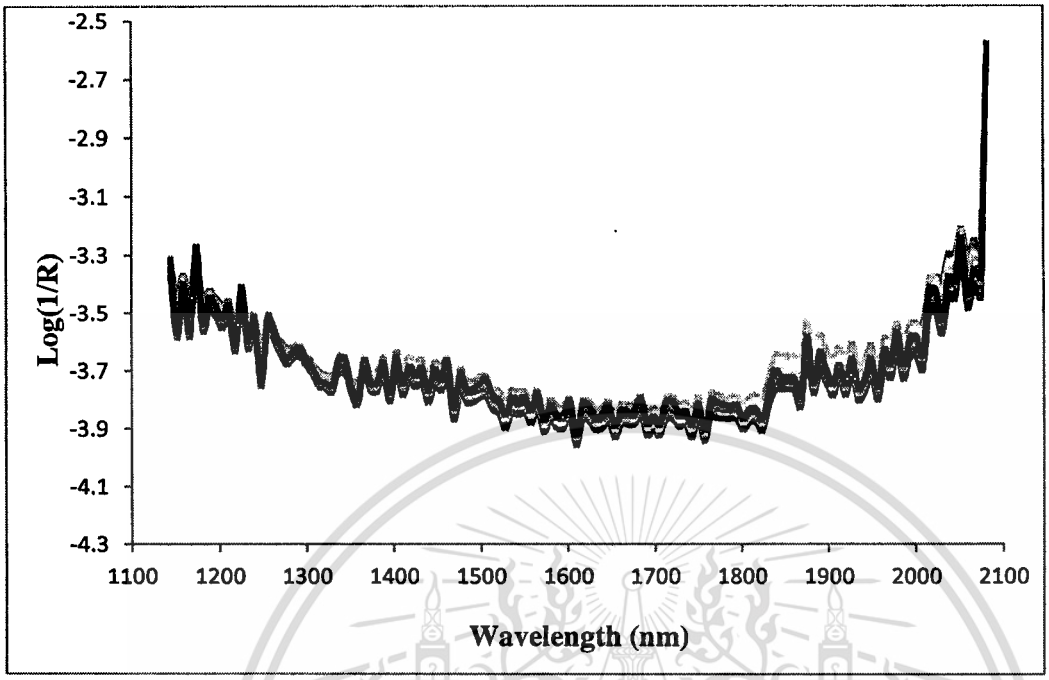

Figure 4: 6 Raw spectra of the grounded bamboo chips scanned by Micro-NIR spectrometer.

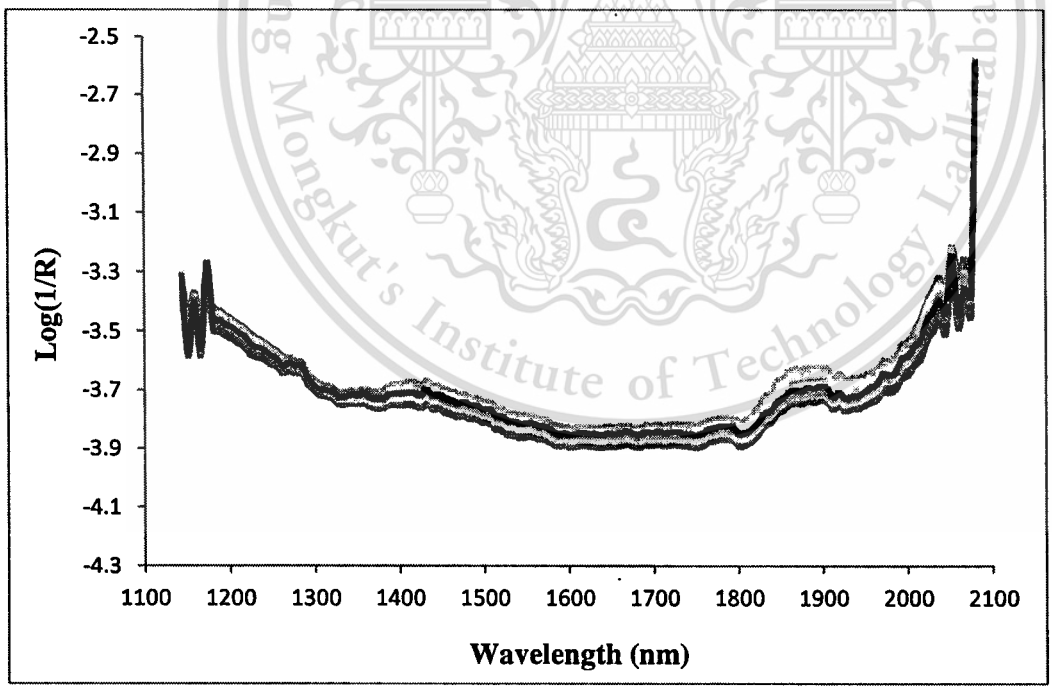

Figure 4: 7 S-G smoothing (second order polynomial with 11 points) of the raw spectra of the grounded bamboo chips scanned by Micro-NIR spectrometer.

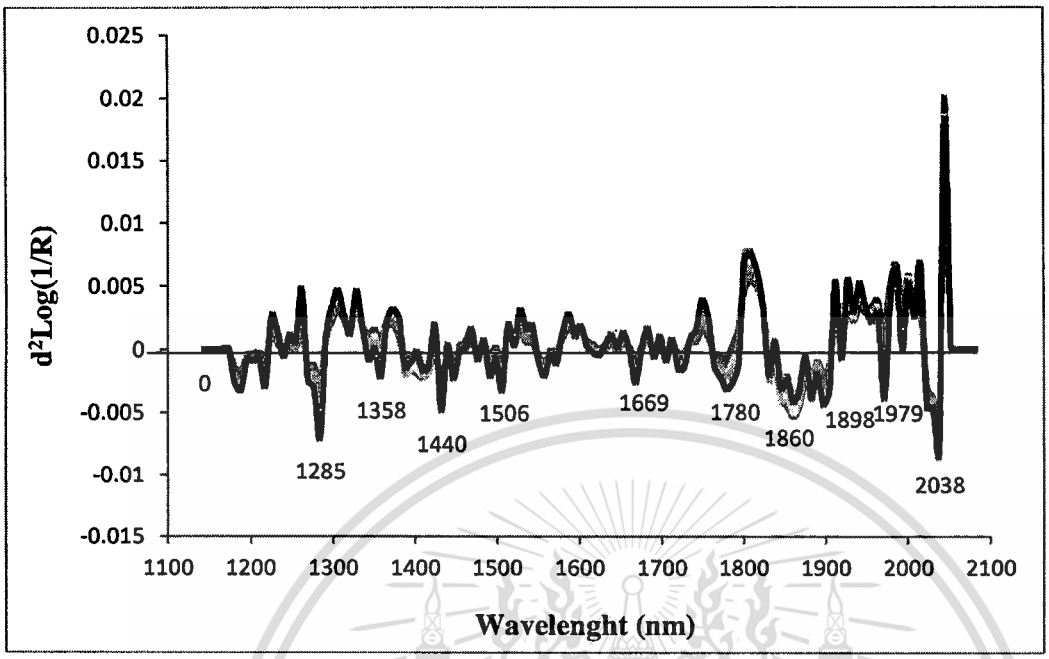

Figure 4: 8 Second derivative (second order polynomial with 5 points) of the raw spectra of the grounded bamboo chips scanned by Micro-NIR spectrometer.

The descriptive statistics for the development of various combustion parameters models of NIR-Gun and Micro-NIR are shown in Table 4:1 and 4:2, respectively. The model calibration and predicted statistics of NIR-Gun scanning for combustion performance parameters are shown in Table 4:3and 4:5. The models used 13-20 PLS factors for the making various models. The models were unable to predict the values of the test set. The reason may be due to the poor spectra scanning which causes more factors to define the spectra. Another reason may be due to the low variability of the calibration set of samples used for making the model (for combustion index 4.613-2.794E-07, ignition index 11.907-6.994E-03, and burnout index 2.040-1.230E-04).

Similarly, the model validation and predicted statistics of Micro-NIR scanning for combustion performance parameters are shown in Table 4:6and4:8. The models used 13-20 PLS factors like NIR-Gun model, and the models were unable to predict the values of the test set. Although the spectra were run in order unlike NIR-Gun scanning spectra and show the similar characteristics, the spectra show lots of noise which causes more factors to define the spectral characteristics and were limited to predict the unknown samples.

Table 4 : 1 Descriptive statistical for the measurement of combustion performance parameters of grounded bamboo chips for developing NIR-Gun model.

Model	Calibration					Prediction				
	N	Max	Min	Mean	SD	N	Max	Min	Mean	SD
Ignition index	59	11.907E-3	7.07E-03	8.750E-03	1.000E-03	19	11.8E-03	7.140E-03	9.120E-03	1.270E-03
Burnout index	59	2.040E-04	1.220E-04	1.550E-04	1.800E-05	19	2.000E-04	1.250E-04	1.590E-04	1.900E-05
Combustion performance	60	4.613E-07	2.794E-07	3.581E-07	4.059E-08	20	4.569E-07	2.872E-07	3.599E-07	4.465E-08

Table 4:2 Descriptive statistical for the measurement of combustion performance parameters of grounded bamboo chips for developing Micro-NIR model.

Model	Calibration					Prediction				
	N	Max	Min	Mean	SD	N	Max	Min	Mean	SD
Ignition index	**60**	**11.907E-03**	**6.994E-03**	**8.853E-03**	**1.084E-03**	**20**	**11.817E-03**	**7.136E-03**	**9.775E-03**	**1.150E-03**
Burnout index	**60**	**2.040E-04**	**1.23E-04**	**1.550E-04**	**1.900E-05**	**20**	**2.000E-04**	**1.250E-04**	**1.580E-04**	**1.900E-05**
Combustion performance	**60**	**4.613E-07**	**2.794E-07**	**3.560E-07**	**4.160E-08**	**20**	**4.569E-07**	**2.934E-07**	**3.661E-07**	**4.080E-08**

Where, N is number of sample, Max is maximum value, Min is minimum value and SD is standard deviation.

Table 4 : 2 PLS models statistics for the measurement of ignition index of grounded bamboo chips scanned by NIR-Gun spectrometer.

S.No.	Method	*Factors*	Calibration			Prediction		
			R_c^2	SECV	BIAS	R_p^2	SEP	BIAS
1	Raw	20	0.940	4.609E-04	2.011E-06	NA	1.500E-03	-1.429E-03
2	S-G (5 points)	20	0.837	6.100E-04	2.870E-06	NA	1.592E-03	-1.900E-03
3	1st Derivative (5 points)	19	0.834	6.200E-04	8.622E-07	NA	1.600E-03	-1.800E-03
4	2nd Derivative (5 points)	20	0.950	4.518E-04	1.054E-05	NA	1.600E-03	-1.100E-03
5	Mean normalization	20	0.932	5.000E-04	7.925E-06		1.600E-03	-2.100E-03
6	Maximum normalization	20	0.943	4.790E-04	-4.625E-06	NA	1.300E-03	-1.500E-03
7	Range normalization	18	0.889	4.841E-04	-1.321E-05	NA	1.100E-03	-1.300E-03
8	Baseline offset	20	0.936	4.838E-04	4.544E-06	NA	1.400E-03	-1.600E-03
9	Linear baseline offset	20	0.946	4.767E-04	1.495E-05	NA	1.300E-03	-7.000E-04
10	SNV	20	0.901	4.934E-04	6.103E-06	NA	1.200E-03	-1.300E-03
11	Detrending	20	0.962	4.251E-04	1.234E-05	NA	1.400E-03	-8.000E-04
12	SNV +Detrending	18	0.877	5.176E-04	2.607E-06	NA	1.100E-03	-9.000E-04
13	MSC	20	0.940	4.609E-04	2.011E-06	NA	1.453E-03	-1.429E-03

Table 4 : 3 PLS models statistics for the measurement of burnout index of grounded bamboo chips scanned by NIR-Gun spectrometer.

S.No.	Method	Factors	Calibration			Prediction		
			R_c^2	SECV	BIAS	R_p^2	SEP	BIAS
1	Raw	20	0.940	8.325E-06	1.704E-07	NA	2.804E-05	-1.949E-05
2	S-G (5 points)	20	0.855	1.051E-05	1.465E-07	NA	3.228E-05	-3.529E-05
3	1st Derivative (5 points)	19	0.821	1.149E-05	1.562E-07	NA	3.083E-05	-3.931E-05
4	2nd Derivative (5 points)	20	0.956	7.788E-06	2.854E-07	NA	3.035E-05	-2.324E-05
5	Mean normalization	20	0.934	9.135E-06	9.486E-06	NA	2.195E-05	-2.423E-05
6	Maximum normalization	20	0.929	8.898E-06	3.850E-07	NA	1.625E-05	-1.737E-05
7	Range normalization	19	0.875	1.039E-05	-6.870E-08	NA	2.159E-05	-1.454E-05
8	Baseline offset	20	0.934	8.864E-07	1.931E-07	NA	2.336E-05	-2.036E-05
9	Linear baseline offset	19	0.934	8.889E-06	1.410E-07	NA	2.299E-05	-1.776E-05
10	SNV	18	0.846	1.090E-05	7.503E-08	NA	2.037E-05	-1.039E-05
11	Detrending	20	0.960	7.503E-06	2.540E-07	NA	2.425E-05	-1.914E-05
12	SNV +Detrending	18	0.851	1.069E-05	8.879E-08	NA	2.037E-05	-1.039E-05
13	MSC	20	0.940	8.254E-06	1.704E-07	NA	2.804E-05	-1.949E-06

Table 4 : 4 PLS models statistics for the measurement of combustion index of grounded bamboo chips scanned by NIR-Gun spectrometer.

S.No.	Method	Factors	Calibration			Prediction		
			R_c^2	SECV	BIAS	R_p^2	SEP	BIAS
1	Raw	20	0.922	2.048E-08	5.214E-10	NA	1.284E-07	-4.793E-08
2	S-G (5 points)	20	0.836	2.562E-08	5.827E-10	NA	1.602E-07	-5.339E-08
3	1st Derivative (5 points)	16	0.699	2.967E-08	3.715E-10	NA	2.191E-07	-7.498E-08
4	2nd Derivative (5 points)	20	0.943	1.944E-08	6.636E-10	NA	2.191E-12	-7.498E-08
5	Mean normalization	20	0.920	2.083E-08	6.949E-10	NA	1.802E-07	-6.212E-08
6	Maximum normalization	20	0.932	1.844E-08	6.223E-10	NA	4.170E-08	-7.605E-08
7	Range normalization	20	0.896	1.983E-08	1.018E-10	NA	4.393E-08	-7.907E-08
8	Baseline offset	20	0.920	2.133E-08	5.668E-10	NA	4.833E-08	-8.781E-08
9	Linear baseline offset	20	0.947	2.248E-08	8.966E-10	NA	1.768E-07	-2.555E-08
10	SNV	16	0.769	2.943E-08	5.877E-11	NA	5.916E-08	-4.629E-08
11	Detrending	20	0.935	2.076E-08	4.705E-10	NA	1.741E-07	-2.883E-08
12	SNV +Detrending	13	0.716	2.913E-08	4.180E-10	NA	5.267E-08	-3.230E-08
13	MSC	20	0.919	2.103E-08	7.755E-10	NA	9.839E-08	-5.215E-09

Table 4 : 5 PLS models statistics for the measurement of ignition index of grounded bamboo chips scanned by Micro-NIR spectrometer.

S.No.	Method	Factors	Calibration			Prediction		
			R_c^2	SECV	BIAS	R_p^2	SEP	BIAS
1	Raw	17	0.880	0.001	-3.043E-05	NA	1.600E-03	5.923E-05
2	S-G (5 points)	12	0.610	0.001	5.952E-07	NA	1.500E-03	1.823E-05
3	1st Derivative (5 points)	20	0.833	0.001	1.053E-05	NA	1.600E-03	1.408E-04
4	2nd Derivative (5 points)	19	0.909	0.001	-1.715E-06	NA	1.700E-03	-2.414E-04
5	Mean normalization	17	0.883	0.001	4.424E-07	NA	1.600E-03	6.841E-05
6	Maximum normalization	18	0.888	0.001	2.991E-06	NA	1.600E-03	2.345E-05
7	Range normalization	17	0.882	0.001	2.546E-09	NA	1.600E-03	6.545E-05
8	Baseline offset	19	0.900	0.001	2.152E-06	NA	1.700E-03	-1.173E-05
9	Linear baseline offset	18	0.892	0.001	5.187E-06	NA	1.630E-03	-5.783E-06
10	SNV	18	0.895	0.001	3.376E-06	NA	1.700E-03	1.089E-05
11	Detrending	15	0.870	0.001	-5.558E-06	NA	1.500E-03	4.462E-05
12	SNV +Detrending	17	0.887	0.001	1.278E-06	NA	1.600E-03	1.583E-05
13	MSC	18	0.898	0.001	4.060E-06	NA	1.600E-03	-2.642E-06

Table 4 : 6 PLS models statistics for the measurement of burnout index of grounded bamboo chips scanned by Micro-NIR spectrometer

S.No.	*Method*	Factors	Calibration			Prediction		
			R_c^2	SECV	BIAS	R_p^2	SEP	BIAS
1	Raw	19	0.929	9.618E-06	5.470E-08	NA	3.369E-05	7.500E-06
2	S-G (5 points)	20	0.818	1.157E-05	-1.997E-08	NA	2.796E-05	-6.675E-05
3	1st Derivative (5 points)	19	0.854	1.063E-05	5.849E-08	NA	2.826E-05	1.593E-07
4	2nd Derivative (5 points)	13	0.805	1.168E-05	3.696E-08	NA	2.456E-05	-7.635E-06
5.	Mean normalization	19	0.939	9.475E-06	-4.592E-08	NA	3.388E-05	9.259E-06
6	Maximum normalization	14	0.876	1.021E-05	-4.012E-08	NA	2.786E-05	1.884E-06
7	Range normalization	16	0.897	9.981E-06	-1.251E-07	NA	2.975E-05	4.787E-06
8	Baseline offset	16	0.898	9.867E-06	-2.936E-07	NA	3.044E-05	5.798E-06
9	Linear baseline offset	15	0.872	1.055E-05	-2.647E-08	NA	2.750E-05	5.838E-06
10	SNV	18	0.934	9.247E-06	-1.181E-07	NA	2.909E-05	7.304E-06
11	Detrending	15	0.888	1.019E-05	-7.460E-08	NA	2.810E-05	7.293E-06
12	SNV +Detrending	14	0.874	1.042E-05	-6.975E-08	NA	2.909E-05	7.304E-05
13	MSC	15	0.889	1.005E-05	6.229E-08	NA	3.021E-05	6.540E-06

Table 4 : 7 PLS models statistics for the measurement of combustion index of grounded bamboo chips scanned by Micro-NIR spectrometer.

S.No.	Method	Factors	Calibration			Prediction		
			R_c^2	SECV	BIAS	R_P^2	SEP	BIAS
1	Raw	17	0.908	2.227E-08	3.373E-10	NA	4.921E-08	-5.789E-09
2	S-G (5 points)	16	0.729	2.983E-08	-4.765E-11	NA	5.966E-08	-1.465E-08
3	1st Derivative (5 points)	20	0.862	2.486E-08	-1.618E-10	NA	5.077E-08	-3.601E-09
4	2nd Derivative (5 points)	14	0.824	2.637E-08	3.416E-10	NA	4.774E-08	-6.019E-09
5	Mean normalization	20	0.944	2.056E-08	1.016E-10	NA	4.338E-08	-3.145E-09
6	Maximum normalization	18	0.922	2.163E-08	2.045E-10	NA	4.755E-08	-3.613E-09
7	Range normalization	19	0.938	2.085E-08	6.390E-10	NA	4.691E-08	-2.315E-09
8	Baseline offset	20	0.943	2.071E-08	2.885E-10	NA	4.403E-08	-2.574E-09
9	Linear baseline offset	20	0.941	2.132E-08	2.748E-10	NA	4.077E-08	-4.144E-09
10	SNV	19	0.942	2.135E-08	8.163E-11	NA	4.704E-08	2.743E-09
11	Detrending	18	0.934	2.150E-08	3.392E-10	NA	4.167E-08	-5.311E-09
12	SNV +Detrending	19	0.944	2.232E-08	4.245E-10	NA	4.083E-08	1.265E-09
13	MSC	19	0.944	2.105E-08	1.925E-10	NA	4.476E-08	5.387E-10

The major components of lignocellulosic biomass are cellulose, hemicellulose, and lignin. Cellulose is a polysaccharide molecule having both a well-ordered structure and a randomly ordered structure which consists of hundreds of glucose molecules linked by glucosidic linkage, and the glucan chains are usually connected by hydrogen bonds [11,12]. While, hemicellulose is another polysaccharide which is more complicated in structure and has higher linkages than cellulose. Hemicellulose, naturally, is connected with cellulose microfibrils by non-covalent linkages [13], and hemicellulose generally consists of more than one type of monosaccharide unit, including both hexose and pentose. Depending on the variety of biomass, hemicellulose may contain xyloglucan, xylan, glucomannans, galactoglucomannans, etc., however, the detailed structure of hemicellulose is still remains unknown [14]. On the other hand, the structure of lignin is very complicated, and it is made of phenolic polymers that consist of three types of phenylpropane untis: p-coumaryl alcohol, coniferyl alcohol, and sinapyl alcohol [15.16]. Damien Sabatier et al. [3] measure the lignocellulosice compounds of sugarcane biomass by near infrared reflectance spectroscopy (400-2500nm), monochromator spectrometer NIRSystems XDS, inc., using modified PLS regression and obtained the coefficient of determination of prediction of sugarcane hemicellulose, cellulose, lignin 0.45, 0.77, 0.44 and RPD 1.9, 4.2 and 1.9 with factors 14, 13 and 14, respectively, and made a conclusion for the poor prediction of hemicellulose and lignin was that it contain several molecules that causes these parameter to define inadequately. Similarly, carbon and hydrogen were predicted poorly (RPD of internal validation 2.1 and 1.3, respectively) by Jesús Mata Sanchez et al. [17] by using the FT-NIR spectrometer (MPA, Bruker Optics, Ettlingen, Germany). The online prediction of lignocellulose compound of corn stover by Junjie Xue et al. [18] were not found accurate as coefficient of determination of prediction for cellulose, hemicellulose and lignin were 0.77, 0.62 and 0.61 were found by using Matrix-F (Bruker Daltonik GmbH, Bremen German) in diffuse reflection mode. Sanderson et al. [19] were also unable to predicted C, H and O of woody and herbaceous feedstocks with any precision or accuracy by using Pacific Scientific Model 6250 scanning monochromator, near infrared reflectance spectrometer, over the range 1100-2500 nm, and concluded that small population size (SD 0.22, 0.3, 2.08 respectively) may have contributed to some of the inaccuracy and imprecision in NIRS prediction.

4.4.2. *Measurement of combustion performance parameters by Fourier transform near infrared instrument (FT-NIR)*

The raw spectrum of the grounded bamboo samples scanned by FT-NIR is shown in Figure 4.9. The absorbance shows the wide range of absorbance over the region 8770-8020 cm^{-1} (1140-1247 nm) but with low absorbance intensity which is normally associated with the second overtone of C—H stretch, carbonyl compounds [8]. The important region of absorption are: 7240-6560 cm^{-1}, 4480-4200 cm^{-1} (1381-1524 nm and 2232-2380 nm, respectively, combination region of C—H band) [1]; 5284-5103 cm^{-1} (1893-1960 nm, first overtone O—H band assign as O—H stretch/O—H deformation combination hydroxyl) [8]; 4980-4640 cm^{-1} (2008-2155 nm, first overtone O—H band C—O, O—H stretching combination, primary alcohol) [8]; 4140-3922 cm^{-1} (2415-2550 nm, second overtone of C—H band, C—H bending) [8].

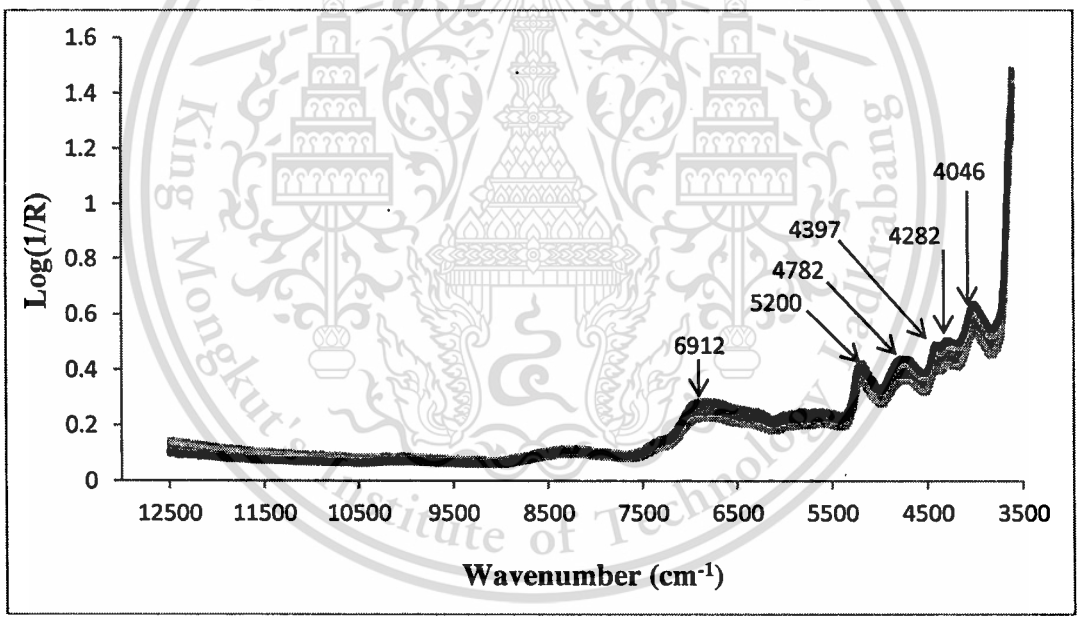

Figure 4: 9 Raw spectra of the grounded bamboo chips samples scanned by FT-NIR spectrometer.

The absorbance shows the peaks at around 6912 cm^{-1} (1447 nm, 2×C—H str. + C—H def., aromatic)[28], 5200 cm^{-1} (1923 nm, O—H str. and HOH deformation bending, O—H molecular water)[7], 4782 cm^{-1} (2091 nm, O—H combination, polymeric .OH), 4397 cm^{-1} (2274 nm, O—H str.+C-C str., starch)[28], 4282 cm^{-1} (2335 nm, C—H str.+C—H def., cellulose)[7], 4046 cm^{-1} (2471 nm, C—H combination, lipids,

aliphatic compounds) [7]. The absorbance is dominated by the C—H bands. The scanning of the FT-NIR seems clearly better than diode array spectrometer NIR-instrument. This is, generally, due to the high signal to noise ratio of FT-NIR spectrometer. However, the FT-NIR spectroscopy was also unable to predict the combustion index with any accuracy, but was able to predict the ignition index and burnout index with lower accuracy.

The total number of the sample used for making the model was 80. The descriptive statistics for the development of combustion parameter models are tabulated under Table 4.9. The various combustion parameter models were developed separately using the same spectra. Various pretreatments were performed on the raw spectra. Min-Max normalization was found to be the effective treatment for the calibration of ignition index, whereas multiplicative scattering correction was found effective for calibration of burnout index. The PLS statistics of the ignition index and burnout index are shown in Table 4.10.

Table 4: 8 The descriptive statistics for the development of combustion performance parameter for FT-NIR models.

Model	Calibration					Prediction				
	N	*Max*	Min	Mean	SD	N	Max	Min	Mean	SD
Ignition index	48	11.908E-03	6.994E-03	8.815E-03	1.041E-03	32	11.817E-03	7.073E-03	8.861E-03	1.186E-03
Burnout index	56	2.040E-04	1.220E-04	1.560E-04	1.800E-05	24	2.000E-04	1.230E-04	1.560E-04	1.900E-05
Combustion performance	56	4.613E-07	2.294E-07	3.5991E-07	3.904E-08	32	4.569E-07	2.811E-07	3.564E-07	4.519E-08

where, N is number of sample, Max is maximum value, Min is minimum value and SD is standard deviation.

Table 4 : 9 PLS statistics of the optimum model of the grounded bamboo chips scanned by FT-NIR spectrometer.

Model	Treatment	Factors	Calibration		Validation			
			R_c^2	RMSEE	R_p^2	RMSEP	Bias	RPD
Ignition index	Min-Max normalization	4	0.297	8.920E-04	0.432	8.870E-3	3.960E-05	1.33
Burnout index	MSC	7	0.683	1.060E-05	0.513	1.380E-05	-2.210E-07	1.43

The R_p^2, bias and RPD of optimum model of ignition index are 0.432, 3.960E-05, and 1.33, with the number of PLS factors of the model 4. The coefficient of determination for prediction set was found higher than calibration set. This may be due to the closeness of the prediction data set to calibration model data set, since the ratio of sample used for prediction and calibration is 1:1.5. The scatter plot of the model is shown in Figure 4.10. The regression coefficient plot and X-loading of first three PLS-factors of ignition index is shown in Figure 4.11 and 4.12, respectively. The most important regions found for the calibration of ignition index were 12007-10036 cm^{-1} (833-996 nm, third overtone of C—H str.) [7], 8706-7876 cm^{-1} (1149-1270 nm, second overtone, C—H str.) [7] and 5404-4575 cm^{-1} (1851-2186 nm, third overtone, C—H bend) [7].

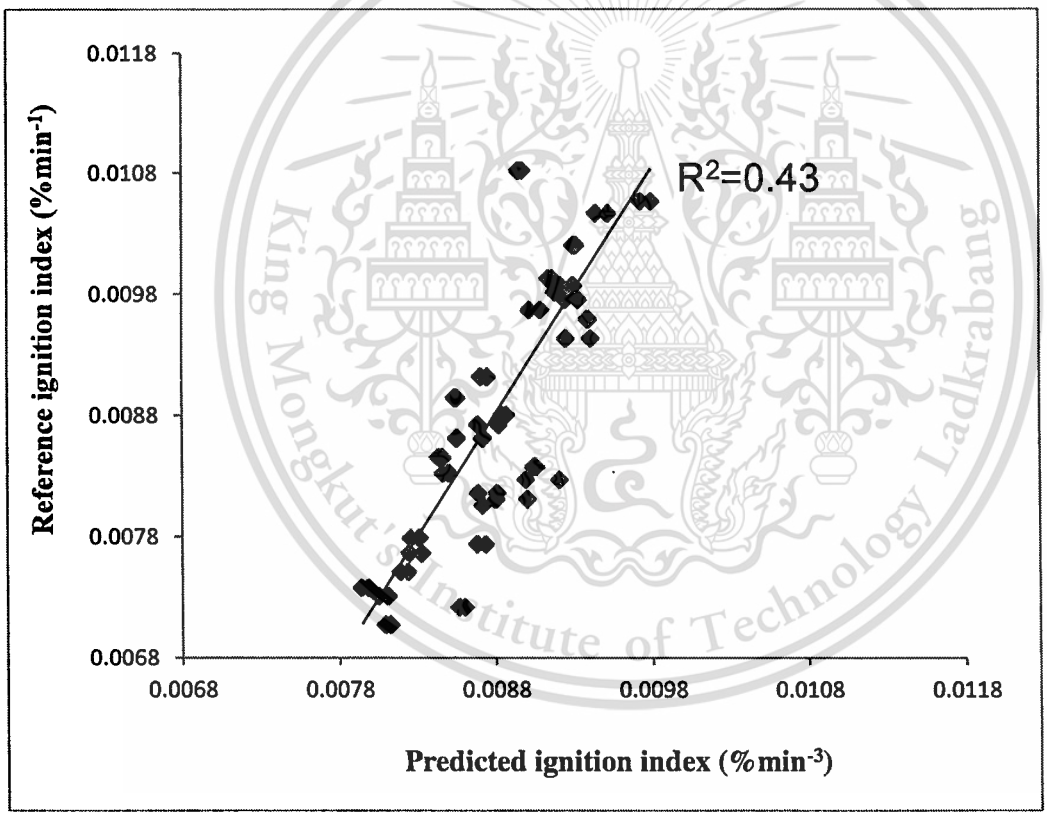

Figure 4: 10 Comparison of ignition index of grounded bamboo chips as predicted by FT-NIR spectroscopy and measured by reference test.

In the regression coefficient plot, several minor peaks are observed in the region 12007-10036 cm^{-1} and 8706-7876 cm^{-1}, while clear sharp peaks are seen in the region 5404-4575 cm^{-1} with independent peaks at around 5404 cm^{-1} (1850 nm, 2×O—H def. + C—O def., starch) [28], 5254 cm^{-1} (1903 nm), 5038 cm^{-1} (1985 nm) and 4879 cm^{-1} (2050 nm). Similarly, in X-loading plot, the most influential region 12007-10036 cm^{-1}, 8706-7876 cm^{-1}, and 5404-4575 cm^{-1}. The most important peaks for factor-1 are 5404 cm^{-1} (1850 nm), 5149 cm^{-1} (1942 nm, O—H str.+O—H def., water) [28], 4694 cm^{-1} (2130 nm); factor-2 are 5404 cm^{-1} (1850 nm), 5257 cm^{-1} (1902 nm), 5022 cm^{-1} (1991 nm), 4732 cm^{-1} (2113 nm); factor-3 are 5404 cm^{-1}(1850 nm), 5350 cm^{-1} (1869 nm), 5254 cm^{-1} (1903 nm), 5072 cm-1, 4856 cm^{-1} (2059 nm), 4674 cm^{-1}(2139 nm). The most important peaks seen in regression coefficient and X-loading and the corresponded vibration bonds are tabulated under Table 4.11.

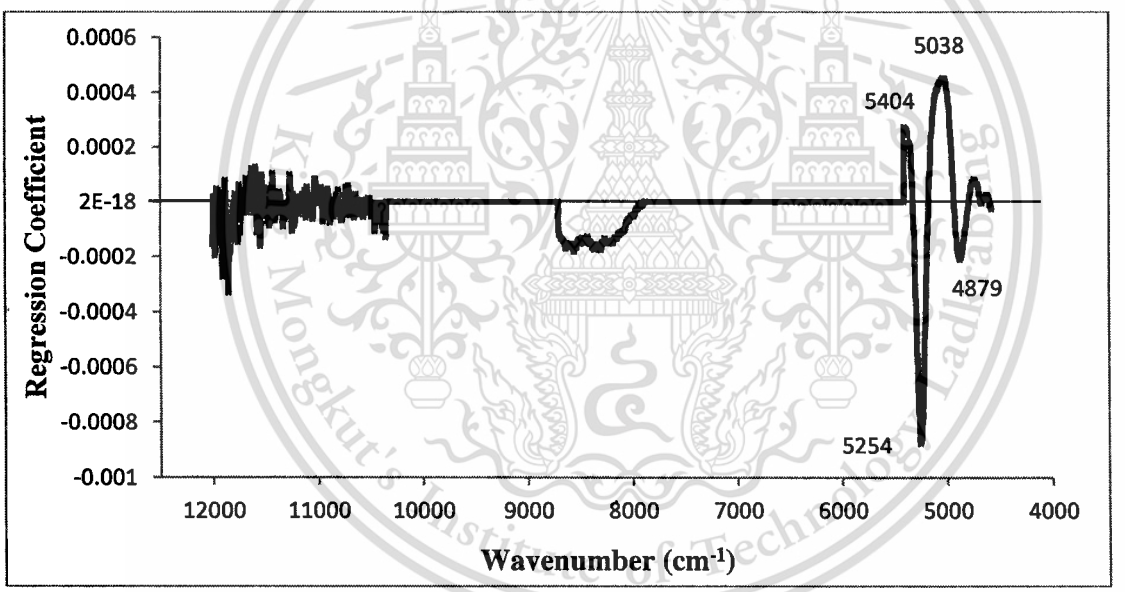

Figure 4: 11 Regression coefficient plot of optimum model of ignition index developed from the spectra of grounded bamboo chips scanned by FT-NIR spectrometer.

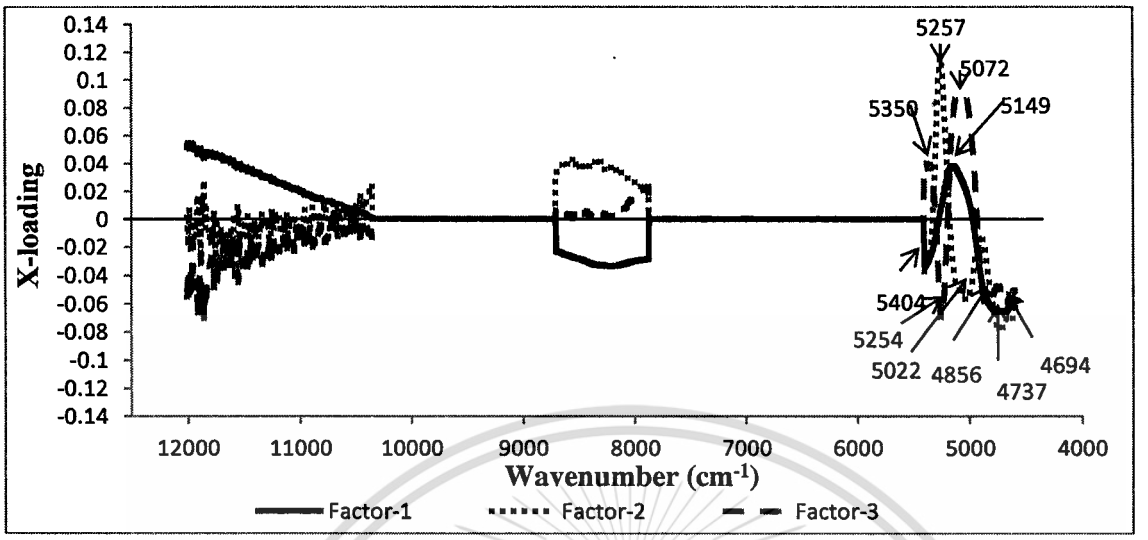

Figure 4: 12 First 3 X-loading plot of optimum model of ignition index developed from the spectra of grounded bamboo chips scanned by FT-NIR spectrometer.

The R_p^2, bias and RPD of optimum model of burnout index are 0.513, -2.210E-07, and 1.43, with the number of PLS factors of the model 7. The scatter plot of the model is shown in Figure 4.13. The most important regions found for the calibration of ignition index were 12003-8697cm^{-1} (833-1149 nm) and 7876-4574 cm^{-1}(1270-2186 nm). The region 12003-8697cm^{-1} is normally associated with the second and third overtone of hydrocarbon, and aromatic amines [1].

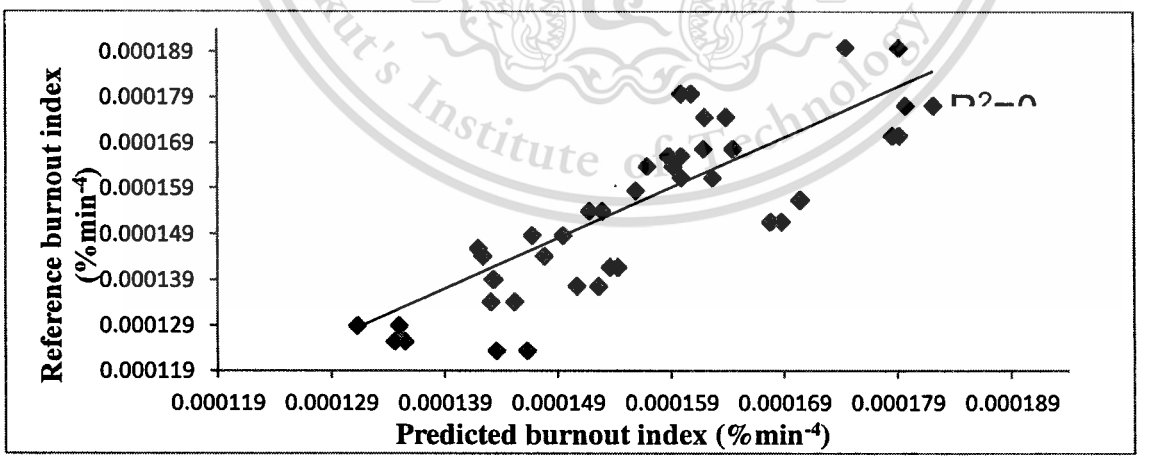

Figure 4: 13 Comparison of burnout index of grounded bamboo chips as predicted by FT-NIR spectroscopy and measured by reference test.

The regression coefficient plot and first 3 X-loading of first three PLS-factors of burnout index is shown in Figure 4.14 and 4.15, respectively. In the regression coefficient plot of burnout index, several narrow peaks are observed in the region 12003-8697 cm^{-1} (833-1149 nm), and the peaks in the region 7876-4574 cm^{-1}(1270-2186 nm) are little broad but with the shoulder peaks. The dominating peaks of X-loading of Factor-1 are 10055 cm^{-1} (995 nm), 8697 cm^{-1} (1150 nm); Factor-2 are 5157 cm^{-1}(1939 nm), 4687 cm^{-1} (2134 nm); Factor-3 are 7047 cm^{-1} (1419 nm), 5253 cm^{-1} (1904 nm). Factor-1 shows the effect of 12003-8697cm^{-1} on the model while factor-2 and factor-3 shows the effect of 7876-4574 cm^{-1} (1270-2186 nm). The most important peaks seen in regression coefficient and X-loading and the corresponded vibration bonds are tabulated in Table 4:11 The regression plot and the X-loading plot are affected mainly by the hydrocarbon (10753, 6120, 6110; 5925, 5900, 5675 cm^{-1}) and aromatic amines (6916, 6791, 6656 cm^{-1}).

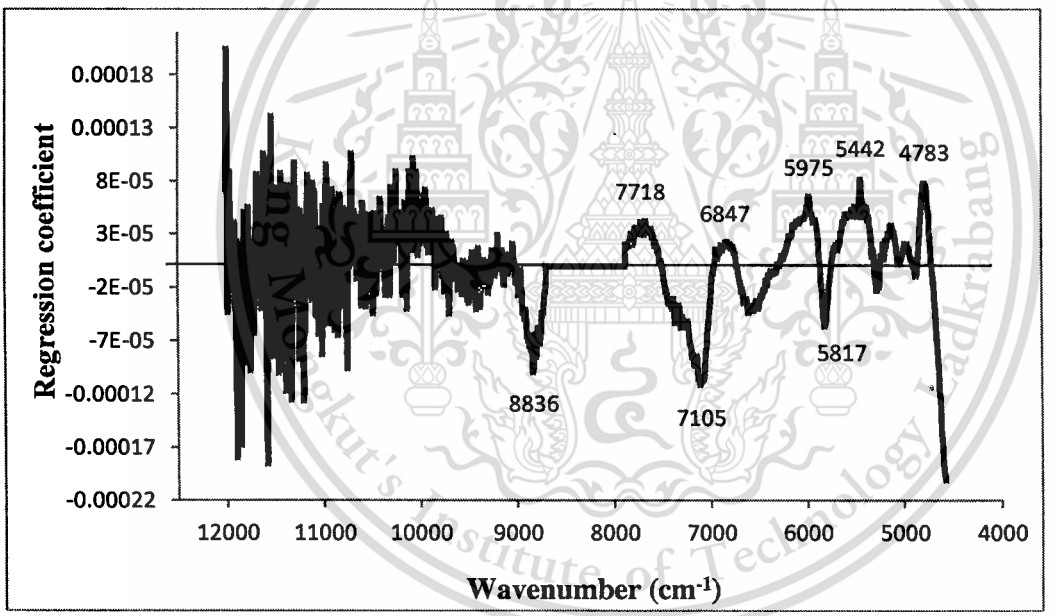

Figure 4: 14 Regression coefficient plot of optimum model of burnout index developed from the spectra of grounded bamboo chips scanned by FT-NIR spectrometer.

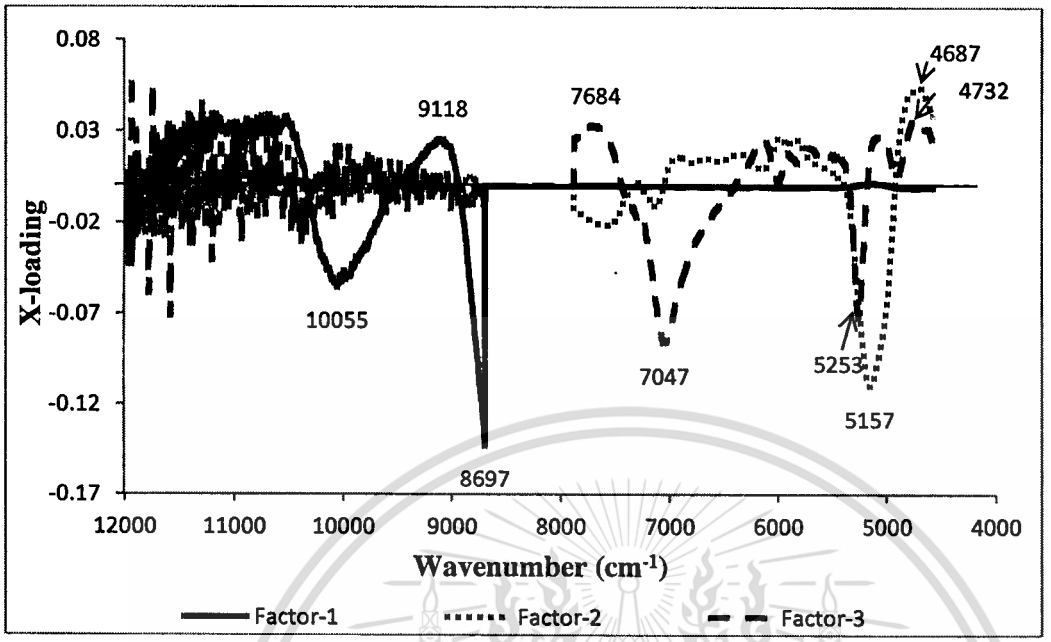

Figure 4: 15 Regression coefficient plot of optimum model of burnout index developed from the spectra of grounded bamboo chips scanned by FT-NIR spectrometer.

Table 4 : 10 The dominant peaks on regression coefficient plot and X-loading plot of ignition index and burnout index of FT-NIR model.

PEAK Wavenumber (cm^{-1})	Wavelength (nm)	Nearest wavelength (nm)	Spectral structure	Material type	Source
10055	995	996	O—H(3U) (—CH_2—OH), primary alcohol	Primary alcohol	[16]
8836	1132				
8697	1150	1152	C—H str. second overtone	CH_3	[28]
7718	1296				
7105	1407	1410	O—H str. first overtone	ROH	[28]
7047	1419	1420	O—H(2U), .O—H	Hydrocarbon,	[16]

				aromatic	
6847	1460	1460	N—H str. first overtone	$CONH_2$	[28]
5975	1674	1671	CHU + CHU (12 + 1), benzene band assignment	C—H aryl	[16]
5817	1719	1725	C—H str. first overtone	CH_2	[28]
5442	1838				
5404	1850	1860	C—CL(7U), .C—CL	Chlorinated hydrocarbons	[16]
5350	1869				
5257, 5254, 5253	1902, 1903, 1904	1900	O—H str.+ 2×C—H str.	Starch	[28]
5157, 5149	1939, 1942	1940	O—H str.+ O—H def.	Water	[28]
5038	1985	1980	N—H(UN—H and Δ N—H combination), primary aromatic amine in CCL_4 as para-NH_2 grouping	Aromatic amine	[16]
5022	1991	1990	N—H for primary amides	Urea	[16]
4879	2050	2050	N—H asym. str. + amide II	protein	[28]
4856	2059	2060	N—H (3Δ) and N—H stretching combination	Amides/protei n	[16]
4783	2091	2090	O—H combination	Polymeric .OH	[16]
4732	2113	2110	N—H sym. str. + amide II	$CONH_2$, CONHR	[28]
4694, 4687	2130, 2134	2132	N—H str. + C═O str.	Ammino acid	[28]
4674	2139	2140	═C—H str. + C═C str.	HC═CH	[28]

4.5. Conclusion

The diode array NIR-instruments were unable to predict the combustion performance parameter of the grounded bamboo chips with any accuracy. All the models of combustion performance parameter used 13-20 PLS factors for the making the model. The models were unable to predict the values of the test set. The spectra were suffered from the noise, and the variability of the calibration set samples used for making the models (for combustion index $4.613\text{-}2.794\times10^{-7}$, ignition index 0.011907-0.006994, burnout index $2.04\text{-}1.23\times10^{-4}$) were low. This may be the reason why the diode array NIR-instrument failed to predict. On the other hand, the FT-NIR was able to predict the ignition index and burnout index with very low accuracy.

However, the model of mine was unable to predict the combustion performance parameter of the bamboo with good accuracy due to low variability of data. So, for the one who want to do research on biomass we would like to suggest to increase the population size of the samples by collecting the different species of same or different biomass, so that the data contains large range and makes the model robust by providing sufficient information while making the model. In addition, we would also like suggest using the whole range of NIR region while making the model.

4.6. References

[1.] Workman J. and Weyer L. Jr. (2008). Practical guide to interpretive Near-Infrared Spectroscopy. Boca Raton: CRC press.

[2] Sirisomboon P., Kaewkuptong A. and Williams P. "Feasibility study on the evaluation of the dry rubber content of field and concentrated latex of Para rubber by diffuse reflectance near infrared spectroscopy.", J. Near Infrared Spectros., vol. 21, 2013. Pp. 81–88.

[3] Sabatier D., Thuries L., Bastianelli D. and Dardenne P. "Rapid prediction of the lignocellulosic compounds of sugarcane biomass by near infrared reflectance spectroscopy: comparing classical and independent cross-validation.", J. Near Infrared Spec., vol. 20, 2012. Pp. 371-385.

[4] He C., Chen L., Yang Z., Hang G., Liao N. and Han L. "A rapid and accurate method for on-line measurement of straw-coal blends using near infrared spectroscopy.", Bioresource

Technol., vol. 110, 2012. Pp. 314-320.

[5] Huang C., Han L., Yang Z., Liu X. "Ultimate analysis and heating value prediction of straw by near infrared spectroscopy.", Waste Manage., vol. 29, 2009. Pp. 1793-1797.

[6] Everard C. D., McDonnell K. P. and Fagan C. C. "Prediction of biomass gross calorific values using visible and near infrared spectroscopy.", Biomass Bioenergy., vol. 45, 2012. Pp. 203-211.

[7] Osborne B.G., Fearn T. and Hindle P.H. 1993. Practical NIR spectroscopy with applications in food and beverage analysis. 2nd ed. UK : Longman Science & Technical.

[8] Murray I. and Williams P. C. 1987. Chemical principles of near-infrared technology. In: William P. and Norris K. eds. Near infrared technology in the agricultural and food industry. Minnesota: American Association of Cereal Chemists, pp. 17-34.

[9] Cozzolino D., Esler M. B., Dambergs R. G., Cynkar W. U., Boehm D. R., Francis I. L. and Gishen M. "Prediction of colour and pH in grapes using a diode array spectrophotometer (400–1100 nm).", J. Near Infrared Spectros., vol. 12, 2004. Pp. 105–111.

[10] Murray I. 1986. The NIR spectra of homologous series of organic compounds. In: Hollo J., Kaffa K.L. and Gonczy J.L. eds. NIR/NIT Conference. Budapest, Akademiai Kiado, pp. 13-28.

[11] Gutierrez A., del Rio J. C. and Martinez A. T. "Microbial and enzymatic control of pitch in the pulp and paper industry.", Appl. Microbiol. Biotechnol., vol. 82, 2009. Pp. 1005–1018.

[12] Kraessig H. A. (1993), Cellulose: Structure, Accessibility and Reactivity, Amsterdam: Gordon & Breach Science Publishers.

[13] Somerville C., Bauer S., Brininstool G., Facette M., Hamann T. and Milne J. "Toward a systems approach to understanding plant cell walls.", Science, vol. 306, 2004. Pp. 2206–2211.

[14] Kacurakova M., Capek P., Sasinkova V., Wellner N. and Ebringerova A. "FT-IR study of plant cell wall model compounds: pectic polysaccharides and hemicelluloses.", Carbohydr. Polym., vol.43, 2000. Pp. 195–203.

[15] Whetten R, MacKay J, and Sederoff R. "Recent advances in understanding lignin biosynthesis.", Annu. Rev. Plant Biol., vol. 49, 1998. Pp. 585–609.

[16] Eriksson T, Borjesson J, and Tjerneld F. "Mechanism of surfactant effect in enzymatic hydrolysis of lignocellulose.", Enzyme Microb. Technol., vol. 31, 2002. Pp. 353–64.

[17] Sáncheza J. M., Jiménez J. A. P., Villanueva M. J. D., Serrano A., Núñez N. and Giménez J. L. "Assessment of near infrared spectroscopy for energetic characterization of olive by products.", Renew. Energ., vol. 74, 2015. Pp. 599-605.

[18] Xue J., Yang Z., Han L., Liu Y. and Liu Y. and Zhou C. "On-line measurement of proximates and lignocellulose components of corn stover using NIRS.", Appl. Energ., vol. 137, 2015. Pp. 18–25.

[19] Sanderson M. A., Agblevor F., Collins M. and Johnson D. K. "Compositional analysis of biomass feedstocks by near infrared reflectance spectroscopy.", Biomass Bioenerg., vol. 11, 1996. Pp. 365–370.

CHAPTER 5

NONDESTRUCTIVE EVALUATION OF KINETICS PARAMETERS OF BAMBOO USING NEAR INFRARED SPECTROSCOPY

5.1. Abstract

NIR spectroscopy analysis was used to evaluate of kinetic parameters of bamboo including activation energy (E_a), pre-exponential factor (A) and order of reaction (n) of milled bamboo. Kinetic parameter was calculated using Coats- Redfern method. The thermal degradation data was measured by a thermogravimetric analyzer and collected from differential thermogravimetric (DTG) curve. PLS regression was used to optimize the models. The results gave the E_a in range of 57-105.90 kJ/mol. The inner relationship between E_a and A at n=1was exponential, they gave relatively equation of $A = 63252e^{0.2198E_a}$ and provided coefficient of determination of 0.990. The PLS model gave coefficient of determination of validation set (R^2_{val}) of 0.890, root mean square error of prediction of 4.37 kJ/mol, bias of 0.19 kJ/mol and RPD of 3.02. The goal point of this studies was the first time but it need to improve to be the global model. The result indicated that PLS model for prediction E_a was good, and could be used with caution for most application.

***Keywords**: Milled Bamboo, kinetic parameters, Renewable energy, Thermal degradation.*

5.2. Introduction

The pyrolysis of biomass presents a complexed process because of overlapping reaction, so kinetic parameter of its reaction depend on the biomass composition i.e. hemicellulose, cellulose and lignin composition ; and thermal condition i.e. heating rate, temperature, particle size[1]. Understanding the thermal degradation and pyrolytic-cracking mechanism of biomass is necessary. Kinetic parameters of reaction are important to design, establish efficient [2,3] that kinetic parameter that activation energy helped to find out the minimum amount of energy need to initial a chemical change, pre-exponential factor and order of reaction helped to calculate the reaction rate. Due to biomass has different element composition on different age, planting area, storage method and so on. These reasons lead to different kinetic parameter i.e the activation energy (E_a), pre-exponential

factor (A) and order of reaction (n) can be determined [4]. These reason can lead to different kinetic parameters even if the same species.

Generally, kinetic analysis of biomass can be conducted using differential thermogravimetric (DTG) measured with a thermogravimetric analyzer [5] Kinetic parameters is calculated using conventional differential or integral methods, i.e. Coats- Redfern method, Kissinger, Flynn-Wall and Ozawa, Vyazovkin and AIC, and Kissinger-Akahira-Sonuse. These calculations are the complicating method. Detail analysis for kinetic parameter of biomass is complicated calculation, expensive and time consuming. Thus, rapid method of analysis should be presented to solve. Then NIR spectroscopy should be requested. Previous studies have trended to concentrate on biomass composition such as compositional analysis of biomass [6], lignocellulosic component of corn stover [7] and so on. But there have no report on kinetic parameters. The goal of this work was to evaluate kinetic parameters of biomass using NIR spectroscopy when kinetic parameters were calculated using Coats- Redfern method [8].

5.3. Materials and methods

5.3.1. Sample

The samples of bamboo, *Dendrocalamus sericeus* cl. Phamon, in this study were of different circumference sizes of culms obtained from the Uttaradit province, Thailand. A total of 80 samples in 12 ranges of culm circumference (16-18, 18-20, 20-22, 22-24, 24-26, 26-28, 28-30, 30-32, 32-34, 34-36, 36-38 and 38-40 cm) were randomly cut of 10 cm above the ground. The each sample was chopped by the chopping machine (P5508, Patipong, Thailand). After that, the sample were dried under the sun until the moisture reached around 5%wb, milled pass through the sieve diameter of 3 mm (60201, QC, UK) and kept in the aluminum bag before experiment.

5.3.2. NIR spectroscopy modeling

The milled sample was scanned using the software program of OPUS version 7.0.129, Bruker Optik GmbH, Germany. The spectrums were recorded using diffuse reflectance mode by log1/R, when R is diffuse reflectance radiation of sample. Models were optimized using partial least squares (PLS) regression with calibration set of 80% from total sample and validation set of 20%

from total sample. Then, performance of models i.e. coefficient of determination (R^2), root mean square error of prediction (RMSEP), bias, and ratio of standard error of prediction to standard deviation (RPD) were determined.

5.3.3. Reference analysis

Kinetic parameters were caculated using Coats- Redfern method, which measured with a thermogravimetric analyzer (TG 209 F3 Tarsus, Netzsch, Germany, 0.1 µg resolution; 6.8 mm diameter aluminum oxide (AL_2O_3) crucible). A 6 mg samples were heated from 32 °C to 700 °C at heating rate of 10°C/min. To complete pyrolysis condition, N_2 was used. The volume flow of N_2 was set up to 20 ml/min, and 10 ml/min for the protective gas. Then, TG/DTG was obtained. After that, these data were used for calculated. All samples were carried on by one time. After that, took out of 10 samples for duplication.

5.4. Determination procedure of kinetic parameter.

In this study, Coats- Redfern method was used to calculate [8]. Thermogravimetric data was used for determination of kinetic parameter using fundamental of Arrhenius equation which was explained by [9] where

$$K(t) = Aexp\left[\frac{-E}{RT}\right] \quad (1)$$

$$\frac{d\alpha}{dt} = Ae^{-\frac{E}{RT}}(1-\alpha)^n \quad (2)$$

Where A is the frequency or pre-exponential factor, E is the activation energy of the reaction, R is the universal gas constant, T is the absolute temperature, n is the order of reaction, t is the time, and α is the fraction of reactant decomposed at time t (min).

And α was obtained from mass lost in the sample which can be obtained by the following equation:

$$\alpha = \frac{W_0 - W}{W_0 - W_f} \quad (3)$$

where w_0, w, and w_f refer to initial, instantaneous and final masses respectively.

For non-isothermal TGA experiments at linear heating rate [10] $= \frac{dT}{dt}$, equation (2) can be written as:

$$\frac{d\alpha}{dT} = \frac{A}{\beta} e^{-\frac{E}{RT}} (1-\alpha)^n \quad (4)$$

This equation expresses the fraction of material consumed in the time. In this work the activation energy was obtained from non-isothermal TGA. The methods used to calculate kinetic parameters are called model-free non-isothermal methods and required a set of experimental tests at different heating rates.

In this study, Coats- Redfern method will be used for determination of kinetic parameter. Equation (4) was integrated and expressed as [11]:

$$\int_0^{\alpha} \frac{d\alpha}{(1-\alpha)^n} = \int_{T_0}^{T} \frac{A}{\beta} \exp\left(-\frac{E}{RT}\right) \quad (5)$$

Integrating both sides followed by taking the logarithm of the obtained equation leads to:

$$ln\left[-\frac{\ln(1-\alpha)}{T^2}\right] = ln\left[\frac{AR}{\beta E}\left(1-\frac{2RT}{E}\right)\right] - \frac{E}{RT} \text{ for } n = 1 \quad (6)$$

and,

$$ln\left[\frac{1-(1-\alpha)^{1-n}}{T^2(1-n)}\right] = ln\left[\frac{AR}{\beta E}\left(1-\frac{2RT}{E}\right)\right] - \frac{E}{RT} \text{ for } n \neq 1 \quad (7)$$

Due to 2RT=E«1, simplifying Equation (8) and (9) gives:

$$ln\left[-\frac{\ln(1-\alpha)}{T^2}\right] = ln\left[\frac{AR}{\beta E} - \frac{E}{RT}\right] \text{ for } n = 1 \quad (8)$$

And

$$ln\left[\frac{1-(1-\alpha)^{1-n}}{T^2(1-n)}\right] = ln\left[\frac{AR}{\beta E} - \frac{E}{RT}\right] \text{ for } n \neq 1 \quad (9)$$

Thus, a plot of $\ln[-\ln(1-\alpha)/T^2)$ against 1/T when n=1 or $\ln[1-(1-\alpha)^{1-n}/(T^2(1-n))]$ versus 1/T when $n \neq 1$ should be a straight line with slope (-E/R) and intercept ($\ln AR/\beta E$) for the correct value of *n*. The kinetic parameters were determined by combining iterative and the least squares method.

5.5. Results and discussion

Fig. 5:1 display typical TGA diagram of milled bamboo in a nitrogen atmosphere. An active pyrolysis zone occurred temperature in range of 180-420 °C. Dehydration zone was temperature in range of 32-180 °C, and Passive pyrolysis zone was temperature in range of 420-700 °C. **Table 5:1** shows the kinetic parameter of milled bamboo for different culm size, and at heating rate of 10 °C/min. Kinetic parameters at active pyrolysis zone were determined using corresponding peaks on the DTG curve of each sample. The results gave the E_a in range of 57-105.90 kJ/mol, mean of 87.02 kJ/mol and SD of 11.425 kJ/mol. **Fig. 5:2.** shows scatters plots between E_a and A factor at n=1. The relationships presented exponential curve, that was $A = 63252e^{0.220E_a}$, when A is pre-exponential factor (1/min) and E_a is activation energy (kJ/mol). Its correlation gave coefficient of determination of 0.990.

Table 5:2 presented PLS calibration results for prediction activation energy of milled bamboo. The PLS model developed using wavenumber region of 9403.8-7498.3 and 6102-4597.7 cm^{-1}, pretreatments of vector normalization (SNV), and PLS factor of 7 gave a best performance with R^2_{val} of 0.890, RMSEP of 4.37 kJ/mol, bias of 0.19 kJ/mol and RPD of 3.02. R^2 and RPD have been recommended by [12], a value between 0.83-0.90 could be used with caution for most application, RPD between 3.1-4.9 correspond to fair and cloud be used for screening.

Scatter plots between measured values versus predicted value for prediction of activation energy was shown in **Fig. 5:3a** . X-loading plots for E_a were shown in **Fig 5:3b**. As seen in **Fig 5:3b** , explicit peaks were at 5238 cm^{-1} (1909 nm), its wavenumber corresponded to O-H stretching first overtone of POH[13]; and 5219 cm^{-1} (1916 nm) which related to C=O stretching second overtone of CONH [13].

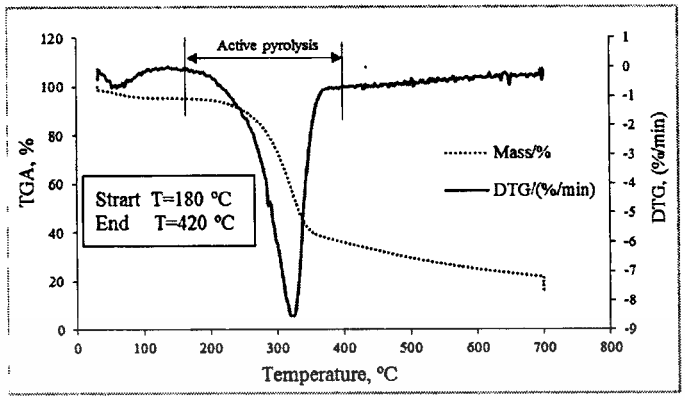

Figure 5 : 1 Typical TGA diagram of milled bamboo in a nitrogen atmosphere.

Table 5 : 1 Statistics of Ea of bamboo chips.

Data set	Maximum	Minimum	Mean	Range	SD
Total set	105.90	57.00	87.02	48.90	11.425
Calibration set	105.90	57.00	87.59	48.90	10.853
Validation set	105.64	59.77	84.71	45.87	13.624

Table 5 : 2 PLS calibration results for predicting activation energy of milled bamboo

Parameters	Wavelength region (cm^{-1})	Pretreatments	F	Calibration		Validation			
				R^2_{cal}	RMSEE	R^2_{val}	RMSEP	Bias	RPD
Activation energy (E_a, kJ/mol)	9403.8-7498.3 6102-4597.7	Vector normalization (SNV)	7	0.814	4.97	0.890	4.37	0.19	3.02

F: The number of factors; R^2_{cal}: the coefficient of determination of calibration set; R^2_{val}: the coefficient of determination of prediction set; RMSEE: root mean square error of estimate, RMSEP: root mean square error of prediction; Bias: the average of differences between reference value and NIR value; RPD: the ratio of standard deviation of reference data in the validation set to SEP; SEP: standard error of prediction.

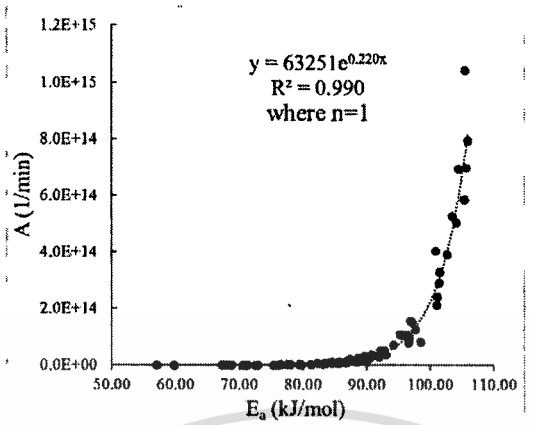

Figure 5 : 2 Scatter plots between pre-exponential factors versus activation energy at n equal to 1.

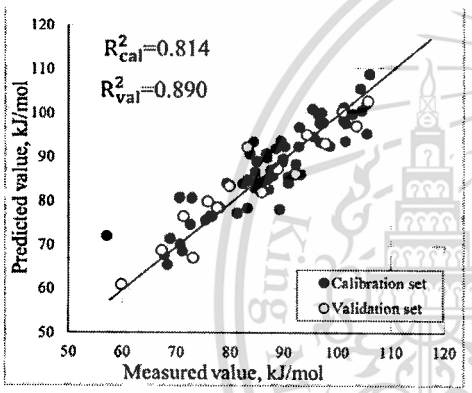

(a)

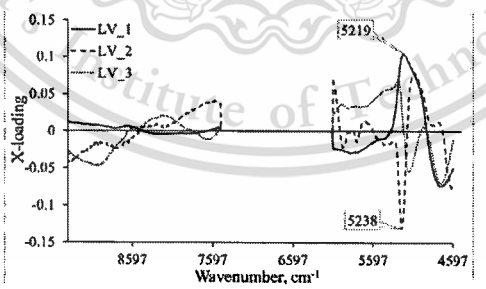

(b)

Figure 5 : 3a) Scatter plots between measured values versus predicted value for Ea, b) X-loading plots for Ea of milled bamboo.

5.6. Conclusion

In the beginning, this model was possible. The result indicated that PLS model for prediction of E_a was good, and could be used with caution for most application. In addition, there were high correlation between E_a and A with high coefficient of determination. This means that A can predicted using a value of E_a. The result indicates that increasing the population size for calibration set was the improving predicting method. Moreover, the models should be improved to be the global model such as the calibration model was carried with many heating rate (such as 5, 10, 15, 20, 25 °C) or many biomass (corn stover, coconut shell, palm shell and so on).

5.7. References

[1] C. Lu, W. Song, W. Lin. (2009). Kinetics of biomass catalytic pyrolysis. Biotechnology Advances 27;583-587.

[2] S. Ceylan, Y. Topçu. (2014). Pyrolysis kinetics of hazelnut husk using thermogravimetric analysis. Bioresource Technology 156;182–188.

[3] P. Parthasarathy, K.S. Narayanan, L. Arockiam. (2013). Study on kinetic parameters of different biomass samples using thermo-gravimetric analysis. Biomass and bioenergy 58; 58-66.

[4] S.A. El-Sayed, M.E. Mostafa. (2014). Pyrolysis characteristics and kinetic parameters determination of biomass fuel powders by differential thermal gravimetric analysis (TGA/DTG). Energy Conversion and Management 85; 165–172.

[5] K. Hashimoto, I. Hasegawa, J. Hayashi, K. Mae. (2011). Correlations of kinetic parameters in biomass pyrolysis with solid residue yield and lignin content. Fuel 90;104–112.

[6] M.A. Sanderson, F. Agblevor, M. Collins, and D.K. Johnson. (1996). Compositional analysis of biomass feedstocks by near infrared spectroscopy. Biomass and bioenergy 11;365-370.

[7] J. Xue, Z. Yang, L. Han, Y. Liu, Y. Liu, and C. Zhou. (2015). On-line measurement of proximates and lignocellulose components of corn stover using NIRS. Applied Energy 137; 18–25.

[8] A.W. Coats, J.P. Redfern. (1964). Kinetic parameters from Thermogravimetric Data. Nature 201(4).

[9] H.H. Sait, A. Hussain, A.A. Salema, F.N. Ani. (2012). Pyrolysis and combustion kinetics of date palm biomass using thermogravimetric analysis. Bioresource Technology 118; 382–389.

[10]K. Slopiecka, P. Bartocci, F. Fantozzi. (2012). Thermogravimetric analysis and kinetic study of poplar wood pyrolysis. Applied Energy 97;491–497.

[11] Q. Dong, Y. Xiong. (2014). Kinetics study on conventional and microwave pyrolysis of moso bamboo. Bioresource Technology 171;127–131.

[12] P. Williams, Near-Infrared Technology—Getting The Best Out Of Light Edition 5.0. A Short Course in the Practical Implementation of Near-Infrared Spectroscopy for the User, PDK Grain, Nanaimo, Canada, 2007.

[13] B.G. Osborne, T. Fearn, Near Infrared Spectroscopy in Food Analysis, Longman Science and Technical, London, 1986.

CHAPTER 6

NONDESTRUCTIVE EVALUATION OF PYROLYSIS PERFORMANCE OF BAMBOO USING NEAR INFRARED SPECTROSCOPY

6.1. ABSTRACT

This paper reports the development of a rapid and low-cost method based on near-infrared spectroscopy as an alternative for thermogravimetric determination of the pyrolysis characteristics, including T_{onset}, T_{sh}, T_{peak}, T_{offset} and DTG_{peak}, of milled bamboo. T_{onset} is the extrapolated onset temperature that is calculated from the partial peak resulting from the decomposition of the hemicellulose component, T_{sh} is the temperature corresponding to the overall maximum of the hemicellulose decomposition rate, DTG_{peak} is the overall maximum of the cellulose decomposition rate, T_{peak} is the temperature corresponding to the overall maximum of the cellulose decomposition rate and T_{offset} is the extrapolated offset temperature of the DTG_{peak} curves determined using thermogravimetric analysis (TGA). The models may be used to control the pyrolysis processes of bamboo to achieve the most economical and environmental conditions. 80 samples of bamboo with various circumferences of culms in the ranges of approximately 16-18, 18-20, 20-22, 22-24, 24-26, 26-28, 28-30, 30-32, 32-34, 34-36, 36-38 and 38-40 cm were randomly collected for optimization of the models. The models were optimized by partial least squares regression (PLSR) with 80 percent of samples for the calibration set and 20 percent for the validation set. For T_{onset}, T_{sh}, T_{peak}, T_{offset} and DTG_{peak}, the models showed coefficients of determination (R^2) of 0.566, 0.845, 0.917, 0.973, and 0.671; root mean square errors of prediction (RMSEP) of 9.7°C, 4.36°C, 3.77°C, 2.66°C, and 0.428 weight loss % /min; ratios of prediction to deviation (RPD) of 1.52, 2.58, 3.48, 3.55, and 1.75; and biases of -0.344°C, -0.765°C, 0.349°C, -5.41°C, and 0.045 weight loss % /min, respectively. In addition, the results showed that pyrolysis characteristics did not depend on the circumference. The vibrational bands of water and CH_3, O–H stretch, first overtones of Ar–OH, CH_2 and HC=CH in the cellulose and lignin structures, O–H hydrogen bonds of polyvinyl alcohol and C–H stretch corresponding to the first overtone of CH_2 had the highest influence on the values of T_{onset}, T_{sh}, T_{peak}, and T_{offset}, respectively. The vibrational band of the C–O–C asymmetrical stretches of cellulose and hemicellulose, and the combination of O–H stretch and HOH bend of polysaccharides influenced the DTG_{peak} value. These results are beneficial for studying the thermal

behaviour of milled bamboo as a potential resource for producing biofuels, especially in the pyrolysis process.

Keywords: Bamboo; Pyrolysis characteristics; Near-infrared spectroscopy; Thermogravimetric analysis; Renewable energy

6.2.Introduction

Biomass has drawn interest because it can act as a renewable and sustainable energy source. Owing to climate change and the increasing demand for fuel, biomass has become more interesting than ever [1]. Bamboo is a renewable energy crop that has been planted in many parts of the world. It is used for furniture, apparatus and fuel. According to literature [2,3], bamboo has a short growth cycle and provides high yields of natural resources. Several studies have reported the advantages of bamboo, such as its fast growth [1, 4], high energy and low ash [5], easy propagation and high productivity [6]. Bamboo is a large, woody grass [5]. In addition, some species can grow up to a foot a day [1]. It has been previously noted that bamboo could be the biomass material and bio-energy resource of the future [4, 7].

The chemical components of biomass are important in the conversion process. Generally, biomass consists of three components, including hemicellulose, cellulose and lignin [8, 9, 10, and 11]. Some studies have reported the content of hemicellulose, cellulose and lignin in bamboo (Table 6:1) . This lignocellulosic matter ~~which each chemical~~ shows different thermal behaviour during pyrolysis [12]. Pyrolysis is thermal decomposition that occurs in the complete absence of oxygen [13]. It is the technology used for converting biomass into energy and chemical products, which consist of liquid bio-oil, solid biochar and gas [14]. Many factors, i.e., temperature, particle size, heating rate and type of biomass affect both the rate and yield of pyrolysis [15]. The proportions of the chemical components of biomass affect the pyrolysis rates [16, 17]. A higher lignin content (corresponding to lower cellulose) results in slower decomposition, while higher hemicellulose and cellulose contents lead to faster decomposition [16, 17, 18, and 19]. Stefanidis et al. [20] reported that pyrolysis of cellulose gave high yields of bio-oil; high yields of hemicellulose gave high gas yields and moderate yields of bio-oil; and high yields of lignin gave the highest solid residue yield. Hemicellulose and cellulose were quickly decomposed at 220–315°C and 315–400°C, respectively, while lignin was decomposed in a wide temperature range from 160 to 900°C [11]. Hemicellulose decomposition had a shoulder peak at 290°C, cellulose decomposition occurred at the highest peak at 347 °C, while

lignin was decomposed in a wide temperature range without an observable peak [21]. Hisham et al. [22] found that the holocellulose, lignin and ash of the specie *Gigantochloa scortechinii* increased as the age were increased over 0.5, 1.5, 3.5, 5.5 and 6.5 years. Cheng et al. [23] showed that cellulose content decreased, and lignin and ash contents increased with the increase in bamboo age from one year to three years. Darabant et al. [2] showed vast differences in the bamboo yield as a result of site and plantation management in eastern Thailand. Thus, even the same species of bamboo may have different characteristics. On the other hand, harvesting age, plantation management and soil fertility also influence the characteristics of bamboo, which have a definite effect on the thermal behaviour. Thus, rapid checking of pyrolysis characteristics of bamboo is required during pyrolysis because temperature influences the quality and yield of the biofuel. The pyrolysis characteristics, i.e., T_{onset}, T_{sh}, T_{peak} and T_{offset}, and DTG_{peak}, are illustrated in Fig. 6:1. El-Sayed and Mostafa [12] indicated that T_{onset} was the extrapolated onset temperature calculated from the partial peak that results from the decomposition of the hemicellulose component, T_{sh} was the temperature corresponding to the overall maximum of the hemicellulose decomposition rate, DTG_{peak} was the overall maximum of the cellulose decomposition rate (dm/dt at the highest peak, weight loss % /min), T_{peak} was the temperature corresponding to the overall maximum of the cellulose decomposition rate and T_{offset} was the extrapolated offset temperature of the DTG_{peak} curves determined using thermogravimetric analysis (TGA). Thermogravimetric (TG) analysis is the direct measurement of weight changes on the TG chart of each sample, and this technique requires a highly skilled technician. These properties can be used to control thermal and chemical conversion during the pyrolysis of biomass.

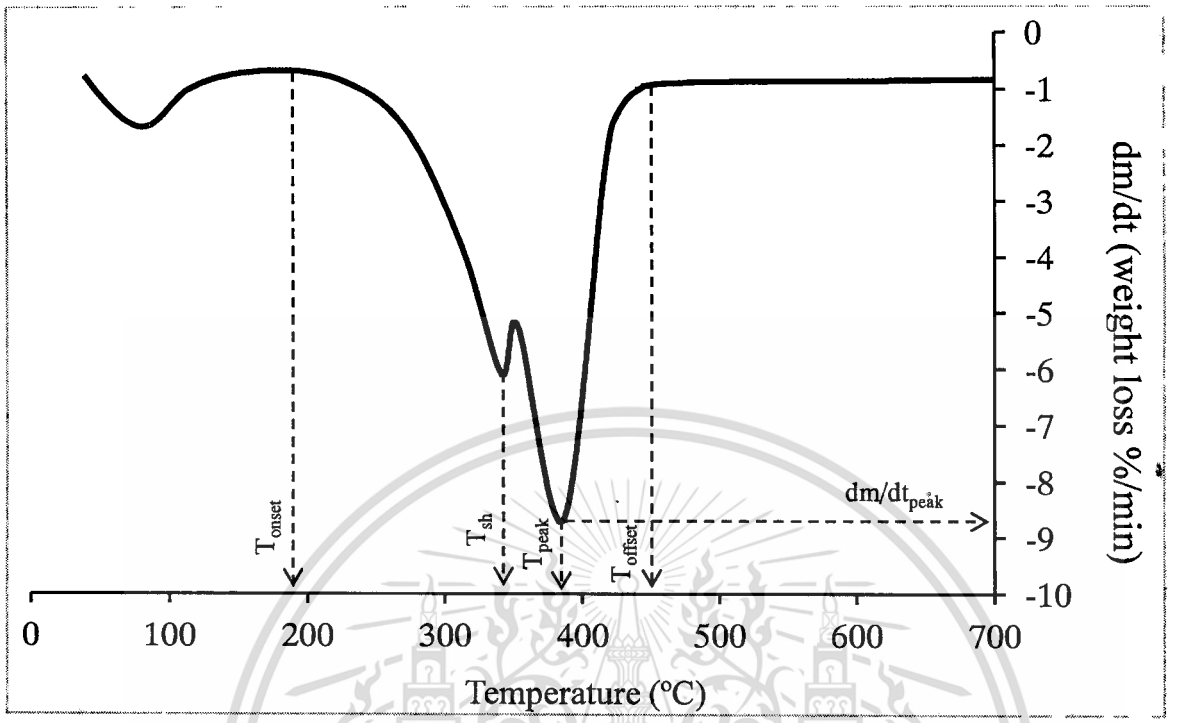

Figure 6 : 1 TG profile for characteristic properties of the material, based on thermal degradation.

Table 6: 1 Hemicellulose, cellulose and lignin content in bamboo.

Material	Hemicellulose	Cellulose	Lignin	Reference
Bamboo	15-20 %	35-45 %	15-25 %	[50]
Bamboo	24.2	43.1	27	[5]
Bamboo Shoots (*Bambusa blumeana*)	27.30 ± 2.8	27.90 ± 1.2	7.92 ± 0.0	[51]
2-Year-old (*Bambusa blumeana*)	27.51 ± 1.7	37.70 ± 1.5	25.73 ± 0.0	
5-Year-old (*Bambusa blumeana*)	22.94 ± 2.1	41.91 ± 1.0	27.11 ± 0.3	
3-year-old moso bamboo culms (*Phyllostachys pubescens*)	22.86±2.19	41.72±2.37	20.91±0.24	[52]

Bamboo, like wood, consists of hemicellulose, cellulose and lignin, which are formed by the atoms C, O and H [24]. Near-infrared (NIR) radiation interacts with structure of O–H, N–H, C–H, C–O, C–O–C, HC=CH, C=C and so on [25, 26]. Hence, biomass is a good absorber of NIR radiation. NIR spectroscopy is an appropriate and rapid method for evaluating the components and physical

properties of agricultural products. Rapid methods are needed to characterize biomass for energy because of the increasing use of biomass in energy systems and the expanding varieties of biomasses available [13]. The different characteristics of biomass are important for controlling thermal processes. These should be monitored to achieve the most economical and environmental conditions. NIR spectroscopy has many advantages, such as being rapid, nondestructive, environmentally friendly due to no or low chemicals, and requiring minimal quantities of samples. Therefore, several recent studies have focused on applying NIR spectroscopy as an alternative method for the assessment of biomass characteristics, such as prediction of composition and bioethanol yield from the cell wall structural components of sweet sorghum biomass [27], evaluation of the thermal properties of *Jatropha curcas* L. kernels [28], prediction of the heating value and moisture content of *Jatropha curcas L.* kernels [29], prediction of moisture, calorific value, ash and carbon content of two dedicated bioenergy crops [30], prediction of biomass composition of switchgrass [31], determination of biochemical methane potential of plant biomass [32] and determination the chemical compositional variability of corn stover and switchgrass [33]. These studies have shown the feasibility of NIR techniques for assessment of the thermal properties and chemical composition of biomass. At present, there has been no report on the application of NIR spectroscopy to study pyrolysis characteristics. Thus, this work is focused on the evaluation of pyrolysis characteristics of milled bamboo, including T_{onset}, T_{sh}, T_{peak} T_{offset} and DTG_{peak} using Fourier Transform-NIR (FT-NIR) spectroscopy as an alternative to thermogravimetric analysis. The reference parameters were obtained from a thermogravimetric apparatus under non-isothermal conditions in a nitrogen atmosphere.

6.3. Material and methods

6.3.1. Sample

The samples of bamboo, *Dendrocalamus sericeus* cl. Phamon, in this study were obtained from the Uttaradit province, Thailand, and had different circumferences of culms. A total of 80 samples in 12 ranges of culm circumference (16-18, 18-20, 20-22, 22-24, 24-26, 26-28, 28-30, 30-32, 32-34, 34-36, 36-38 and 38-40 cm) were randomly cut 10 cm above the ground. Each sample was chopped by a chopping machine (P5508, Patipong, Thailand). After this, the samples were dried under the sun until the moisture reached approximately 5 %wb. The milled were passed through a sieve of diameter 3 mm (60201, QC, UK) and kept in an aluminium bag till the experiment.

6.3.2. *Near Infrared spectroscopy*

The milled sample was filled in a sample cup of 43 mm diameter and 50 mm height, the bottom of which was made of quartz. The sample was scanned using a FT-NIR spectrometer (MPA, Bruker, Germany) with the diffuse reflection mode, and the spectrum was recorded in the range of 12500 cm^{-1}-3800 cm^{-1}, as an average of 64 scans with a resolution of 8 cm^{-1} at room temperature, i.e., 25±2 °C. The sample at the bottom of the cup, irradiated by NIR radiation, was collected to determine the reference values because it contained more NIR spectral information than the remaining part of the cup.

6.3.3. *Reference methods*

The reference value of pyrolysis characteristics, including T_{onset}, T_{sh}, T_{peak} T_{offset} and DTG_{peak} (dm/dt at the highest peak), of a milled sample of 6±0.5 mg were determined using a thermogravimetric analyser (TG 209 F3 Tarsus, Netzsch, Germany, 0.1 µg resolution; 6.8 mm diameter aluminium oxide (Al_2O_3) crucible). The experiments were conducted at a heating rate of 10 °C/min. The samples were heated from 32°C to 700 °C with a flow rate of 20 ml/min of N_2 and zero-O_2 environment for pyrolysis. The temperature was maintained at 700°C for 1 hour to ensure completion of the pyrolysis process. The derivative thermogravimetry (DTG) curve is shown in Fig. 1. After the pyrolysis characteristics were measured, the outliers were then calculated using equation (1).

$$\frac{(X_i - \bar{X})}{SD} \geq \pm 3 \qquad (1)$$

where X_i is the measured value of sample i. $\bar{X}$ and SD are the average and standard deviation of the measured values of all samples, respectively. If the equation was satisfied, the sample was an outlier and it was then removed from the reference data set.

6.3.4. *Repeatability, Reproducibility and Maximum R^2*

The precision of pyrolysis characteristics measured and spectral data scanned were determined using the parameters of repeatability and reproducibility. Maximum R^2 (R^2_{Max}) is the maximum coefficient of determination, when there are no errors in the spectra. For the pyrolysis characteristic reference data; repeatability was the standard deviation of the difference between duplicates; while reproducibility was the standard deviation of the difference between duplicates from blind samples.

In addition, the precision of the NIR instrument was also determined using repeatability and reproducibility. The absorbance value at the wavenumber of 5176 cm^{-1} (1932 nm) was used for the determination. Any wavenumber could be used to determine the repeatability and reproducibility of NIR scans. Therefore, we used the wavenumber 5176 cm^{-1} (1932 nm). This was the absorption band of water in the milled bamboo spectrum. The NIR absorption band of water was the highest peak that was obviously visible in the spectrum. The peak was easily changed when the scanning conditions were varied. The repeatability of the NIR instrument was the standard deviation of the absorbance values when the sample was re-scanned 10 times in the same position, and the reproducibility of spectral data was the standard deviation of the absorbance values when the sample was re-loaded and re-scanned 10 times. According to Dardenne [34], R^2_{Max} can be calculated using equation (2):

$$R^2_{Max} = \frac{SD_y^2 - Rep^2}{SD_y^2} \quad (2)$$

Where, SD_y is the standard deviation of the measured values in the calibration set. Rep is the repeatability of the pyrolysis characteristic reference data. R^2_{Max} Is possible only when there are no errors in the spectra or the model, and it depends on the range and precision of the reference data.

6.3.5. Spectrum pre-processing and NIR spectroscopy modelling

The model was optimized using the OPUS software, Version 7.0.129, Bruker Optik GmbH, Germany, with partial least squares (PLS) regression using the test set validation method. The samples were randomly sub-divided into 80 % for the calibration sample set and 20 % for the validati

on sample set. The wavenumber range of 12500-3800 cm^{-1} was equally divided into five sub-ranges. Spectrum preprocessing was performed by the constant offset elimination; straight line subtraction; vector normalization, min-max normalization; multiplicative scatter correction (MSC); first derivatives, second derivatives; first derivatives+straight line subtraction; first derivatives+ vector normalization and first derivatives+MSC techniques. The models were developed using a combination of sub-ranges of wavenumbers and spectrum pre-processing techniques, and the corresponding root mean square error of prediction (RMSEP) was determined. The model with the

optimal sub-range of wavenumbers and spectrum pre-processing technique was selected by the lowest root RMSEP. Spectral pre-processing techniques are required for model development to remove any irrelevant information that cannot be properly handled by regression techniques [35]. The outliers were determined by the Mahalanobis distance limit. The regression coefficient and X-loading weight of each PLS latent variable was also determined by the software programme and plotted.

6.3.6. Evaluation of the performance of models

When the best model was selected, the model performance was determined by statistical terms i.e., coefficient of determination (R^2), root mean square error of prediction (RMSEP), ratio of prediction to deviation (the standard deviation to standard error of prediction, RPD) and bias. R^2 can be calculated as follows:

$$R^2 = 1 - \frac{\sum_1^m (Y_i - Y_{pre})^2}{\sum_1^m (Y_i - \bar{Y}_i)^2} \quad (3)$$

Where, Y_i is the reference data of the validation set, Y_{pre} is the predicted value, $\bar{Y}_i$ is the average of the reference data of the validation set and m is the number of samples. It shows the proportion of the variance in absorption data that can be explained by the variance in the pyrolysis characteristics data. For example, if R^2 equals 0.95, this means that 95 % variance of pyrolysis characteristics data can be explained by spectral data, while 5 % is the unexplained variance. RMSEP can be calculated as follows:

$$RMSEP = \sqrt{\frac{\sum_1^m (Y_i - Y_{pre})^2}{m}} \quad (4)$$

Nicolaï et al. [35] defined RMSEP as the average uncertainty that could be expected for predictions of future samples. The bias was calculated as follows:

$$Bias = \frac{\sum_1^m (Y_i - Y_{pre})}{m} \quad (5)$$

The bias is the mean difference between the reference and predicted NIR spectra, which describes the overall accuracy of the calibration model [36]. RPD is calculated by:

$$RPD = \frac{SD}{SEP} \quad (6)$$

SD is the standard deviation of the reference data of the validation set and SEP is the standard error of prediction. A low RPD means that the reference data are so narrow or have such a high SEP that the model development is unnecessary [36].

6.4. Results and discussion

6.4.1. Pyrolysis characteristics of milled bamboo

The T_{onset}, T_{sh}, T_{peak}, T_{offset}, and DTG_{peak} of milled bamboo are shown Table 6:2. There were 2 different levels for T_{onset} and DTG_{peak}, and 3 different levels for T_{sh}, T_{peak}, and T_{offset}. As seen in Table 6:2, the standard deviations were high, indicating the difference in pyrolysis characteristics, even for equal circumferences of culms. Thus, the pyrolysis characteristics did not depend on circumference. However, the age may have a significant influence on the properties of the fast-pyrolysis products [23]. Moreover, the different pyrolysis characteristics were affected by the lignin, cellulose and hemicellulose contents [16, 17, 18, 19, and 20].

Table 6: 2 Tonset, Tsh, Tpeak, Toffset and DTGpeak of milled bamboo obtained from bamboo trunks with culms of different circumferences

Range (mm)	N	T_{onset} (°C)	T_{sh} (°C)	T_{peak} (°C)	T_{offset} (°C)	DTG_{peak} (weight loss % /min)
16<L≤18	8	141.725±12.454ab	295.375±10.796abc	332.818±14.814abc	385.562±10.959abc	-8.835±0.739ab
18<L≤20	6	136.233±14.417b	303.250±17.394a	343.541±15.531a	390.833±11.910a	-9.486±1.046b
20<L≤22	6	133.550±8.519b	294.000±15.241abc	335.916±15.635abc	385.166±12.363abc	-8.733±0.678a
22<L≤24	7	141.657±9.866ab	289.857±12.821abc	326.471±12.958bc	380.928±8.757abc	-8.498±0.579a
24<L≤26	6	137.916±9.370ab	285.083±1.357c	322.000±2.393c	377.333±5.988c	-8.638±0.351a
26<L≤28	6	144.600±8.728ab	289.5±9.746abc	322.950±8.474c	376.583±5.219c	-8.623±0.574a
28<L≤30	8	139.162±13.116ab	288.875±8.096bc	323.812±8.110bc	378.812±8.668bc	-8.451±0.521a
30<L≤32	8	146.250±14.576ab	293.750±6.181abc	332.587±9.794abc	383.625±6.968abc	-8.402±0.261a
32<L≤34	7	138.442±11.296ab	290.428±10.357abc	327.685±12.020bc	379.500±7.643bc	-8.387±0.520a
34<L≤36	7	153.842±19.677a	294.214±10.676abc	332.028±11.605abc	383.928±8.115abc	-8.261±0.653a
36<L≤38	5	146.160±8.838ab	301.800±4.868ab	342.700±7.316a	389.900±6.328ab	-8.834±0.406ab
38<L≤40	6	141.883±8.628ab	298.583±9.951abc	338.183±8.857ab	387.500±7.661abc	-8.471±0.589a

Different letters in the same column indicate different means that are significant at p>0.05, as per the Duncan multiple range test. N is the number of samples. L is the circumference of the bamboo culms.

6.4.2. *NIR spectral characteristics of milled bamboo*

The vibrational bands of milled bamboo can be observed in Fig.6:2, which shows the NIR spectra of 80 samples. The main spectral regions were at 6823 cm^{-1} (1466 nm), 5192 cm^{-1} (1926 nm), 4752 cm^{-1} (2104 nm) and 3992 cm^{-1} (2505 nm). The waveband at 1471 nm is the first overtone of N–H stretching of CONHR [25], 1930 nm is the combination band of O–H stretching + H–O–H bending polysaccharides [26], 2103 nm is the band for α-D- glucose, and 2500 nm is the band corresponding to C–H stretching + C–C stretching of starch [25]. Similar results were also reported by Yang et al. [37] for mature bamboo (two years old) and juvenile bamboo (one month old), with many absorption bands in the wavelength region of 1100-2500 nm, including peaks at approximately 1473, 1925, 2095, 2267 and 2328 nm.

The NIR spectra obtained by scanning the milled bamboo raw material changed when the scanning environment, i.e., ambient temperature and water dissolved in the ambient air penetrating into the spectrometer, was changed [38]. In our scanning protocol, this environment was kept constant by means of an air conditioning temperature controller and a spectrometer humidity controller using a molecular sieve. However, parameters such as heating rate, inert gas flow rate and pyrolysis temperature, which were the reference test conditions, might have an effect on the pyrolysis characteristics. Further, the change of pyrolysis characteristics might affect the prediction models. Some researchers concluded that the maximum weight loss rate (DTG_{peak}) decreased with increasing heating rate because their curves shifted obviously towards the high temperature range as the heating rate rose [39,40,41]. By observing the DTG curves of these reports, it might be concluded that T_{onset}, T_{sh}, T_{peak} and T_{offset} increased with increasing heating rate. Modifications of reference test conditions, such as heating rate, pyrolysis temperature and inert gas flow rate, would affect the product and residue yield. Oyedun et al. [1] reported that residue yields increased with increasing heating rate, but were very similar. Higher heating rates lead to higher liquid yields, while lower heating rates lead to higher biochar yields [14]. The pyrolysis temperature influences the bio-product yield. Thus, Irfan et al. [42] reported that for pyrolysis of *Achnatherum splendens* L. under three different pyrolysis temperatures (300, 500, and 700 °C), the biochar yield decreased and syngas yield increased when pyrolysis temperature was increased, and the maximum bio-oil yield was obtained at 500 °C. In addition, the pyrolysis temperature also has an effect on the

product properties. Lower pyrolysis temperatures and heating rates promote higher mass and energy yields of biochar, while higher pyrolysis temperatures and heating rates lead to higher mass and energy yields of the non-condensable gas [43]. Kim et al. [44] reported that increasing the N_2 gas flow rate from 20 to 40 L/min did not change the yield of the pyrolysis products. However, it did change the bio-oil properties, e.g., by decreasing the water content and increasing the amount of organic compounds. In our experiment, both scanning and thermogravimetric protocols were fixed. When the models are proven to be suitable for use, the developed protocol must be applied to update the model.

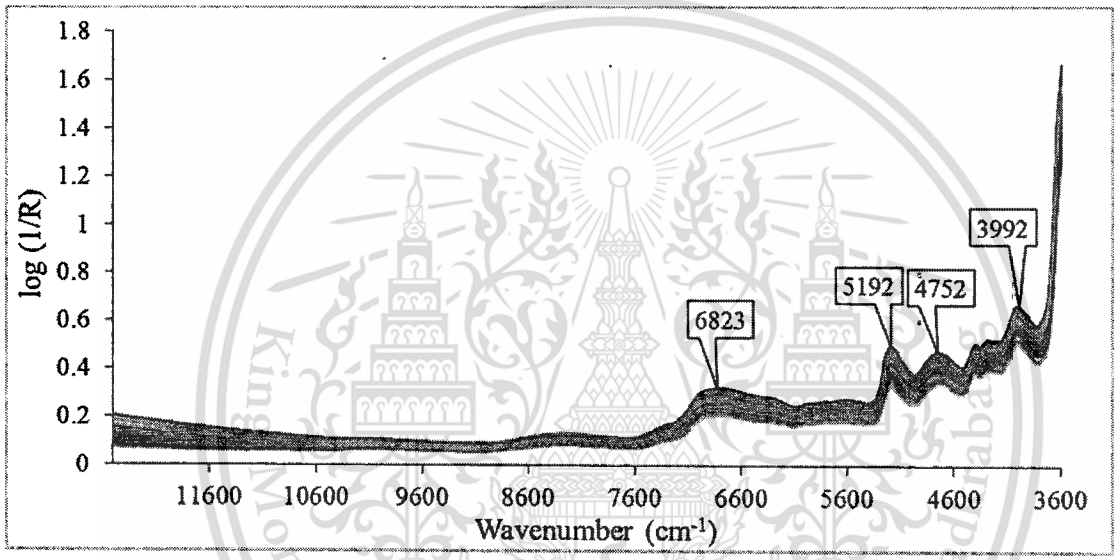

Figure 6 : 2 NIR spectra of 80 samples of milled bamboo.

6.4.3. Overall precision of reference test

The repeatability, reproducibility and R^2_{max} of T_{onset}, T_{sh}, T_{peak}, T_{offset}, DTG_{peak} and the absorption at 5176 cm^{-1} (1932 nm) of milled bamboo are shown in Table 6:3. They had the same precision as the reference laboratory and NIR spectrometer. While R^2_{Max} is possible only when there are no errors in the spectra [34], it can be used to indicate whether the NIR model should be developed or not. R^2_{Max} of T_{onset} was the lowest, and it was not reasonable to develop a NIR model for this parameter. However, those of T_{sh}, T_{peak}, T_{offset}, and DTG_{peak} were high, due to which it was reasonable that NIR models should be developed for these.

6.4.4. *Performance of PLS models*

Statistical data for T_{onset}, T_{sh}, T_{peak}, T_{offset}, and DTG_{peak} of milled bamboo in the total samples, calibration set and validation set are shown in Table 6:3. The data were used for model development and validation. The results of the optimal PLS models for the studied properties are shown in Table 6:5, where the wavenumber range, spectrum pre-processing method, number of PLS latent variables, coefficients of determination (R^2) of both calibration and validation, root mean square error of estimate (RMSEE), root mean square error of prediction (RMSEP), ratio of prediction to deviation (RPD) and bias are shown. The R^2_{max} in Table 6:4 was determined when there was no error in the scanning and the only error was from the reference laboratory source. It was the maximum possible value of R^2. In Table 6:5, the R^2 was the normal R^2, where the sources of error came from NIR scanning, reference laboratory as well as other unknown sources. Fig. 6:3 displays the scatter plots of measured versus predicted values of the prediction sample set. The best models for prediction were developed using the wavenumber range of 6102-5446.3 cm^{-1} for T_{onset}; 8046-7155 and 6267.9-4485.9 cm^{-1} for T_{sh}; 5874.5-4246.7 cm^{-1} for T_{peak}; and 9403.8-7498.3 and 6102-4597.7 cm^{-1} for T_{offset}; and 9403.8-7498.3 and 5450.2-4246.7 cm^{-1} for DTG_{peak}. The second-derivative spectrum pre-processing method was used for model development of T_{onset} and T_{sh}, and first derivative+vector normalization was used for T_{peak}, T_{offset}, and DTG_{peak}. The PLS latent variable numbers were 7, 7, 9, 9 and 9 for T_{onset}, T_{sh}, T_{peak}, T_{offset} and DTG_{peak}, respectively.

The R^2 were 0.566, 0.847, 0.917, 0.894, 0.671; RMSEP were 9.7°C, 4.87°C, 3.77°C, 3.32°C, 0.428 weight loss % /min; RPD were 1.52, 2.59, 3.48, 3.08, 1.75; and biases were -0.344°C, -0.78°C, 0.349°C, 0.352°C, 0.0452 weight loss % /min for T_{onset}, T_{sh}, T_{peak}, T_{offset} and DTG_{peak}, respectively. Our results show that the models for T_{onset} and DTG_{peak} yielded low R^2 of 0.566 and 0.671, respectively. Those models were not applicable due to the following reasons: R^2 of 0.566 indicates that 56.6 % of the total variation can be explained by NIR spectra, while 43.4 % (100-56.6) of the total variation is unexplained variance that cannot be explained by NIR spectra. R^2 of 0.671 indicates that 67.1 can be explained by NIR spectra while the remaining 32.9 % cannot be explained by NIR spectra. If R^2 is too low, the model results in a high error (unexplained variance). Many researchers have suggested guidelines for R^2 and RPD. For example, the model that gives R^2 between 0.50-0.64 could be used for rough screening, 0.66-0.81 for screening and some other "approximate" calibrations, 0.83-0.90 could be used with caution for most applications and 0.92-0.96 could be usable for most applications [36]; the model shows excellent predictions if R^2>0.90 and RPD>3, good predictions if 0.81<R^2<0.90 and 2.5<RPD<3, only approximate predictions if

$0.66<R^2<0.80$ and $2.0<RPD<2.5$ and poor predictions if $R^2<0.66$ and $RPD<2$ [45]; RPD between 1.5 and 2 means that the model can discriminate between low and high values of the response variable; a value between 2 and 2.5 indicates that coarse quantitative predictions are possible; and a value between 2.5 and 3 or above corresponds to good and excellent prediction accuracies, respectively [35]. Therefore, the T_{onset} prediction model is not recommended due to low R^2 and RPD. T_{onset} showed 43.4 percent variance, which cannot be explained by absorption data. Although the measured data were in a wide range, it had high values of repeatability and reproducibility. The T_{sh} model showed low bias (approximately -0.765°C), low RMSEP, and high R^2 and RPD. The ratio between RMSEP and the mean of the reference value (4.36 °C/293.437°C) was approximately 1.48 %. Therefore, the T_{sh} model showed good predictions and could be used with caution for most applications. For T_{peak}, the model showed high R^2 and RPD, low RMSEP and bias. The ratio between RMSEP and the mean of the reference value (3.77°C /333.368 °C) was approximately 1.13 %. This model is excellent and could be used for most applications. For T_{offset}, the model displayed excellent predictive accuracy with high R^2 and RPD and low RMSEP and bias, and may be used with caution for most applications. The ratio between RMSEP and the mean of the reference value (2.66°C/383.687°C) was approximately 0.693 %. On the other hand, for DTG_{peak}, the ratio between RMSEP and the mean of the reference value (0.428 weight loss %/min /-8.525 weight loss %/min) was approximately 5.020 %. It only permitted approximate predictions and could be used for screening. Moreover, all parameters showed low bias. This means that a better model could be provided with a wider range of reference data.

Table 6: 3 Statistical data of Tonset, Tsh, Tpeak, Toffset and DTGpeak of milled bamboo used in model development.

Parameters	Data set	N[a]	Max	Min	Mean	Range	SD[b]
T_{onset} (°C)	Total sample	80	182.6	115.7	141.882	66.9	12.574
	Calibration set	64	182.6	115.7	141.540	66.9	11.941
	Prediction set	16	172.5	117.3	143.250	55.2	15.213
T_{sh} (°C)	Total sample	79	319	277	293.063	42	10.471
	Calibration set	63	319	277	292.777	42	10.336

	Prediction set	16	316	278	293.437	38	11.458
	Total sample	80	357	313.2	331.007	43.8	12.283
T_{peak} (°C)	Calibration set	64	357	313.2	330.407	43.8	12.003
	Prediction set	16	353.8	313.2	333.368	40.6	13.476
	Total sample	78	403.5	367	382.565	36.5	8.646
T_{offset} (°C)	Calibration set	62	403.5	367	382.270	36.5	8.457
	Prediction set	16	398	368	383.687	30	9.539
	Total sample	80	-7.25	-11.27	-8.618	4.02	0.638
DTG_{peak} (weight loss % /min)	Calibration set	64	-7.25	-11.27	-8.641	4.02	0.605
	Prediction set	16	-7.43	-10.25	-8.525	2.82	0.771

Number of samples.

[b] Standard deviation.

Table 6: 4 Repeatability, reproducibility and R_Max^2 of reference laboratory for Tonset, Tsh, Tpeak, Toffset and DTGpeak and of absorption at 5176 cm-1 (1932 nm) of milled bamboo.

Parameter	Repeatability	Reproducibility	R^2_{max}
T_{onset}	8.8	7.0	0.465
T_{sh}	3.9	5.2	0.877
T_{peak}	1.81	2.39	0.979
T_{offset}	1.58	1.89	0.970
DTG_{Peak}	0.199	0.333	0.903
Absorptive value at 5167 cm-1(1932nm) of sample	0.00467	0.01816	-

Table 6: 5 Results of partial least squares regression models for determination of Tonset, Tsh, Tpeak, Toffset and DTGpeak of milled bamboo

R^2 is the coefficient of determination. RMSEE is the root mean square error of estimation. RMSEP is the root mean square error of prediction. RPD is the ratio of standard deviation. Bias is the average error of prediction.

Parameters	Wavenumber range (cm^{-1})	Pre-processing	Calibration			Validation			
			PLS latent variables	R^2	RMSEE	R^2	RMSEP	RPD	Bias
onset	6102-5446.3	Second derivative	7	0.545	8.55	0.566	9.70	1.52	-0.344
sh	8046-7155 6267.9-4485.9	Second derivative	7	0.865	4.02	0.845	4.36	2.58	-0.765
peak	5874.5-4246.7	First derivative + vector normalization	9	0.921	3.66	0.917	3.77	3.48	0.349
offset	9403.8-7498.3 6102-4597.7	First derivative + vector normalization	9	0.939	2.27	0.917	2.66	3.55	-0.541
TG_{peak}	9403.8-7498.3 5450.2-4246.7	First derivative + vector normalization	9	0.692	0.363	0.671	0.428	1.75	0.0452

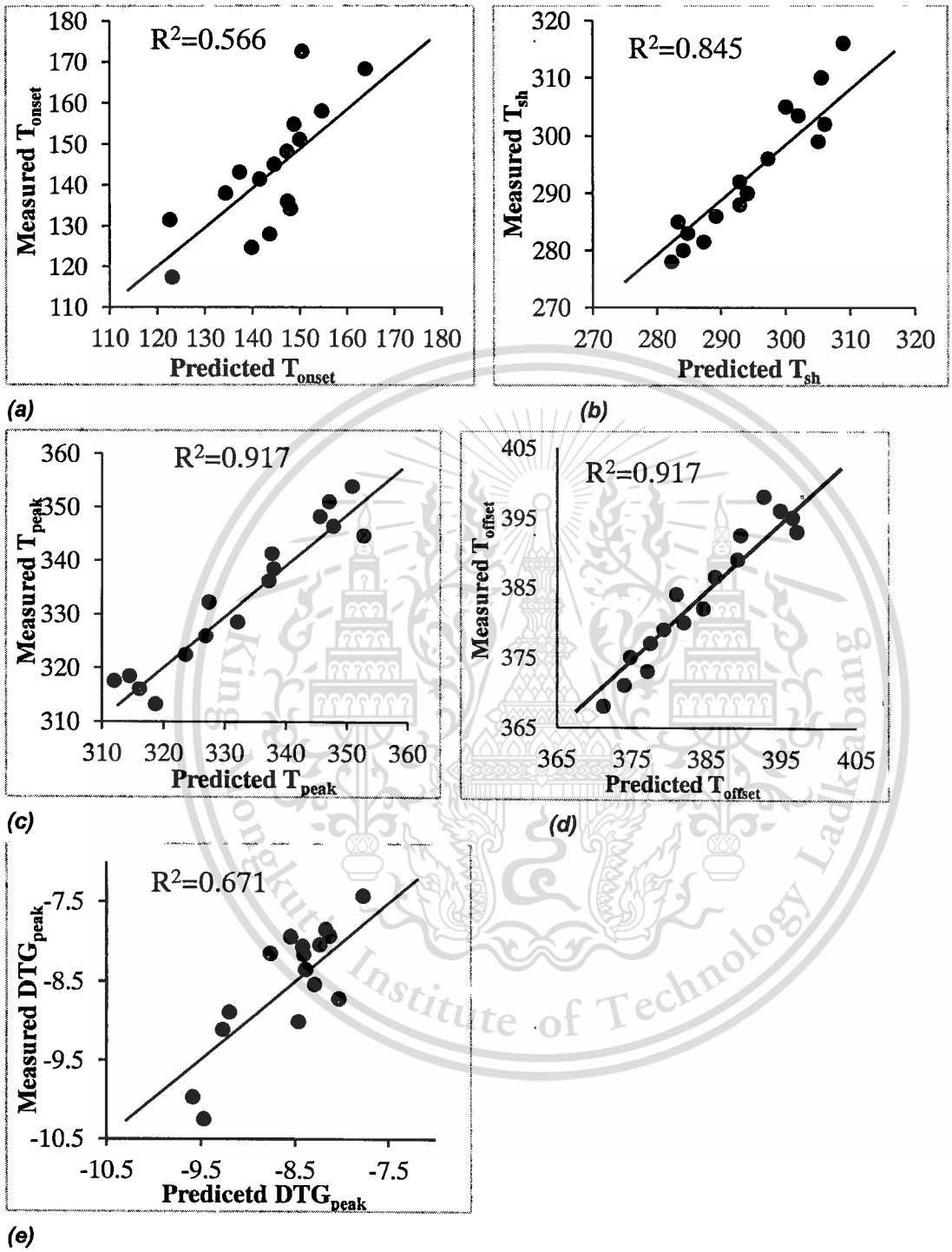

Figure 6 : *3* **Scatter plots of measured vs predicted a) Tonset, b) Tsh, c) Tpeak, d) Toffset and e) DTGpeak of the validation set.**

6.4.5. Regression coefficient and X-loading

The regression coefficient plots of the models developed for T_{onset}, T_{sh}, T_{peak}, T_{offset} and DTG_{peak} are shown in Fig.6 : 4, while the X-loading plots of the first three factors are shown in Fig.6: 5. The high values of the regression coefficient and X-loading weight at any wavenumber meant that the vibration of a particular bond at that wavenumber was the main factor influencing the model prediction.

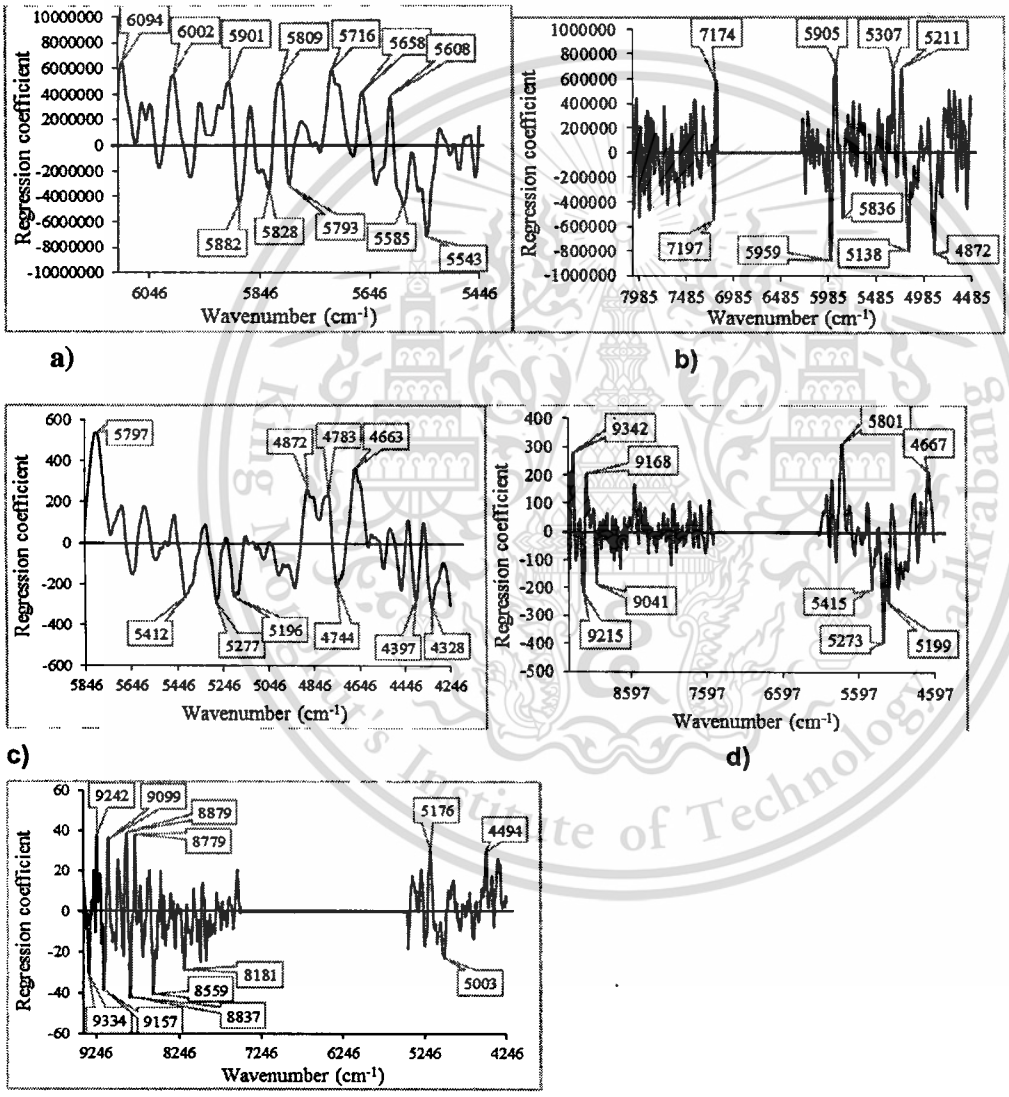

Figure 6 : 4 Regression coefficient plots of the models for a) Tonset, b) Tsh, c) Tpeak, d) Toffset and e) DTGpeak.

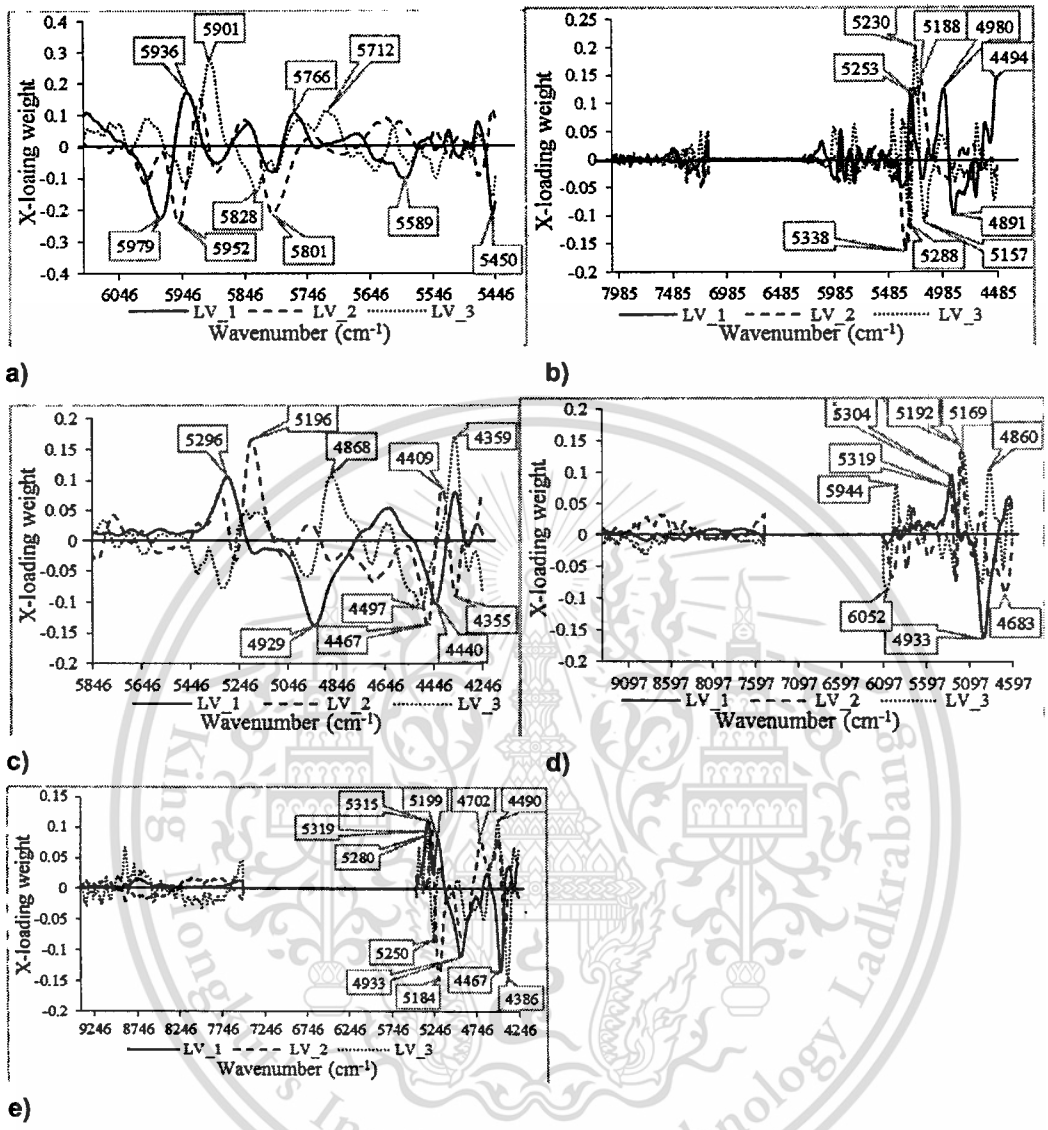

Figure 6 : 5 X-loading weight plots of the models for a) Tonset, b) Tsh, c) Tpeak, d) Toffset and e) DTGpeak. LV_1, LV_2 and LV_3 are the PLS latent variables 1, 2 and 3, respectively.

➢ T_{onset}

The regression coefficient plot of T_{onset} is displayed in Fig.6 :4a. The most important peaks are at approximately 5543 cm^{-1} (1804 nm) (O–H combination of water) [26], 6094 cm^{-1} (1641 nm) (first overtone of C–H stretching of R–C_2H_2O) [25] and 5716 cm^{-1} (1750 nm) (related to the structure of α-D glucose) [25]. While the corresponding X-loading weight plot is also shown in Fig. 6:5a, the

most important peaks are at approximately 5901 cm^{-1} (1695 nm) (related to first overtone of C–H stretching of CH_3), 5952 cm^{-1} (1680 nm) (related to aromatic C–H of hydrocarbon or aromatic) and 5979 cm^{-1} (1673 nm) (related to C–H aromatic C–H (aryl)). The corresponding absorption bands with high regression coefficients and X-loading weights are displayed in Table 6:6. The results indicate that the O–H vibrations of water and C–H vibrations of CH_3 had the highest influence because there was no volatilization of water during the initial decomposition of hemicellulose [12]. The CH_3 is found in the hemicellulose structure. Guimarães et al. [27] also reported that the most important peaks affecting the hemicellulose evaluation model were the first overtone of O–H stretching, the first overtone of C–H stretching and the combination of the C–H stretching.

Table 6: 6 Absorption bands with high regression coefficients and X-loading weights in the model for Tonset of milled bamboo.

Regression coefficient				
Wavenumber (cm^{-1})	**Wavelength (nm)**	**Wavelength (nm) referred from reference**	**Bond vibration**	**Structure**
5543	1804	1790[26]	O–H combination	Water
6094	1641	1645[25]	C–H stretching first overtone	
5716	1750	1750[25]	-	α-D-glucose
6002	1666	1664[26]	C–H methyl, OH associated as $ROHCH_3$	Alcohols, diols
5585	1790	1790[26]	O–H combination	Water
5882	1700	1700[26]	C–H methyl, CH_3Cl	Halogenated (CH_3Cl) (gas phase)
5901	1695	1695[26]	C–H methyl, CH_3Br	Halogenated (CH_3Br) (gas phase)
5809	1721	1725[25]	C–H stretching first overtone	CH_2
5658	1767	1765[25]	C–H stretching first overtone	CH_2

5608	1783	1780[25]	C–H stretching first overtone		Cellulose
5828	1715	1711[26]	C–H methyl, CH_3Br		Halogenated (CH_3I)
5793	1726	1728[25]	-		Hemicellulose
X-loading weight					
Wavenumber (cm^{-1})	**Wavelength (nm)**	**Wavelength(nm) referred from reference**	**PLS latent variable**	**Bond vibration**	**Structure**
5901	1695	1695[25]	3	C–H stretching first overtone	CH_3
5952	1680	1680[26]	2	Aromatic C–H	Hydrocarbon, aromatic
5979	1673	1671[26]	1	C–H aromatic C–H (aryl)	C–H aryl
5936	1685	1685[26]	1	C–H aromatic C–H	Hydrocarbon, aromatic
5450	1835	1834[25]	1	-	α–D–glucose
5801	1724	1725[25]	2	C-H stretching first overtone	CH_2
5712	1751	1750[25]	3	-	α–D–glucose
5766	1734	1733[26]	1	C–H methyl C–H, ether associated as (R–O–CH_3)	Ether
5828	1716	1711[26]	3	C-H methyl, CH_3Br	Halogenated (CH_3I)
5589	1789	1789[25]	1	-	α–D–glucose

➢ T_{sh}

For T_{sh}, the regression coefficient and X-loading weight plots of the first three factors are shown in Fig.6:4b and 6:5b, respectively. The most important peaks of the regression coefficient plots are at

approximately 5959 cm^{-1} (1678 nm) (C-H methyl, carbonyl adjacent to (.C=OCH_3) of ketones) [26], 5138 cm^{-1} (1946 nm) (C=O esters and acids (.C=OOR) of acids and esters) [26] and 4872 cm^{-1} (2052 nm) (N–H combination from polyamide II of polyamide II) [26]. For the X-loading weight plots, the most important peaks are at approximately 5338 cm^{-1} (1873 nm), 4494 cm^{-1} (2225 nm) (related to CHO) [26] and 5230 cm^{-1} (1912 nm) (related to O–H stretch first overtone of Ar–OH) [46]. The corresponding absorption bands with high regression coefficients and X-loading weights are displayed in Table 6:7. Guimarães et al. [27] also reported that the first overtone of the O–H stretch and first overtone of the C–H stretch affected the hemicellulose predictions.

Table 6: 7 Absorption bands with high regression coefficients and X-loading weights in the model for Tsh of milled bamboo.

Regression coefficient				
Wavenumber (cm^{-1})	**Wavelength (nm)**	**Wavelength (nm) referred from reference**	**Bond vibration**	**Structure**
5959	1678	1678[26]	C–H methyl, carbonyl adjacent as (.C=OCH_3)	Ketones
5138	1946	1950[26]	C=O esters and acids (.C=OOR)	Acids and esters
4872	2052	2053[26]	N–H combination from polyamide II	Polyamide II
5905	1693	1694[26]	C–H methyl C–H, (.CH_3)	Hydrocarbons, aliphatic
5307	1884	1892[26]	O–H hydrogen bonding between water and exposed polyvinyl alcohol OH	Water and polyvinyl
5211	1919	1920[25]	C=O stretching second overtone	CONH
7174	1394	1395[25]	2×C–H stretching + C–H deformation	CH_2
7197	1389	1390[26]	Si–OH	Silica; optical fibres

5836	1714	1711[26]	C–H methyl C–H, iodine (CH_3I)		Halogenated (CH_3I)
X-loading weight					
Wavenumber (cm^{-1})	**Wavelength (nm)**	**Wavelength(nm) referred from reference**	**PLS latent variable**	**Bond vibration**	**Structure**
5338	1873	-	2	-	-
4494	2225	2230[26]	1	CHO	-
5230	1912	1910 [46]	3	O-H stretch first overtone	Ar-OH
5188	1928	1928[26]	2	O–H stretching and HOH deformation combination from water in the 3-aminopropyltriethoxysilane-ethanol-water system	3-aminopropyltriethoxysilane-ethanol-water system
4980	2008	2008[25]	1	-	Sucrose
5253	1904	1900[25]	1	O–H stretching second overtone	Starch
5288	1891	1892[26]	3	O–H hydrogen bonding between water and exposed polyvinyl alcohol OH	Water and polyvinyl alcohol OH
5157	1939	1940[25]	3	O–H stretching + O–H deformation	Water
4891	2045	2050[25]	1	N-H asym. Stretching+ amide III	$CONH_2$

➢ T_{peak}

For T_{peak}, the regression coefficient plots are shown in Fig. 6:4c . The most important peaks are at approximately 5797 cm^{-1} (1725 nm) (related to the first overtone of C–H stretching of CH_2) [25], 4663 cm^{-1} (2144 nm) (=C–H stretching + C=C stretching of HC=CH) [25] and 4328 cm^{-1} (2310 nm) (C–H stretching + C–H deformation of CH_2) [25]. The X-loading plots of the first three factors are shown in Fig. 5c. The high peaks are at approximately 4359 cm^{-1} (2294 nm) (related to the C–H aromatic C–H (aryl) of C–H aryl) [26], 5196 cm^{-1} (1925 nm) (related to the assigned O–H) [26] and 4929 cm^{-1} (2029 nm) (related to the second overtone of the C=O stretch of $CONH_2$) [25]. The corresponding absorption bands with high regression coefficients and X-loadings are displayed in Table 6:8. T_{peak} is the temperature corresponding to the overall maximum of the cellulose decomposition rate [12]. The peaks of CH_2 and HC=CH, found in the cellulose and lignin structures, had the highest influence. The results are similar to those reported by Guimarães et al. [27], where the vibration band of the first overtone of C–H stretching was the most important for cellulose prediction. The T_{peak} of the milled bamboo samples had a range of 313.2 to 357 °C (Table 6:4), in agreement with the result of Jiang et al. [4], where the critical temperature of maximum weight loss was 347 °C with 10 °C/min for moso bamboo in the pyrolysis process. Cellulose was quickly decomposed at 315–400 °C [11] and highly decomposed at 347 °C [21]. Lignin was degraded in a wide temperature range of 200-600 °C [47]. Accordingly, it may be concluded that not only cellulose but lignin was also degraded at T_{peak}.

Table 6: 8 Absorption bands with high regression coefficients and X-loading weights in the model for Tpeak of milled bamboo.

Regression coefficient				
Wavenumber (cm^{-1})	**Wavelength (nm)**	**Wavelength (nm) referred from reference**	**Bond vibration**	**Structure**
5797	1725	1725[25]	C–H stretching first overtone	CH_2
4663	2144	2140[25]	=C–H stretching + C=C stretching	HC=CH

4328	2310	2310[25]	C–H stretching + C–H deformation		CH_2
5412	1847	-	-		-
4397	2274	2276[25]	O–H stretching + C–C stretching		Starch
5277	1895	1900[25]	O–H stretching + 2×C–O stretching		Starch
5196	1925	1923[26]	O–H assigned to molecular water (O-H stretching and HOH deformation)		O–H molecular water
4744	2108	2110[25]	-		Hemicellulose
4872	2053	2053[26]	N–H combination from polyamide 11		Polyamide 11
4783	2090	2090[26]	O–H combination		Polymeric OH
X-loading weight					
Wavenumber (cm^{-1})	**Wavelength (nm)**	**Wavelength(nm) referred from reference**	**PLS latent variable**	**Bond vibration**	**Structure**
4359	2294	2294[26]	3	C–H aromatic C–H (aryl)	C–H aryl
5196	1925	1923[26]	2	O–H assigned to molecular water	O–H molecular water
4929	2029	2030[25]	1	C=O stretching second overtone	$CONH_2$
4467	2239	-	2	-	-
4868	2054	2053[26]	3	N–H combination from polyamide II	Polyamide II
5296	1888	1900[25]	1	O–H stretching + 2× C–O stretching	Starch
4497	2224	2220[26]	3	NH combination band from urea (N–	NH from urea

				H_2–C=O–NH_2)	
4440	2252	2252[25]	1	O–H stretching + O–H deformation	Starch
4409	2268	2270[26]	2	O–H stretching and C–O stretching combination	Cellulose
4355	2296	2294[25]	2	N–H stretching + C=O stretching	Amino acid

The intensity of the peaks runs in descending order.

➢ T_{offset}

For T_{offset}, the regression coefficient and X-loading weight plots of the first three factors are displayed in Fig. 6:4d and 6:5d , respectively. The important peaks of the regression coefficient are at approximately 5273 cm^{-1} (1896 nm) (related to the O–H hydrogen bonding between water and exposed polyvinyl alcohol OH of water and polyvinyl alcohol) [26], 5801 cm^{-1} (1724 nm) (first overtone of C–H stretching of CH_2) [25], and 9342 cm^{-1} (1070 nm) (O–H combination band, alcohol or water of alcohols as R–C–O–H) [26]. The X-loading weight plots showed important peaks at 4933 cm^{-1} (2027 nm) (related to C=O stretching + second overtone of $CONH_2$) [25], 5192 cm^{-1} (1926 nm) (combination of O–H stretching and HOH deformation from water molecules in the 3-aminopropyltriethoxysilane-ethanol-water system) [26]. The corresponding absorption bands with high regression coefficients and X-loading weight plots are shown in Table 6:9. T_{offset} is the extrapolated offset temperature. It is the temperature at the end of the DTG curves at which there is little or no volatilization of the biomass. The O-H bond of polyvinyl alcohol, found in the lignin structure, had a significant influence. The CH_2 bond, present in both lignin and cellulose structures, also had a high influence.

Table 6: 9 Absorption bands with high regression coefficients and X-loading weights in the model for Toffset of milled bamboo.

Regression coefficient					
Wavenumber (cm^{-1})	**Wavelength (nm)**	**Wavelength (nm) referred from reference**	**Bond vibration**		**Structure**
5273	1896	1892[26]	O–H hydrogen bonding between water and exposed polyvinyl alcohol OH		Water and polyvinyl alcohol
5801	1724	1725[25]	C–H stretching first overtone		CH_2
9342	1070	1065[26]	O–H combination band, alcohol or water		Alcohols as R–C–O–H
5199	1923	1920[25]	C=O stretching second overtone		CONH
9215	1085	1080[25]	2×C–H stretching + 2×C–C stretching		Benzene
5415	1847	-	-		-
9168	1091	1097[25]	2×C–H stretching + 2×C–C stretching		Cyclopropane
4667	2143	2140[25]	=C–H stretching + C=C stretching		HC=CH
9041	1106	-	-		-
X-loading weight					
Wavenumber (cm^{-1})	**Wavelength (nm)**	**Wavelength(nm) referred from reference**	**PLS latent variable**	**Bond vibration**	**Structure**
4933	2027	2030[25]	1	C=O stretching + second overtone	$CONH_2$
5192	1926	1928[26]	2	O–H stretching and HOH deformation combination from water molecules in the 3-aminopropyltriethoxysilane-ethanol-water system	3-aminopropyltriethoxysilane-ethanol-water system
5169	1935	1933[26]	3	Si–O–H stretching + Si–O–Si combination from silicone	Silicone (dimethyl

					siloxane)
4860	2058	2060[26]	3	N–H combination band from secondary amide in proteins	N–H from protein
4683	2135	2132[25]	2	N–H stretching + C=O stretching	Amino acid
5304	1885	1892[26]	1	O–H hydrogen bonding between water and exposed polyvinyl alcohol OH	Water and polyvinyl alcohol OH
6052	1652	1654[26]	3	C–H methyl C–H, nitro (CH_3NO_2)	Nitro (CH3) as (CH_3NO_2)
5319	1880	-	2	-	-
5944	1682	1685[25]	3	C–H stretching first overtone	Aromatic

The intensity of the peaks runs in descending order.

➢ ***DTG_{peak}***

For DTG_{peak}, the regression coefficient and X-loading weight plots of the first three factors are displayed in Fig. 6:4e and 6:5e, respectively. The important peaks are at approximately 8837 cm^{-1} (1132 nm), 8559 cm^{-1} (1168 nm) (C–O–C asymmetrical stretch of cellulose and hemicellulose) [48], and 9157 cm^{-1} (1092 nm) (2×C–H stretches + 2× C–C stretches of cyclopropane) [26]. The important peaks in the X-loading weight plots are at 5184 cm^{-1} (1929 nm) (combination of O–H stretch and HOH bend of polysaccharides) [26] and 4386 cm^{-1} (2280 nm) (C–H stretch + C–H stretch deformation of CH_3) [25]. The corresponding absorption bands with high regression coefficients and X-loading weights are shown in Table 6:10.. The results show that polysaccharides strongly influence DTG_{peak} prediction. Polysaccharides, such as hemicellulose, holocellulose and cellulose, have a similar molecular structure of –OH groups [49]. The DTG_{peak}, which was the overall maximum of the cellulose decomposition rate [12], increased with increasing cellulose content [16, 17, 18, and 19].

Table 6: 10 Absorption bands with high regression coefficients and X-loading weights in the model for DTGpeak of milled bamboo.

Regression coefficient					
Wavenumber (cm^{-1})	**Wavelength (nm)**	**Wavelength (nm) referred from reference**	**Bond vibration**		**Structure**
8837	1132	-	-		-
8559	1168	1160[48]	C–O–C asymmetrical stretching		Cellulose, hemicellulose
9157	1092	1097[25]	2×C–H stretching + 2× C–C stretching		Cyclopropane
8879	1126	-	-		-
8779	1139	1142[26]	C–H (3*v*), aromatic C–H		Hydrocarbon, aromatic
9242	1082	1080[25]	2×C–H stretching + 2× C–C stretching		Benzene
9099	1099	1097[25]	2×C–H stretching + 2× C–C stretching		Cyclopropane
5176	1932	1930[26]	O–H stretching and HOH bending combination		Polysaccharides
9334	1071	1065[26]	O–H combination band, alcohols or water		Alcohols as R–C–O–H
4494	2225	2230[26]	CHO		-
8181	1222	1225[25]	C–H stretching second overtone		CH
5003	1999	2000[25]	2× O–H stretching and C–O deformation		Starch
X-loading weight					
Wavenumber (cm^{-1})	**Wavelength (nm)**	**Wavelength(nm) referred from reference**	**PLS latent variable**	**Bond vibration**	**Structure**
5184	1929	1930[26]	2	O–H stretching and HOH bending combination	Polysaccharides
4386	2280	2280[25]	3	C–H stretching + C–H stretching deformation	CH_3

4467	2239	-	1	-	-
5315	1882	1900[25]	1	O–H stretching + 2×C–O stretching	Starch
4933	2027	2030[25]	1, 2	C=O stretching overtone	$CONH_2$
4490	2227	2230[26]	3, 2	CHO	-
5319	1880	1900[25]	3	O–H stretching + 2×C–O stretching	Starch
5280	1894	1892[26]	2	O–H hydrogen bonding between water and exposed polyvinyl alcohol OH	Water and polyvinyl alcohol OH
5250	1905	1908[25]	3	O–H stretching + O–H deformation	POH
4702	2127	2027[26]	2	N–H/C=O combination from polyamide II	Polyamide II
5199	1923	1923[26]	1	O–H assigned to molecular water (O–H stretching and HOH deformation combination)	O–H molecular water

The intensity of the peaks runs in descending order.

6.5.Conclusions

This study focused on NIR spectroscopic methods as an alternative for thermogravimetric analysis (TGA) to determine T_{onset}, T_{sh}, T_{peak}, T_{offset} and DTG_{peak} of milled bamboo. The results show that the pyrolysis characteristics did not depend on the culm circumference, and the lignocellulosic content in the bamboo influenced the predictions of the models. The models developed for T_{sh} and T_{offset} may be used as a nondestructive technique with caution for most applications, and the model developed for T_{peak} is usable for most applications. On the other hand, the model for DTG_{peak} may be used for screening. However, the predictive model for T_{onset} is not usable due to high RMSEP and low R^2. However, all models showed low bias. This indicates that the developed protocol could be used to control the pyrolysis processes of bamboo to achieve the most economical and environmental conditions. In the authors' opinion, T_{onset} and T_{offset} can be used to set the starting

temperature and the final target temperature of the pyrolysis, both of which are very important parameters. Oyedun et al. [1] explained that the final target temperature could greatly influence the amount of energy used during pyrolysis, and its value could significantly affect the energy cost and completion time. If the value is too low, the biomass will contain some volatile gas and the process will take a long time to complete, thus leading to a low amount of bio-oil. On the other hand, if the value is too high, the amount of energy used by the heater is too high, which affects the energy cost. T_{onset} is the temperature at which biomass starts to decompose, and it can be used to set the gas collection time. If the gas is collected before the biomass starts to decompose, there will be a high amount of moisture in the gas, which results in low-quality bio-oil. T_{peak} is the temperature at the highest degradation rate and DTG_{peak} is the maximum rate of decomposition. Their values can significantly affect the processing time. It was assumed that if the biomass pyrolysis was carried out at the temperature T_{peak}, it will give the highest decomposition rate of DTG_{peak}, thus resulting in the highest processing rate. The NIR spectroscopic model for these pyrolysis characteristics could be applied to control the process online in real time. The information found in this research can be used to manage the bamboo biomass feedstock, pyrolysis process, and storage. In addition, the authors recommend the development of a universal model using different types of biomass, where the reference value will be in a wide range. Such a model may be useful for many types of biomass materials.

6.6. Acknowledgments

The authors thank the Near-Infrared Spectroscopy Research Center for Agricutultural Products and Food (www.nirsresearch.com) at King Mongkut's Institute of Technology, Ladkrabang, Bangkok, Thailand, for instruments. We also acknowledge the financial support from the Royal Golden Jubilee PhD scholarship (PHD/0070/2557) of Thailand research fund (TRF).

6.7. References

[1] A.O. Oyedun, T. Gebreegziabher, C.W. Hui, Mechanism and modelling of bamboo pyrolysis, Fuel Process Technol 106 (2013) 595-604.

[2] A. Darabant, M. Haruthaithanasana, W. Atklaa, T. Phudphonga and E. Thanavata, Bamboo biomass yield and feedstock characteristics of energy plantations in Thailand, Energy Procedia 59 (2014) 134 – 141.

[3] E.V. Villar-Cociña, S.F. Morales, H.S. Santos, b. Jr, M. Frías, Pozzolanic behaviour of bamboo leaf ash: Characterization and determination of the kinetic parameters, Cem Concr Compos 33 (2011) 68–73.

[4] Z. Jiang, Z. Liu, Benhua Fei, Z. Cai, Y. Yu, X. Liu, The pyrolysis characteristics of moso bamboo, J. Anal Appl Pyrol 94 (2012) 48–52.

[5] J.M.O. Scurlock, D.C. Dayton, B. Hames, Bamboo: an overlooked biomass resource?, Biomass Bioenerg 19 (2000) 229-244.

[6] C.M.D. Montaño, J.R. Pels, L.E. Fryda, R.W.R. Zwart, Evaluation of torrefied bamboo for sustainable bioenergy production, in: J. Gielis (Ed.) 9th World Bamboo Congress, World Bamboo Organization, Antwerpen, (2012) 809-818.

[7] Z. Liu, Z. Jiang, Z. Cai, B. Fei, Y. Yu, X. Liu, The Manufacturing Process of Bamboo Pellets, Proceedings of the 55th International Convention of Society of Wood Science and Technology. August 27-31, 2012 - Beijing, CHINA.

[8] Y. Long, L. Ruan, X. Lv, Y. Lv, J. Su, Y. Wen, TG–FTIR analysis of pyrolusite reduction by major biomass components, Chinese J Chem Eng 23 (2015) 1691–1697.

[9] S. Wang, B. Ru, H. Lin, W. Sun, Pyrolysis behaviours of four O-acetyl-preserved hemicelluloses isolated from hardwoods and softwoods. Fuel 150 (2015) 243–251.

[10] S. Ren, H. Lei, L. Wang, Q. Bu, S. Chen, J. Wu, Thermal behaviour and kinetic study for woody biomass torrefaction and torrefied biomass pyrolysis by TGA, Biosyst Eng 116 (2013) 420-426.

[11] H. Yang, R. Yan, H. Chen, D.H. Lee, C. Zheng, Characteristics of hemicellulose, cellulose and lignin pyrolysis, Fuel. 86 (2007) 1781–1788.

[12] S.A. El-Sayed, M.E. Mostafa, Pyrolysis characteristic and kinetic parameters determination of biomass fuel powders by differential thermal gravimetric analysis (TGA/DTG), Energ Convers Manage 85 (2014) 165-172.

[13] D.T. Chadwick, K.P. McDonnell, L.P. Brennan, C.C. Fagan, C.D. Everard, Evaluation of infrared techniques for the assessment of biomass and biofuel quality parameters and conversion technology processes: A review. Renew Sust Energ Rev 30 (2014) 672–681.

[14] T. Kan, V. Strezov, T.J. Evans, Lignocellulosic biomass pyrolysis: A review of product properties and effects of pyrolysis parameters, Renew Sust Energ Rev 57 (2016) 1126–1140.

[15] E. Părpăriță, M. Brebu, Md.A. Uddin, J. Yanik, C. Vasile, Pyrolysis behaviours of various biomasses, Polym Degrad Stabil 100 (2014) 1-9.

[16] J. Wannapeera, N. Worasuwannarak, S. Pipatmanomai, Product yields and characteristics of rice husk, rice straw and corncob during fast pyrolysis in a drop-tube/fixed-bed reactor. Songklanakarin J Sci Technol 30 (3) (2008) 393-404.

[17] D. Lv, M. Xu, X. Liu, Z. Zhan, Z. Li, H. Yao, Effect of cellulose, lignin, alkali and alkaline earth metallic species on biomass pyrolysis and gasification, Fuel Process Technol 91 (2010) 903–909.

[18] L. Burhenne, J. Messmer, T. Aicher, M-P. Laborie, The effect of the biomass components lignin, cellulose and hemicellulose on TGA and fixed bed pyrolysis, J Anal Appl Pyrol 101 (2013) 177–184.

[19] G. Dorez, L. Ferry, R. Sonnier, A. Taguet, J.-M. Lopez-Cuesta, Effect of cellulose, hemicellulose and lignin contents on pyrolysis and combustion of natural fibres, J Anal Appl Pyrol 107 (2014) 323–331.

[20] S.D. Stefanidis, K.G. Kalogiannis, E.F. Iliopoulou, C.M. Michailof, P.A. Pilavachi, A.A. Lappas, A study of lignocellulosic biomass pyrolysis via the pyrolysis of cellulose, hemicellulose and lignin, J Anal Appl Pyrol 105 (2014) 143–150.

[21] Y. Guan, Y. Ma, K. Zhang, H. Chen, G. Xu, W. Liu, Y. Yang, Co-pyrolysis behaviours of energy grass and lignite, Energ Convers Manage 93 (2015) 132–140.

[22] H.N. Hisham, S. Othman, H. Rokiah, M.A. Latif, S. Ani, M.M. Tamizi, Characterization of bamboo *gigantochloa Scortechinii* at different ages, J Tropical Forest Science 18 (4) (2006) 236–242.

[23] L. Cheng, S. Adhikari, Z. Wang, Y. Ding, Characterization of bamboo species at different ages and bio-oil production, J Anal Appl Pyrol 116 (2015) 215–222.

[24] T.A. Lestander, B. Johnsson, M. Grothage, NIR technique create added value for the pellet and biofuel industry, Bioresource Technol 100 (2009) (1589-1594)

[25] B.G. Osborne, T. Fearn, Near Infrared Spectroscopy in Food Analysis, Longman Science and Technical, London, 1986.

[26] J. Workman, J.R.L. Weyer, Practical Guide to Interpretive Near-Infrared Spectroscopy, Taylor and Francis, Boca Raton, FL, 2007, pp. 240–262.

[27] C.C. Guimarães, M.L. Simeone, R.A.C. Parrella, M.M. Sena, Use of NIRS to predict composition and bioethanol yield from cell wall structure components of sweet sorghum biomass, Microchem J 117 (2014) 194-201.

[28] J. Posom, P. Sirisomboon, Evaluation of the thermal properties of Jatropha curcas L. kernels using near-infrared spectroscopy. Biosystem Eng 125 (2014) 45-53.

[29] J. Posom, P. Sirisomboon, Evaluation of the moisture content of *Jatropha curcas* kernels and the heating value of the oil extracted residue using near-infrared spectroscopy, Biosystem Eng 130 (2015) 52-59.

[30] C.C. Fagan, C.D. Everard, K. McDonnell, Prediction of moisture, calorific value, ash and carbon content of two dedicated bioenergy crops using near-infrared spectroscopy, Bioresour Technol 102 (2011) 5200–5206.

[31] J.I. Park, L. Liu, X.P. Ye, M.K. Jeong, Y-S Jeong, Improved prediction of biomass composition for switchgrass using reproducing kernel methods with wavelet compressed FT-NIR spectra, Expert Syst Appl 39 (2012) 1555–1564.

[32] J.M. Triolo, AJ. Ward, L. Pedersen, M.M. Løkke, H. Qu, S.G. Sommer, Near infrared reflectance spectroscopy (NIRS) for rapid determination of biochemical methane potential of plant biomass, Appl Energ 116 (2014) 52–57.

[33] L. Liu, X.P. Ye, AR. Womac, S. Sokhansanj, Variability of biomass chemical composition and rapid analysis using FT-NIR techniques, Carbohyd Polym 81 (2010) 820–829.

[34] P. Dardenne, Some considerations about NIR spectroscopy, Closing speech at NIR-2009, NIR news 21(1) (2010) 8–14.

[35] B.M, NicolaÏ, K, Beullens, E, Bobelyn, A, Peirs, W, Saeys, K.I, Theron, J, Lammertyn, Nondestructive measurement of fruit and vegetable quality by means of NIR spectroscopy: A review, Postharvest Biol Technol 46 (2007) 99–118.

[36] P. Williams, Near-Infrared Technology—Getting The Best Out Of Light Edition 5.0. A Short Course in the Practical Implementation of Near-Infrared Spectroscopy for the User, PDK Grain, Nanaimo, Canada, 2007.

[37] Z. Yang, K. Li, M. Zhang, D. Xin, J. Zhang, Rapid determination of chemical composition and classification of bamboo fractions using visible–near infrared spectroscopy coupled with multivariate data analysis, Biotechnol Biofuels (2016) 1-18.

[38] JP. Conzen, Selection criteria for a PLS calibration; Method optimization. "Multivariate calibration". Bruker Optik GmbH; 2006, 2rd edition.

[39] B. Peters, Prediction of pyrolysis of pistachio shells based on its components hemicellulose, cellulose and lignin, Fuel Process. Technol. 92 (2011) 1993–1998.

[40] D. Chen, J. Zhou, Q. Zhang. Effects of heating rate on slow pyrolysis behaviour, kinetic parameters and products properties of moso bamboo. Bioresour. Technol. 169 (2014) 313–319.

[41] L. Sanchez-Silva, D. LÒpez-González, J. Villase, P. Sánchez, J.L. Valverde, Thermogravimetric–mass spectrometric analysis of lignocellulosic and marine biomass pyrolysis, Bioresour. Technol. 109 (2012) 163–172.

[42] M. Irfan, Q. Chen, Y. Yue, R. Pang, Q. Lin, X. Zhao, H. Chen, Co-production of biochar, bio-oil and syngas from halophyte grass (*Achnatherum splendens* L.) under three different pyrolysis temperatures. Bioresour. Technol. 211 (2016) 457–463.

[43] D. Chen, Y. Li, K. Cen, M. Luo, H. Li, B Lu, Pyrolysis poly generation of poplar wood: Effect of heating rate and pyrolysis temperature. Bioresour. Technol. 218 (2016) 780–788.

[44] P. Kim, S. Weaver, N. Labbé, Effect of sweeping gas flow rates on temperature-controlled multistage condensation of pyrolysis vapors in an auger intermediate pyrolysis system. J. Anal. Appl. Pyrolysis 118 (2016) 325–334.

[45] R. Zornoza, C. Guerrero, J. Mataix-Solera, K.M. Scow, V. Arcenegui, J. Mataix-Beneyto, Near infrared spectroscopy for determination of various physical, chemical and biochemical properties in Mediterranean soils. Soil Biol Biochem 40 (7) (2008) 1923–1930.

[46] H. Baillères, F. Davrieux, F. Ham-Pichavant, Near infrared analysis as a tool for rapid screening of some major wood characteristics in a eucalyptus breeding program, Annal Forest Sci 59 (2002) 479–90.

[47] S. Gaur, T.B, Reed, Thermal data for natural and synthetic fuels, Pyrolysis of the components of biomass. Marcel Dekker, Inc. New York. Basel. Hong Kong, 1998, pp. 83.

[48] D.L. Sills, J.M. Gossett, Using FTIR to predict saccharification from enzymatic hydrolysis of alkali pretreated biomasses. Biotechnol Bioeng 109 (2012) .62–353

[49] W. Jiang, G. Han, B.K. Via, M. Tu, W. Liu, O. Fasina, Rapid assessment of coniferous biomass lignin carbohydrates with near-infrared spectroscopy, Wood Sci Technol 48 (2014) 109–122.

[50] G. Xiao, M-J. Ni, H. Huang, Y. Chi, R. Xiao, Z-P. Zhong, K-F. Cen. Fluidized-bed pyrolysis of waste bamboo, J Zhejiang Univ Sci A 2007 8(9) 1495-1499.

[51] Z. Jiang, B. Fei, Z. Li, Pretreatment of bamboo by ultra-high pressure explosion with a highpressure homogenizer for enzymatic hydrolysis and ethanol fermentation, Bioresource Technology 214 (2016) 876–880.

[52] J. Xie, C-Y. Hse, C.F.D. Hoop, T. Hu, J. Qi, T.F. Shupe, Isolation and characterization of cellulose nanofibres from bamboo using microwave liquefaction combined with chemical treatment and ultrasonication, Carbohydr. Polym. 151 (2016) 725–734.

CHAPTER 7

OUTPUT

7.1 International journal publication

1) Jetsada Posom, Wanphut Saechua, Panmanas Sirisomboon, Evaluation of pyrolysis characteristics of milled bamboo using near-infrared spectroscopy. Renewable Energy, In Press, Available online 4 November 2016.
2) Jetsada Posom and Panmanas Sirisomboon, Evaluation of lower heating value and elemental composition of bamboo using near infrared spectroscopy, Energy, (Under first revision).

7.2 International conference publication

1) Jetsada Posom, Panmanas Sirisomboon, Axel Funke, Jessica Heinrich, Jessica Maier, Pia Griesheimer, Near infrared spectroscopy as an alternative method to thermogravimetric analysis for evaluation of volatile matter of bamboo wood chips presented by The 9th TSAE International Conference (TSAE2016), IMPACT Exhibition and Convention Center, Hall 7, Bangkok, Thailand, during September 8-10, 2016.

รายงานสรุปการเงิน ประจำปีงบประมาณ 2559

รหัสโครงการ สกอ.-2559A11862003

โครงการส่งเสริมการวิจัยในอุดมศึกษาและพัฒนามหาวิทยาลัยวิจัยแห่งชาติ

สำนักงานคณะกรรมการการอุดมศึกษา

ชื่อมหาวิทยาลัย สถาบันเทคโนโลยีพระจอมเกล้าเจ้าคุณทหารลาดกระบัง

ชื่อโครงการ (ไทย) การใช้เนียร์อินฟราเรดสเปกโทรสโกปีแทนวิธีเทอร์โมกราวิเมทรี และบอมบ์แคลอริเมทรีในการวิเคราะห์สมรรถนะการแยกสลายด้วยความร้อน การเผาไหม้ พารามิเตอร์เชิงจลน์ และค่าความร้อนสูงของชิ้นไม้ไผ่สับ

(อังกฤษ) Near infrared spectroscopy as an alternative for thermogravimetry and bomb calorimetry in evaluation of pyrolysis, combustion performance, kinetics parameter and higher heating value of bamboo wood chips

ชื่อ-สกุลหัวหน้าโครงการวิจัยผู้รับทุน/ผู้วิจัย (อ./ดร./ผศ./รศ./ศ.) ปานมนัส ศิริสมบูรณ์

รายงานในช่วงตั้งแต่วันที่ 1 เดือน.ตุลาคม. พ.ศ. 2558 ถึงวันที่ 30 เดือน กันยายน พ.ศ. 2559

ระยะเวลาดำเนินการ 12 เดือน ตั้งแต่วันที่ 1 เดือน.ตุลาคม. พ.ศ. 2558 ถึงวันที่ 30 เดือน กันยายน พ.ศ. 2559

รายจ่าย

หมวด	งบประมาณรวมทั้งโครงการ (บาท)	ค่าใช้จ่ายงวดปัจจุบัน	คงเหลือ (หรือเกิน)
1. ค่าตอบแทน	-	-	-
2. ค่าจ้าง	**105,000**	**105,000**	**0**
3. ค่าวัสดุ	**66,900**	**120,000**	**- 53,100**
4. ค่าใช้สอยอื่นๆ	**178,100**	**125,000**	**53,100**
4.1 ค่าเช่าเหมาพาหนะ	90,000	90,000	0
4.2 ค่าที่พัก	21,000	0	21,000
4.3 ค่าจ้างสับต้นไผ่	22,500	20,000	2,500
4.4 ค่าจ้างบดชิ้นไผ่สับ	9,000	15,000	-6,000
4.5 ค่าบำรุงรักษา	30,000	0	30,000
4.6 ค่าปรับเทียบเครื่องชั่ง	5,000	0	5,000
4.7 ค่าถ่ายเอกสาร	600	0	600
รวม	350,000	350,000	0

จำนวนเงินที่ได้รับและจำนวนเงินคงเหลือ

จำนวนเงินที่ได้รับ 350,000 บาท

งวดที่ 1 210,000 บาท เมื่อ 8 มีนาคม 2559

งวดที่ 2 140,000 บาท เมื่อ 18 พฤษภาคม 2559

รวม 350,000 บาท

....

ลงนามหัวหน้าโครงการวิจัยผู้รับทุน

...../...../.....

ลงนามเจ้าหน้าที่การเงินโครงการ

...../...../.....

ข้อมูลประวัติคณะผู้วิจัย (รูปแบบปรับได้ตามความเหมาะสม)

ประวัติส่วนตัวหัวหน้าโครงการวิจัย

1. ชื่อ (ภาษาไทย) **นางสาว ปานมนัส ศิริสมบูรณ์**

   (ภาษาอังกฤษ) **Ms. Panmanas Sirisomboon**

2. รหัสประจำตัวนักวิจัยแห่งชาติ **38-50-0171**
3. เลขหมายบัตรประจำตัวประชาชน 4-1009-00107-43-1
4. ตำแหน่งปัจจุบัน **รองศาสตราจารย์**
5. หน่วยงานที่อยู่ที่ติดต่อได้พร้อมเบอร์โทรศัพท์และโทรสารหลักสูตรวิศวกรรมเกษตร สาขาวิชาวิศวกรรมเครื่องกล คณะวิศวกรรมศาสตร์

   สถาบันเทคโนโลยีพระจอมเกล้าเจ้าคุณทหารลาดกระบัง

   กรุงเทพฯ 10520

   โทรศัพท์ 02-329800 ต่อ 5120, 5008

   โทรสาร 02-33298336
6. ประวัติการศึกษา

   ปริญญาตรี (พ.ศ.2519 - พ.ศ.2523) วศ.บ. (วิศวกรรมเกษตร) มหาวิทยาลัยเกษตรศาสตร์

   ปริญญาโท (พ.ศ.2525 - พ.ศ. 2527) M.Eng. (Farm machinery and management) Asian Institute of Technology (Thailand)

   ปริญญาเอก (พ.ศ.2540 - พ.ศ.2544) Ph.D. (Agric. Science) United Graduate School of Kagoshima University (Saga University), Japan.
6. สาขาวิชาที่มีความชำนาญเป็นพิเศษ (แตกต่างจากวุฒิการศึกษา) ระบุสาขาวิชาการ

   สมบัติทางกายภาพและวิศวกรรมของวัสดุเกษตรและอาหาร

   สมบัติทางเนื้อสัมผัสของวัสดุเกษตรและอาหาร

   การตรวจสอบคุณภาพของวัสดุเกษตรและอาหารโดยใช้ Near Infrared Spectroscopy

   เทคโนโลยีการขนถ่ายวัสดุ

รางวัลงานวิจัยคุณภาพในการประชุมวิชาการ มหาวิทยาลัยเกษตรศาสตร์ วิทยาเขตกำแพงแสน ครั้งที่ 6 ประจำปี 2552 (The 6th Conference of Kasetsart University Kamphaeng Saen Campus)

สาขาวิศวกรรมศาสตร์

ระดับดีเด่น

ปานมนัส ศิริสมบูรณ์ และ พัชรี คล้ายมณี
เรื่อง : สมบัติเชิงกายภาพของข้าวโพดหวาน
(Physical Properties of Sweet Corn)

Scientific Award of Excellence for 2011 selected by the American Biographical Institute, Inc., USA

7. ประสบการณ์ที่เกี่ยวข้องกับการบริหารงานวิจัยทั้งภายในและภายนอกประเทศ โดยระบุสถานภาพในการทำการวิจัยว่าเป็นผู้อำนวยการแผนงานวิจัย หัวหน้าโครง การวิจัย หรือผู้ร่วมวิจัยในแต่ละข้อเสนอการวิจัย เป็นต้น
   7.1 ผู้อำนวยการแผนการวิจัย : ชื่อแผนงานวิจัย -
   7.2 หัวหน้าโครงการวิจัย : ชื่อโครงการวิจัย
   1. **โครงการ เครื่องเกี่ยวนวดถั่วเหลือง** (ทุนวิจัยกระทรวงวิทยาศาสตร์และสิ่งแวดล้อม)
   2. **โครงการ เครื่องคัดแยกถั่วเหลืองฝักสด** (ทุนวิจัยเงินรายได้คณะวิศวกรรมศาสตร์ สจล.)
   3. **โครงการ การศึกษาสมบัติทางกายภาพและวิศวกรรมของมะม่วงพันธุ์น้ำดอกไม้ซึ่งเป็นพันธุ์ที่มีการส่งออก** (ทุนวิจัยงบประมาณแผ่นดินโดยพิจารณาโครงการโดยสภาวิจัย 496,280 บาท)
   4. **โครงการเครื่องทำน้ำกะทิเข้มข้นแบบที่ระเหยที่ความดันต่ำกว่าบรรยากาศ** (เงินรายได้คณะวิศวกรรมศาสตร์ สจล. 147,000 บาท ปี 2549)
   5. **โครงการการออกแบบและพัฒนาเครื่องผลิตเนยแข็งขนาดเล็ก** (เงินรายได้คณะวิศวกรรมศาสตร์ สจล. 152,500 บาท ปี 2550)
   6. **โครงการการออกแบบและพัฒนาเครื่องทำไอศกรีมโดยใช้ระบบการทำความเย็นเบื้องต้นที่ความดันสุญญากาศ** (เงินรายได้คณะวิศวกรรมศาสตร์ สจล. 67,060 บาท ปี 2551)
   7. **การประเมินดัชนีคุณภาพภายในและภายนอกของส้มโอเพื่อการส่งออกที่ระยะเวลาเก็บรักษาต่าง ๆ กันด้วยวิธีไม่ทำลายโดยใช้เทคนิคเนียร์อินฟราเรดสเปคโตสโคปี** (ทุนวิจัยมหาบัณฑิต สกว. สาขาวิทยาศาสตร์และเทคโนโลยี 200,000 บาท ปี2551)

8. **โครงการเครื่องทำแห้งเนื้อมะพร้าวขูดด้วยความดันสูญญากาศเพื่อการผลิตน้ำมันมะพร้าวบริสุทธิ์** (เงินรายได้คณะวิศวกรรมศาสตร์ สจล. 100,000 บาท ปี 2552)
9. **โครงการการวิเคราะห์ค่าปริมาณเนื้อยางแห้งและความหนืดของน้ำยางข้นสำหรับห้องปฏิบัติการในโรงงานด้วยวิธีไม่ทำลายโดยใช้เทคนิคเนียร์อินฟราเรดสเปคโตรสโคปี** (สกว. ฝ่ายอุตสาหกรรม ในโครงการวิจัยขนาดเล็กเรื่องยางพารา ปี 2552 **132,000** บาท)
10. **โครงการเครื่องทำแห้งเนื้อมะพร้าวขูดด้วยความดันสูญญากาศร่วมกับคลื่นอินฟราเรดเพื่อการผลิตน้ำมันมะพร้าวบริสุทธิ์** (เงินรายได้คณะวิศวกรรมศาสตร์ สจล. 59,000 บาท ปี 2553)
11. **โครงการการวิเคราะห์ปริมาณเนื้อยางแห้งในน้ำยางสดและน้ำยางข้นโดยการวัดที่ต้นยางพาราโดยตรงด้วยวิธีไม่ทำลายโดยใช้เทคนิคเนียร์อินฟราเรดสเปคโตรสโคปี** (ทุนวิจัยงบประมาณแผ่นดิน ประจำปี 2553-2554โดยพิจารณาโครงการโดยสภาวิจัย 551,200 บาทและ สกอ. 192,800บาท)
12. **โครงการการวิเคราะห์ปริมาณไลโคปีนในเนื้อแตงโมด้วยเทคนิคที่ไม่ทำลายด้วยวิธีเนียร์อินฟราเรดสเปกโตรสโคปี** (ทุนวิจัยงบประมาณแผ่นดิน ประจำปี 2554โดยพิจารณาโครงการโดยสภาวิจัย 242,500บาท)
13. **โครงการการพัฒนาเทคนิคมาตรฐานการวัดเนื้อสัมผัสข้าวสวยเพื่อใช้ในอุตสาหกรรมผลิตข้าวสารและข้าวแปรรูป** (เงินรายได้คณะวิศวกรรมศาสตร์ สจล. 72,000 บาท ปี 2555)
14. **โครงการการตรวจสอบคุณภาพของส้มโอพันธุ์ขาวน้ำผึ้ง โดยวิธีแบบไม่ทำลายด้วยเทคนิค Near Infrared Spectroscopy** (เงินรายได้คณะวิศวกรรมศาสตร์ สจล. 72,000 บาท ปี 2555)
15. **โครงการเครื่องกะเทาะเปลือกผลและเปลือกเมล็ดสบู่ดำ** (เงินรายได้คณะวิศวกรรมศาสตร์ สจล. 72,000 บาท ปี 2555)
16. **โครงการการวิเคราะห์สารแกมมาอะมิโนบิวทิริกแอซิดหรือสารกาบาในข้าวกล้องงอกด้วยเทคนิคเนียร์อินฟราเรดสเปคโตรสโคปี** (ทุนวิจัยงบประมาณแผ่นดิน ประจำปี 2555โดยพิจารณาโครงการโดยสภาวิจัย 1,207,000บาท)
17. โครงการการจำแนกพันธ์ข้าวหอมมะลิจากพันธุ์ปลอมปนโดยวิธีไม่ทำลายด้วยเทคนิคการประมวลผลภาพ (เงินรายได้คณะวิศวกรรมศาสตร์ สจล. 80,000 บาท ปี 2556)

18. โครงการการตรวจวัดสารที่มีสรรพคุณต่อสุขภาพและสมบัติที่เกี่ยวข้องบางประการในน้ำพริกแกงแดงของไทยโดยเทคนิคเนียร์อินฟราเรดสเปกโทรสโกปี (เงินรายได้คณะวิศวกรรมศาสตร์ สจล. 80,000 บาท ปี 2556)
19. โครงการการพัฒนาเทคนิคการวัดปริมาณน้ำมันและสมบัติเชิงความร้อนของชีวมวลโดยวิธีไม่ทำลายด้วยเนียร์อินฟราเรดสเปกโตรสโคปี: กรณีศึกษา เนื้อในเมล็ดสบู่ดำ (ประจำปี 2556โครงการทุนวิจัยมหาบัณฑิต สกว. สาขาวิทยาศาสตร์และเทคโนโลยี 270,000บาท)
20. โครงการการวิเคราะห์ปริมาณเกลือของปลาซาร์ดีนในอุตสาหกรรมผลิตปลาซาร์ดีนกระป๋องด้วยเทคนิคเนียร์อินฟราเรดสเปกโทรสโกปี (ประจำปี 2556 ทุนพัฒนานักวิจัย กองทุนวิจัย สถาบันเทคโนโลยีพระจอมเกล้าเจ้าคุณทหารลาดกระบัง 924,000 บาท)
21. โครงการเทคนิคแบบไม่ทำลายสำหรับการวัดความหนืด ปริมาณความเป็นด่าง และจำนวนโพแทสเซียมไฮดรอกไซด์ในน้ำยางพาราข้นโดยเนียร์อินฟราเรดสเปกโทรสโกปี(โครงการทุน พวอ. ระดับปริญญาโท ประจำปี 2556 300,000 บาท)
22. โครงการการวิเคราะห์อิสตามีนและความสดของปลาซาร์ดีนด้วยเทคนิคเนียร์อินฟราเรดสเปกโทรสโกปี(ทุนวิจัยงบประมาณแผ่นดิน ประจำปี 2557โดยพิจารณาโครงการโดยสภาวิจัย 729,000บาท)
23. โครงการการศึกษาความเป็นไปได้ในการตรวจวัดปริมาณความชื้นในแป้งมันสำปะหลังหมาดโดยเนียร์อินฟราเรดสเปกโทรสโกปี (เงินรายได้คณะวิศวกรรมศาสตร์ สจล. 60,000 บาท ปี 2557)
24. โครงการการวิเคราะห์องค์ประกอบหลักของน้ำผึ้งโดยใช้เนียร์อินฟราเรดสเปกโทรสโกปี (เงินรายได้คณะวิศวกรรมศาสตร์ สจล. 60,000 บาท ปี 2557)
25. โครงการการวิเคราะห์คุณภาพของน้ำแกงเขียวหวานและน้ำแกงเผ็ดแดงด้วยเนียร์อินฟราเรดสเปกโทรสโกปี (โครงการพัฒนานักวิจัยและงานวิจัยเพื่ออุตสาหกรรม (พวอ.): ระดับปริญญาโท ประจำปี 2557 300,000 บาท)
26. โครงการการใช้เนียร์อินฟราเรดสเปกโทรสโกปีแทนวิธีเทอร์โมกราวิเมทรีและบอมบ์แคลอริเมทรีในการวิเคราะห์สมรรถนะการแยกสลายด้วยความร้อน พารามิเตอร์เชิงจลน์และค่าความร้อนสูงของไม้ไผ่อัดเม็ด (โครงการปริญญาเอกกาญจนาภิเษก(คปก) สาขาวิทยาศาสตร์และเทคโนโลยี 1,838,000 บาท ปี 2557)
27. โครงการการประเมินความสุกแก่ของทุเรียนพันธุ์หมอนทองเพื่อการส่งออกและการประเมินคุณภาพการรับประทานของเนื้อทุเรียนพันธุ์หมอนทองเพื่อการขายในห้างสรรพสินค้าโดยใช้เทคนิคเนียร์อินฟราเรดสแปกโทรสโกปี(ทุนวิจัยงบประมาณแผ่นดิน ประจำปี 2558โดยพิจารณาโครงการโดยสภาวิจัย 297,900 บาท)

28. โครงการการตรวจการปลอมปนของน้ำส้มสดโดยสารละลายน้ำตาลโดยใช้เนียร์อินฟราเรดสเปกโทรสโกปี (เงินรายได้คณะวิศวกรรมศาสตร์ สจล. 50,000 บาท ปี 2558)
29. โครงการการประเมินความสุกแก่และคุณภาพการรับประทานของเมลอนโดยใช้เทคนิคเนียร์อินฟราเรดสแปกโทรสโกปี (ทุนพัฒนานักวิจัย กองทุนวิจัย สถาบันเทคโนโลยีพระจอมเกล้าเจ้าคุณทหารลาดกระบัง ประจำปี 2558 675,000 บาท)
30. โครงการการใช้เนียร์อินฟราเรดสเปกโทรสโกปีแทนวิธีเทอร์โมกราวิเมทรี และบอมบ์แคลอริเมทรีในการวิเคราะห์สมรรถนะการแยกสลายด้วยความร้อน การเผาไหม้ พารามิเตอร์เชิงจลน์ และค่าความร้อนสูงของชิ้นไม้ไผ่สับ(โครงการส่งเสริมการวิจัยในอุดมศึกษาและพัฒนามหาวิทยาลัยวิจัยแห่งชาติ สำนักงานคณะกรรมการการอุดมศึกษาประจำปีงบประมาณ พ.ศ. 2559 350,000 บาท)
31. โครงการการประยุกต์เทคนิคเนียร์อินฟราเรดสเปกโทรสโกปีเพื่อวิเคราะห์ความหนาแน่นของพันธะเชื่อมขวาง ปริมาณสบู่แอมโมเนียมลอเรตและปริมาณเตตระเมทธิลไทยูแรมไดซัลไฟด์ของน้ำยางธรรมชาติและผลิตภัณฑ์จากน้ำยาง(งบประมาณทุนวิจัยมุ่งเป้าของสำนักงานคณะกรรมการวิจัยแห่งชาติประจำปีงบประมาณ 2559 960,200 บาท)

7.3 งานวิจัยที่ทำเสร็จแล้ว :

1. โครงการ เครื่องเกี่ยวนวดถั่วเหลือง (หัวหน้าโครงการ)

Sirisomboon, P., W. Tangcharoenchai, and R.Nochai, 1994. Performance of Rice Reaper and Reaper Binder in Harvesting Soybean. Proceedings of World Soybean Research Conference V, 21-27 February 1994. Chiang Mai, Thailand. 8 p.

Nochai, R., P. Sirisomboon, and W. tangcharoenchai, 1994. Soybean Growers and Mechanization Situation Case Study: Sukhothai Province. Proceedings of World Soybean Research Conference V, 21-27 February 1994. Chiang Mai, Thailand. 5 p.ปานมนัส ศิริสมบูรณ์, วรรณา ตั้งเจริญชัย และ รังสรร โนชัย, 2537. การออกแบบหัวเกี่ยวถั่วเหลืองติดรถไถเดินตาม. รายงานการประชุมทางวิชาการทางวิศวกรรมเกษตร. 18-20 พฤษภาคม 2537. มหาวิทยาลัยเกษตรศาสตร์ วิทยาเขตกำแพงแสน นครปฐม. หน้า 1-4.

Chanchai Rojanasaroj, Panmanas Sirisomboon, Rangsan Nochai, Wanna Tangjaroenchai: Small Soybean Harvester Implementing a Two-wheel Tractor, Electronic-only Proceedings of the

International Conference on Crop Harvesting and Processing, 9-11 February 2003, Louisville, Kentucky, USA.

2. โครงการวิจัย เครื่องคัดแยกถั่วเหลืองฝักสด (หัวหน้าโครงการ)

ปานมนัส ศิริสมบูรณ์, ธีรนุต ร่มโพธิ์ภักดิ์ และ พิมพ์เพ็ญ พรเฉลิมพงศ์, 2545. เครื่องคัดแยกถั่วเหลืองฝักสด. รายงานการประชุมทางวิชาการสมาคมวิศวกรรมเกษตรแห่งประเทศไทย ครั้งที่ 3. 23-24 พฤษภาคม 2545. วิศวกรรมเกษตรกับการพัฒนาภูมิปัญญาท้องถิ่น. โรงแรมอิมพีเรียลแม่ปิง เชียงใหม่. หน้า 19-25.

ปานมนัส ศิริสมบูรณ์, ธีรนุต ร่มโพธิ์ภักดิ์ และ พิมพ์เพ็ญ พรเฉลิมพงศ์, 2547. สมบัติทางกายภาพของถั่วเหลืองฝักสด. รายงานการประชุมทางวิชาการสมาคมวิศวกรรมเกษตรแห่งประเทศไทย ครั้งที่ 5. 26-27 เมษายน 2547. นวัตกรรมทางวิศวกรรมเกษตรเพื่อการเพิ่มผลผลิต. ภาควิชาวิศวกรรมเกษตร คณะวิศวกรรมศาสตร์ สถาบันเทคโนโลยีพระจอมเกล้าเจ้าคุณทหารลาดกระบัง. หน้า 360-367.

Panmanas Sirisomboon, Pimpen Pornchaloeampong, and Teeranud Romphophak, 2005. Physical properties of green soybean: Criteria for sorting. Proceedings of the 2nd International Conference on Innovations in food processing technology and engineering. 11-13 January 2005. Asian Institute of Technology, Bangkok, Thailand.

Panmanas Sirisomboon, Pimpen Pornchaloeampong, and Teeranud Romphophak, 2007. Physical properties of green soybean: Criteria for sorting. J. Food Engineering. 79: 18-22.

Panmanas Sirisomboon, Yuki Hashimoto and Munehiro Tanaka, 2008. Study on Non-destructive Evaluation Methods for Defect Pods for Green Soybean Processing by Near-Infrared Spectroscopy. Annual Meeting on the Japanese Society of Agricultural Machinery, 27 - 30 March 2008. Miyazaki Kanko Hotel 1-1-1 Matsuyama, Miyazaki-city, Miyazaki-prefecture, Japan.

Panmanas Sirisomboon, Yuki Hashimoto, Munehiro Tanaka. Study on non-destructive evaluation methods for defect pods for green soybean processing by near-infrared spectroscopy Journal of Food Engineering, 93 (4), 502-512 (2009)

3. โครงการวิจัย Study on the relationship between texture and pectin constituents of Japanese pear (ผู้ร่วมวิจัย)

Panmanas Sirisomboon, Munehiro Tanaka, Takayoshi Akinaga and Takayuki Kojima 2001. Evaluation of the texture properties of Japanese pear, Journal of Texture Studies 31. 665-677. (be cited by Thompson A.K.: Fruit ripening conditions. In Fruit and vegetables-

harvesting, handling and storage. 2nd editions. Blackwell Publishing. UK p. 88 (2003))

Panmanas Sirisomboon, Munehiro Tanaka, Shuji Akinaga and Takayuki Kojima 2001. Relationship between the texture and pectin constituents of Japanese pear, Journal of Texture Studies 31. 679-690.

Panmanas Sirisomboon, Munehiro Tanaka, Shuji Fujita,Takayoshi Akinaga and Takayuki Kojima 2001. A simplified method for the determination of total oxalate soluble pectin content of Japanese pear. Journal of food Composition and Analysis. 14, 14: 83-91.

Takayuki Kojima, Shuji Fujita, Munehiro Tanaka, Panmanas Sirisomboon 2004 Chapter 11, Plant Compounds and Fruit Texture: the Case of Pear. In Texture in Food, Volume 2: Solid Foods, David Kilcast Editor. Woodhead publishing limited. Cambridge, England. 1st edition p 259-294.

Panmanas Sirisomboon, Munehiro Tanaka, Shuji Fujita, Takayuki Kojima 2007. Evaluation of pectin constituents of Japanese pear by near infrared spectroscopy, J. Food Engineering 78(2): 701-707.

4. โครงการ การศึกษาสมบัติทางกายภาพและวิศวกรรมของมะม่วงพันธุ์น้ำดอกไม้ซึ่งเป็นพันธุ์ที่มีการส่งออก

ปานมนัส ศิริสมบูรณ์, และ ศุภสมบูรณ์ อึงรัตนากร, 2548. การใช้เครื่องจักรกลเกษตรในสวนมะม่วง. รายงานการประชุมทางวิชาการสมาคมวิศวกรรมเกษตรแห่งประเทศไทย ครั้งที่ 6. 30-31 มีนาคม 2548. วิศวกรรมเกษตรนำไทยสู่ครัวโลก. โรงแรมมิราเคิลแกรนด์ กรุงเทพมหานคร. หน้า 40-41.

Panitnat Yimyam, Thanarat Chalidabhongse, Panmanas Sirisomboon and Suwanee Boonmung, 2005. Physical Properties Analysis of Mango using Computer Vision, Proceedings of the International Conference on Control, Automation, and Systems (ICCAS 2005) June 2-5, 2005, KINTEX (Korea International Exhibition Center) The Province of Gyeonggi, Korea. (Best Presentation Award)

ปานมนัส ศิริสมบูรณ์, ศุภสมบูรณ์ อึงรัตนากร, ดนัย ปัญจพิทยากุล, 2548. การใช้อุปกรณ์และเครื่องจักรกลเกษตรในสวนมะม่วง. วารสารเกษตรพระจอมเกล้า 23(3): 28-40

ปานมนัส ศิริสมบูรณ์, ศุภสมบูรณ์ อึงรัตนากร, ดนัย ปัญจพิทยากุล, 2549. ความเมื่อยล้าในการใช้เครื่องมือและเครื่องจักรกลเกษตรในสวนมะม่วง. รายงานการประชุมทางวิชาการสมาคมวิศวกรรมเกษตรแห่งประเทศไทย ครั้งที่ 7. 23-24 มกราคม 2549. งานวิจัยเพื่อเพิ่มศักยภาพสินค้าเกษตรไทยในตลาดโลก. คณะวิศวกรรมศาสตร์ มหาวิทยาลัยมหาสารคาม มหาสารคาม. หน้า 32-38.

Thanarat H Chalidabhongse, Panitnat Yimyam, Panmanas Sirisomboon, 2006. 2D/3D Vision-Based Mango's Feature Extraction and Sorting, Proceedings of the 9th International Conference on Control, Automation, Robotics and Vision (ICARCV 2006), December 5-8,

2006, Grand Hyatt, Singapore.

Sirisomboon, P., Boonmung, S., Pornchaloempong P., and Pithuncharurnlap, M. A Preliminary Study on Classification of Mango Maturity by Compression Test. International Journal of Food Properties, 11: 206-212 (2008).

P. Sirisomboon, P. Pornchaloempong. Instrumental textural properties of mango (cv Nam Doc mai) at commercial harvesting time. International Journal of Food Properties, 14, 441-449 (2011).

Panitnat YIMYAM, Somkit JAITRONG, **Panmanas SIRISOMBOON**. Mango Maturity Classification by using Physical Properties, The 12th Annual Conference of Thai Society of Agricultural Engineering "International Conference on Agricultural Engineering" (Novelty, Clean and Sustainable) Chon-Chan Pattaya Resort, Chonburi, Thailand; 31 March-1 April 2011, p 50-1 -50-4.

5. โครงการ เครื่องจักรกลเกษตรและอาหาร

Panmanas Sirisomboon, Vasu Udompetaikul and Yaowaluk Suraphantapisit, 2007. Design and Development of A Simple Meat Quality-Improving Machine. Proceedings of International Conference on Agricultural, Food, and Biological Engineering & Post Harvest/Production Technology, January 21-24, 2007. Sofitel Raja Orchid Hotel, Khon Kaen, Thailand.

Vipa Jayranaiwachira and Panmanas Sirisomboon, 2007. Effect of Agitation Parameters on Viscosity Properties of Concentrated Coconut Milk. Proceedings of International Conference on Agricultural, Food, and Biological Engineering & Post Harvest/Production Technology, January 21-24, 2007. Sofitel Raja Orchid Hotel, Khon Kaen, Thailand.

Panmanas Sirisomboon, Yothin Prempraneerach, Phornsuk Ratiroch-anant, and Yaowaluk Suraphantapisit 2008. Automatic Table Top Stuffer for Sausage. CR1-15, Proceedings of the 9th Thai Society of Agricultural Engineering annual meeting –Technology for Sustainable Agriculture and Agro-Industry- January 31- February 1, 2008, Faculty of Engineering and Agricultural Industry, Maejo University, Thailand. (in Thai).

Nuthvipa Jayranaiwachira and Panmanas Sirisomboon 2008. Physical Properties of Concentrated Coconut Milk by Evaporating at Vacuum Pressure. CR1-21, Proceedings of the 9th Thai Society of Agricultural Engineering annual meeting –Technology for Sustainable Agriculture and Agro-Industry- January 31- February 1, 2008, Faculty of Engineering and

Agricultural Industry, Maejo University, Thailand. (in Thai).

ปานมนัส ศิริสมบูรณ์, และ มงคล สกุลทองอร่าม, 2553. สมรรถนะของเครื่องทำแห้งเนื้อมะพร้าวขูดระบบสุญญากาศร่วมกับการนำความร้อนด้วยน้ำร้อน. รายงานการประชุมทางวิชาการสมาคมวิศวกรรมเกษตรแห่งประเทศไทย ครั้งที่ 11. 6-7 พฤษภาคม 2553. นวัตกรรมทางวิศวกรรมเกษตรเพื่อเศรษฐกิจพอเพียงและชุมชนเข้มแข็ง. มหาวิทยาลัยเกษตรศาสตร์ วิทยาเขตกำแพงแสน นครปฐม. หน้า 242-246.

Panmanas SIRISOMBOON, Mongkol SKUNTHONGARLAM. The optimal condition for coconut flakes dryer with vacuum and infrared heater, The 12th Annual Conference of Thai Society of Agricultural Engineering "International Conference on Agricultural Engineering" (Novelty, Clean and Sustainable) Chon-Chan Pattaya Resort, Chonburi, Thailand; 31 March-1 April 2011, p 55-1 -50-5.

6. โครงการ สบู่ดำและชีวมวล

Panmanas Sirisomboon, Prakob Kitchaiya, Teerapong Pholpho and Wiroj Mahuttanyavanitch: Physical and mechanical properties of Jatropha curcas L. fruits, nuts and kernels, Biosystems Engineering, 2007, 97:201-207.

P. Sirisomboon, P. Kitchaiya, Physical properties of *Jatropha curcas* L. kernels after heat treatments. Biosystems Engineering, 2009, 102 (2), 244-250.

Panmanas Sirisomboon, Jetsada Posom, Thermal properties of Jatropha curcas L. kernels. Biosystems Engineering, 113(4), 402-409.

Jetsada Posom and **Panmanas Sirisomboon**. Development of the technique for measuring of oil content and thermal properties of biomass by non-destructive method using near infrared spectroscopy: case study of Jatropha curcas kernels. RRI-MAG Congress I, the Twin Tower, Bangkok, Thailand Thailand during April 3-5, 2014 (in Thai).

Jetsada Posom, Panmanas Sirisomboon, Evaluation of the thermal properties of Jatropha curcas L. kernels using near-infrared spectroscopy, Biosystems Engineering, 125, 45-53 (2014).

Jetsada Posom, Panmanas Sirisomboon, Evaluation of the moisture content of Jatropha curcas kernels and the heating value of the oil-extracted residue using near-infrared spectroscopy. Biosystems Engineering, 130, 52-59 (2015).

Amrit Shrestha, Wanphut Saechua, Panmanas Sirisomboon, Some physical and combustion

characteristic of Leucaena leucophala pellet, The 8th TSAE International conference, Bitec, Bangkok, Thailand during March 17-19, 2015.

Jetsada Posom, Amrit Shrestha, Wanphut Saechua, Panmanas Sirisomboon, Rapid non-destructive evaluation of moisture content and higher heating value of Leucaena leucocephala pellets using near infrared spectroscopy. Energy, 107, 464-472, (2016).

Jetsada Posom, Panmanas Sirisomboon, Axel Funke, Jessica Heinrich, Jessica Maier, Pia Griesheimer, Near infrared spectroscopy as an alternative method to thermogravimetric analysis for evaluation of volatile matter of bamboo wood chips presented by The 9th TSAE International Conference (TSAE2016), IMPACT Exhibition and Convention Center, Hall 7, Bangkok, Thailand, during September 8-10, 2016.

7. โครงการตรวจสอบคุณภาพส้มโอโดยไม่ทำลาย

ปานมนัส ศิริสมบูรณ์, จรูญพงศ์ เทียมประทีป, รวิภัทร ลาภเจริญสุข, จิตรา ด้วงช้าง. 2551. คุณภาพของเนื้อส้มโอพันธุ์ขาวน้ำผึ้งที่อายุการเก็บเกี่ยวต่างๆ. รายงานการประชุมทางวิชาการและเสนอผลงานวิจัย มหาวิทยาลัยทักษิณครั้งที่ 18 ประจำปี 2551, การวิจัยกับการแก้ปัญหาวิกฤติชาติ 25-26 กันยายน 2551. โรงแรมกรีนเวิลด์ พาเลซ อำเภอเมือง จังหวัดสงขลา หน้า 27 (6 หน้า)

ปานมนัส ศิริสมบูรณ์ และ รวิภัทร ลาภเจริญสุข. 2552. การศึกษาสมบัติทางกายภาพและเชิงกลของผลส้มโอพันธุ์ขาวน้ำผึ้งระหว่างระยะเวลาการเก็บรักษาต่างๆ. เรื่องเต็มการประชุมทางวิชาการครั้งที่ 47 มหาวิทยาลัยเกษตรศาสตร์ "เกษตรนำไทย : อาหารและพลังงานทดแทนสู่สมดุลอย่างยั่งยืน" เล่มที่ 7 สาขาสถาปัตยกรรมศาสตร์และวิศวกรรมศาสตร์ 17-20 มีนาคม 2552 มหาวิทยาลัยเกษตรศาสตร์ วิทยาเขตบางเขน กรุงเทพมหานคร

Panmanas Sirisomboon, Jittra Duangchang. 2009. Prediction and analysis of peel essential oil of pomelo by NIR spectroscopy. 10th International Conference of Thailand Society of Agricultural Engineering on "Innovations of Agricultural, Food and Renewable Energy Productions for Mankind" 1-3 April 2009 , Suranaree Univeristy of Technology, THAILAND.

Panmanas Sirisomboon, Warunee Thanapase, Ravipat Lapcharoensuk 2009. Identification of Different Storage Duration of Pomelo (Kao Num Peung Variety) by Near Infrared Spectroscopy using SIMCA. 10th International Conference of Thailand Society of Agricultural Engineering on "Innovations of Agricultural, Food and Renewable Energy Productions for

Mankind" 1-3 April 2009 , Suranaree Univeristy of Technology, THAILAND.

Panmanas Sirisomboon, Charoonpong Theamprateep 2009. Maturity Classification of Kao Nampueng Pomelo Fruit using Visible Range Spectrum. 10th International Conference of Thailand Society of Agricultural Engineering on "Innovations of Agricultural, Food and Renewable Energy Productions for Mankind" 1-3 April 2009 , Suranaree Univeristy of Technology, THAILAND.

Panmanas Sirisomboon, Warunee Thanapase, Ravipat Lapcharoensuk. Identification of Different Storage Duration of Pomelo (Kao Num Peung Variety) by Near Infrared Spectroscopy using PLS-DA. The 3rd Asian Near Infrared Symposium (ANS2012) Amari Watergate Hotel, Bangkok, Thailand; 14-18 May 2012.

P. Sirisomboon and C. Theamprateep, Physicochemical and Textural Properties of Pomelo (Citrus maxima Merr. cv. Kao Num Peung) at Preharvest, Postharvest and During the Commercial Harvest Period. The Philippine Agricultural Scientist, 95 (1), 43-52 (2012).

P. Sirisomboon, R. Lapchareonsuk, Evaluation of the physicochemical and texture properties of pomelo fruit following storage. Fruits, 67 (6), 399-414 (2012).

Panmanas Sirisomboon, Warunee Thanapase, Ravipat Lapcharoensuk. Identification of Different Storage Duration of Pomelo (Kao Num Peung Variety) by Near Infrared Spectroscopy using PLS-DA. The 3rd Asian Near Infrared Symposium (ANS2012) Amari Watergate Hotel, Bangkok, Thailand; 14-18 May 2012.

8. โครงการยางพารา

ปานมนัส ศิริสมบูรณ์ และรวิพันธ์ ชาวบ้านกร่าง 2552. สมบัติเชิงความหนืดของน้ำยางข้นที่อายุการเก็บรักษาต่างๆ. การประชุมวิชาการ มหาวิทยาลัยเกษตรศาสตร์ วิทยาเขตกำแพงแสน ครั้งที่ 6, 8-9 ธันวาคม 2552. มหาวิทยาลัยเกษตรศาสตร์ วิทยาเขตกำแพงแสน นครปฐม

ปานมนัส ศิริสมบูรณ์, และ อภิดุลย์ แก้วกับทอง, 2553. ผลของอายุการเก็บรักษาน้ำยางข้นต่อปริมาณเนื้อยางแห้ง. รายงานการประชุมทางวิชาการสมาคมวิศวกรรมเกษตรแห่งประเทศไทย ครั้งที่ 11. 6-7 พฤษภาคม 2553. นวัตกรรมทางวิศวกรรมเกษตรเพื่อเศรษฐกิจพอเพียงและชุมชนเข้มแข็ง. มหาวิทยาลัยเกษตรศาสตร์ วิทยาเขตกำแพงแสน นครปฐม. หน้า 382-385.

Panmanas SIRISOMBOON and Apidul KEAWKUPTONG. Evaluation of dry rubber content of concentrated latex by Near-infrared Spectroscopy, The 12th Annual Conference of

Thai Society of Agricultural Engineering "International Conference on Agricultural Engineering" (Novelty, Clean and Sustainable) Chon-Chan Pattaya Resort, Chonburi, Thailand; 31 March-1 April 2011, p 49-1 -49-5.

ปานมนัส ศิริสมบูรณ์, รวิพันธ์ ชาวบ้านกร่างและ อภิดุลย์ แก้วกับทอง, 2554. .การวิเคราะห์ค่าความหนืดและปริมาณเนื้อยางแห้งของน้ำยางสดและน้ำยางข้นสำหรับห้องปฏิบัติการในโรงงานด้วยเทคนิคเนียร์อินฟราเรดสเปคโตรสโคปี วิจัยยางพารา เล่มที่ 6, 297-308.

Panmanas Sirisomboon, Rawiphan Chowbankrang, Phil Williams, Evaluation of apparent viscosity of Para rubber latex by diffuse reflection near infrared spectroscopy. Applied Spectroscopy, 66(5), 595-599 (2012).

Tetsuya Inagaki, Panmanas Sirisomboon, Chang Liu, Warunee Thanapase, and Satoru Tsuchikawa, High accuracy in-line prediction and feasibility of on-site nondestructive estimation of Para rubber quality by spectroscopic methods. Journal of Wood Science, 59(2), 119-126, 2013.

P. Sirisomboon, A. Kaewkuptong and P. Williams, Feasibility study on the evaluation of the dry rubber content of field and concentrated latex of Para rubber by diffuse reflectance near infrared spectroscopy. J. Near Infrared Spectrosc. 21, 81–88 (2013).

Aphichart Sompiw and **Panmanas Sirisomboon**. Nondestructive evaluation technique for viscosity, alkalinity and potassium hydroxide number in concentrated para rubber latex by near infrared spectroscopy. RRI-MAG Congress I, the Twin Tower, Bangkok, Thailand during April 3-5, 2014 (in Thai).

Aphichart Sompiw and **Panmanas Sirisomboon**. Evaluation of Para rubber latex viscosity using shortwave near infrared spectroscopy. The 7th TSAE International conference, Krungsri River Hotel, Ayudhya, Thailand during April 2-4, 2014.

Jiraporn Onmankong, Panmanas Sirisomboon, Feasibility study of evaluation of ammonium laurate soap content in natural rubber latex by near infrared spectroscopy. The 9th TSAE International Conference (TSAE2016), IMPACT Exhibition and Convention Center, Hall 7, Bangkok, Thailand, during September 8-10, 2016.

9. โครงการข้าว

Areerat Imsil, Ronnarit Rittiron, **Panmanas Sirisomboon** and Varipat Areekul, Classification of Hom Mali rice with different degrees of milling based on physicochemical measurements by principal component analysis. Kasetsart Journal: Natural Science, 45(5), 863-873 (2011)

Somchai Kladsuk, **Panmanas Sirisomboon**, Selection of cooking method for cooked rice texture determination and sensory panel training in research work. International Conference on Engineering, Applied Sciences, and Technology (ICEAST - 2012) November 21 - 24, 2012, SwissÔtel Le Concorde, Bangkok, Thailand (Paper ID 00136)

Nuttagorn Sonsanguan, **Panmanas Sirisomboon**, Jiraporn Sripinyowanich Jongyingcharoen, Selection of objective test for cooked rice texture determination in research and industrial work. International Conference on Engineering, Applied Sciences, and Technology (ICEAST - 2012) November 21 - 24, 2012, SwissÔtel Le Concorde, Bangkok, Thailand (Paper ID 00137)

C. Dachoupakan Sirisomboon, R. Putthang, P. Sirisomboon, Application of near infrared spectroscopy to detect aflatoxigenic fungal contamination in rice. Food Control, 33(1), 207-214, 2013.

Ravipat Lapcharoensuk and **Panmanas Sirisomboon.** Some physical properties of rice in rice improvement plant. The 7th TSAE International conference, Krungsri River Hotel, Ayudhya, Thailand during April 2-4, 2014.

Kannapot Kaewsorn and Panmanas Sirisomboon. Feasibility study for evaluation of gamma-aminobutyric acid (GABA) content of germinated brown rice by visible and near infrared spectroscopy. The 7th TSAE International conference, Krungsri River Hotel, Ayudhya, Thailand during April 2-4, 2014.

K. Kaewsorn and Panmanas Sirisomboon, Determination of the gamma-aminobutyric acid content of germinated brown rice by near infrared spectroscopy, J. Near Infrared Spectrosc. 22(1), 45–54 (2014).

Ravipat Lapchareonsuk and Panmanas Sirisomboon, Alternative method for measuring of whiteness and transparency of rice using mathematic model of color values, The 8th

TSAE International conference, Bitec, Bangkok, Thailand during March 17-19, 2015.

Ravipat Lapchareonsuk & Panmanas Sirisomboon, Sensory Quality Evaluation of Rice Using Visible and Shortwave Near-Infrared Spectroscopy. International Journal of Food Properties, 18(5), 1128-1138, 2015.

10. โครงการมะเขือเทศ

Panmanas Sirisomboon, Munehiro Tanaka and Takayuki Kojima, 2008. Intensive Evaluation of Tomato 'Momotaro' Textural Properties. Annual Meeting on the Japanese Society of Agricultural Machinery, 27 - 30 March 2008. Miyazaki Kanko Hotel 1-1-1 Matsuyama, Miyazaki-city, Miyazaki-prefecture, Japan

Panmanas Sirisomboon, Munehiro Tanaka, Takayuki Kojima, Evaluation of tomato textural mechanical properties. Journal of Food Engineering, 111(4), 618-624, 2012.

Panmanas Sirisomboon, Munehiro Tanaka, Takayuki Kojima, Phil Williams, Nondestructive Estimation of Maturity and Textural Properties on Tomato 'Momotaro' by Near Infrared Spectroscopy. Journal of Food Engineering, 112(3), 218-226, 2012.

11. ทุเรียน

Phalanon Onsawai and **Panmanas Sirisomboon**. Color and soluble solids content of Durian pulp at different maturity stages. The 7th TSAE International conference, Krungsri River Hotel, Ayudhya, Thailand during April 2-4, 2014.

Phalanon Onsawai and Panmanas Sirisomboon, Determination of dry matter and soluble solids of durian pulp using diffuse reflectance near infrared spectroscopy. Journal of Near Infrared Spectroscopy, 23(3), 167–179, (2015).

Phalanon Onsawai, Panmanas Sirisomboon, Near infrared spectral and physicochemical characteristic of durian pulp at different maturities. The 9th TSAE International Conference (TSAE2016), IMPACT Exhibition and Convention Center, Hall 7, Bangkok, Thailand, during September 8-10, 2016.

12. แป้งมันสำปะหลัง

Wantanee Phoonphatthanachai and **Panmanas Sirisomboon**. Feasibility study for the evaluation of moisture content in tapioca starch cake by near Infrared spectroscopy. The 3rd International Conference on Engineering, Applied Sciences, and Technology (ICEAST 2013), The Sukosol, Bangkok, Thailand during August 21-24, 2013.

Kittisak Phetpan and **Panmanas Sirisomboon**. Feasibility study for the evaluation of moisture content in tapioca starch cake by near infrared reflectance spectroscopy. The 7th TSAE International conference, Krungsri River Hotel, Ayudhya, Thailand during April 2-4, 2014.

Kittisak Phetpan, Panmanas Sirisomboon, Evaluation of the moisture content of tapioca starch using near-infrared spectroscopy, J. Innovative Optical Health Sciences, 8(2), (2015) 1550014 (12 pages).

13. น้ำแกงสำเร็จรูป

Natcha Thitibunjan and **Panmanas Sirisomboon**. Feasibility study on evaluation of salt content of Massaman curry soup using near infrared spectroscopy. The 7th TSAE International conference, Krungsri River Hotel, Ayudhya, Thailand during April 2-4, 2014.

Jutharat Nawayon and **Panmanas Sirisomboon**. Feasibility study on evaluation of total solids of Massaman curry soup using near infrared spectroscopy. The 7th TSAE International conference, Krungsri River Hotel, Ayudhya, Thailand during April 2-4, 2014.

Panmanas Sirisomboon and Jutharat Nawayon, Evaluation of total solids of curry soup containing coconut milk by near infrared spectroscopy. J. Near Infrared Spectrosc. 24(2), 191–198 (2016).

14. ปลาซาร์ดีนกระป๋อง

Panmanas Sirisomboon, Pimpen Pornchaloempong, Peerawat Ramsiri, Skaow Pongkuan and Sarocha Srikornkarn, Evaluation of the salt content of canned sardines in tomato ketchup by diffuse reflection near infrared spectroscopy. J. Near Infrared Spectrosc. 22(5), 329–336 (2014)

Sarocha Srikornkarn, Panmanas Sirisomboon, Feasibility of evaluation of salt content in canned sardine in oil by near infrared spectroscopy. Agriculture and Agricultural Science Procedia, 2, 381-385 (2014).

Srocha Srikornkarn and Panmanas Sirisomboon, Feasibility of evaluation of salt content of canned sardines in oil by near infrared spectroscopy. The Second International Conference on Agricultural and Food Engineering (**CAFEI2014**), Berjaya Times Square Hotel, Kuala Lumpur, Malaysia, during 1-3 December 2014.

Sakaow Pongkuan and Panmanas Sirisomboon, Feasibility study on evaluation of salt content in canned sardines in brine by near infrared spectroscopy. The Second International Conference on Agricultural and Food Engineering (**CAFEi2014**), Berjaya Times Square Hotel, Kuala Lumpur, Malaysia, during 1-3 December 2014.

15. น้ำส้ม

Panmanas Sirisomboon, Teerapong Pholpho and Jutharat Nawayon, Classification of orange juice adulterated by table sugar solution using principal component analysis, The 11th International Conference "Inter-University Cooperation Program" "ASIAN Community Knowledge Networks for the Economy, Society, Culture, and Environmental Stability" 30 March – 3 April 2015 at Soaltee Crowne Plaza Kathmandu Hotel, Federal Democratic Republic of Nepal.

Jutharat Nawayon and Panmanas Sirisomboon, Detection of Sugar Solution Adulteration of Fresh Orange Juice by Near Infrared Spectroscopy. International Journal of Bioprocess and Biotechnological Advancements, Volume:1, Issue:1, April 24, 2015.

16. อ้อย

Kittisak Phetpan, Vasu Udompetaikul, Panmanas Sirisomboon, A study of the influence of sugarcane variety on sugar content prediction using shortwave near-infrared spectroscopy. The 9th TSAE International Conference (TSAE2016), IMPACT Exhibition and Convention Center, Hall 7, Bangkok, Thailand, during September 8-10, 2016.

17. อื่น ๆ

ธีรพงศ์ ผลโพธิ์, บัณฑิต จริโมภาส และ ปานมนัส ศิริสมบูรณ์, 2551. ความเสียหายหลังการเก็บเกี่ยวและสมบัติทางกายภาพบางประการของผลลำไยสด. การประชุมวิชาการสมาคมวิศวกรรมเกษตรแห่ง ประเทศไทย ครั้งที่ 9 ประจำปี 2551. 31 มกราคม 2551-1 กุมภาพันธ์ 2551, คณะวิศวกรรมและ อุตสาหกรรมเกษตร มหาวิทยาลัยแม่โจ้ เชียงใหม่. CR 3-12

ปานมนัส ศิริสมบูรณ์, โยธิน เปรมปราณีรัชต์, พรสุข รติโรจน์อนันต์, เยาวลักษณ์ สุรพันธพิศิษฐ์, 2551. เครื่องบรรจุไส้กรอกอัตโนมัติแบบตั้งโต๊ะการประชุมวิชาการสมาคมวิศวกรรมเกษตรแห่งประเทศไทย ครั้งที่ 9 ประจำปี 2551. 31 มกราคม 2551 - 1 กุมภาพันธ์ 2551. คณะวิศวกรรมและอุตสาหกรรมเกษตร มหาวิทยาลัยแม่โจ้ เชียงใหม่. CR1-15

ณัตวิภา เจียระไนวชิระ และ ปานมนัส ศิริสมบูรณ์ 2551, สมบัติทางกายภาพของน้ำกะทิเข้มข้น โดยการระเหยด้วยความดันสุญญากาศ, การประชุมวิชาการสมาคมวิศวกรรมเกษตรแห่ง ประเทศไทย ครั้งที่

9 ประจำปี 2551. 31 มกราคม 2551-1 กุมภาพันธ์ 2551, คณะวิศวกรรมและ อุตสาหกรรมเกษตร มหาวิทยาลัยแม่โจ้ เชียงใหม่. CR1-21

Yuki Hashimoto, Nobuyuki Hayashi, Munehiro Tanaka, Keiji Hoaki, and **Panmanas Sirisomboon**, 2008. Case Study on Rice Husk Power Generation in Thailand. Annual Meeting on the Japanese Society of Agricultural Machinery, 27 - 30 March 2008. Miyazaki Kanko Hotel 1-1-1 Matsuyama, Miyazaki-city, Miyazaki-prefecture, Japan.

Panmanas Sirisomboon 2009. Physical properties of some oil seeds for biodiesel. The 1st AUN/SEED-Net Regional Conference on Materials 2009. RCM 2009. 16-17 February, 2009. Equatorial Hotel, Penang, Malaysia.

Panmanas Sirisomboon, Suppakit Howvimanporn 2009. Determination of soluble solids of honey by near infrared spectroscopy. 10th International Conference of Thailand Society of Agricultural Engineering on "Innovations of Agricultural, Food and Renewable Energy Productions for Mankind" 1-3 April 2009 , Suranaree Univeristy of Technology, THAILAND.

Teerapong Pholoho, Bandit Jarimopas, **Panmanas Sirisomboon**, Siwalak Pathaveerat 2009. Mechanical bruising of fresh longan fruit. 10th International Conference of Thailand Society of Agricultural Engineering on "Innovations of Agricultural, Food and Renewable Energy Productions for Mankind" 1-3 April 2009 , Suranaree Univeristy of Technology, THAILAND.

P. Sirisomboon, W. Thanapase, S. Kasemsumran and S. Howvimanporn 2009. Identification of honey authenticity by NIRS. The 14th International Conference on Near Infrared Spectroscopy. NIR 2009 Breaking the Dawn. 7-16 Novemebr 2009, Amari Watergate Hotel, Bangkok, Thailand.

ปานมนัส ศิริสมบูรณ์ และพัชรี คล้ายมณี 2552. สมบัติเชิงกายภาพของข้าวโพดหวาน. การประชุมวิชาการ มหาวิทยาลัยเกษตรศาสตร์ วิทยาเขตกำแพงแสน ครั้งที่ 6, 8-9 ธันวาคม 2552. มหาวิทยาลัยเกษตรศาสตร์ วิทยาเขตกำแพงแสน นครปฐม

ปานมนัส ศิริสมบูรณ์, และ สฤษฏ์ เชื้อชาติ, 2553. การเปลี่ยนแปลงปริมาณของแข็งที่ละลายได้ (ความหวาน) ของแตงโมพันธุ์กินรีที่อายุการเก็บเกี่ยวต่างๆ. รายงานการประชุมทางวิชาการสมาคมวิศวกรรมเกษตรแห่งประเทศไทย ครั้งที่ 11. 6-7 พฤษภาคม 2553. นวัตกรรมทางวิศวกรรมเกษตรเพื่อเศรษฐกิจพอเพียงและชุมชนเข้มแข็ง. มหาวิทยาลัยเกษตรศาสตร์ วิทยาเขตกำแพงแสน นครปฐม. หน้า 247-250.

ธีรพงศ์ ผลโพธิ์, ศิวลักษ์ ปฐวีรัตน์ และ ปานมนัส ศิริสมบูรณ์, 2553. การพัฒนาและทดสอบเครื่องสั่นสะเทือนสำหรับทดสอบบรรจุภัณฑ์ผักและผลไม้. รายงานการประชุมทางวิชาการสมาคมวิศวกรรม

เกษตรแห่งประเทศไทย ครั้งที่ 11. 6-7 พฤษภาคม 2553. นวัตกรรมทางวิศวกรรมเกษตรเพื่อเศรษฐกิจพอเพียงและชุมชนเข้มแข็ง. มหาวิทยาลัยเกษตรศาสตร์ วิทยาเขตกำแพงแสน นครปฐม. หน้า 116-121.

T. Pholpho, S. Pathaveerat, **P. Sirisomboon**, Classification of longan fruit bruising using visible spectroscopy Journal of Food Engineering, 104 (1), 169-172 (2011)

Panmanas SIRISOMBOON, Sarid CHURCHART. Prediction of soluble solids content in cut watermelons using near infrared Spectroscopy, The 12th Annual Conference of Thai Society of Agricultural Engineering "International Conference on Agricultural Engineering" (Novelty, Clean and Sustainable) Chon-Chan Pattaya Resort, Chonburi, Thailand; 31 March-1 April 2011, p 48-1 -48-5.

Sirisomboon, P. and Jayranaiwachira, N. Characteristics of ice-cream under vacuum pressure pre-cooling condition, The 13th Annual Conference of Thai Society of Agricultural Engineering "The International conference of the Thai Society of Agricultural Engineering 2012" (Agro-Techno Fusion for Global Sustainability) Imperial Mae Ping Hotel, Chiang Mai, Thailand; 4-5 April 2012. FOE 08, 161

Jutharat Nawayon and Panmanas Sirisomboon, Detection of adulteration of orange juice by sugar solution using near infrared spectroscopy. The Second International Conference on Agricultural and Food Engineering (**CAFEi2014**), Berjaya Times Square Hotel, Kuala Lumpur, Malaysia, during 1-3 December 2014.

Kittisak Phetpan and Panmanas Sirisomboon, Application of near infrared spectroscopy for detection of steroid adulteration in traditional Thai medicine. The Second International Conference on Agricultural and Food Engineering (**CAFEi2014**), Berjaya Times Square Hotel, Kuala Lumpur, Malaysia, during 1-3 December 2014.

Natcha Thitibunjan and Panmanas Sirisomboon, Detection of adulteration of soy sauce by brine using near infrared spectroscopy. The Second International Conference on Agricultural and Food Engineering (**CAFEi2014**), Berjaya Times Square Hotel, Kuala Lumpur, Malaysia, during 1-3 December 2014.

Panmanas Sirisomboon, Overview on texture of agricultural produce and food, The 8th TSAE International conference, Bitec, Bangkok, Thailand during March 17-19, 2015.

Thanakorn Kamfuu, Surapong Kanchanalertchai, Napassanan Saksagiam, Panmanas Sirisomboon, Design and development of cutter for E-san mackerel powder in cooked rice, The 8th TSAE International conference, Bitec, Bangkok, Thailand during March 17-19, 2015, in Thai.

Panmanas Sirisomboon, Natthanant Bangkha, Tanatip Buranavanitkul, Pattawee Wutthigarn, Evaluation of nutrition in oil palm leaves using near-infrared spectroscopy presented by The 9th TSAE International Conference (TSAE2016), IMPACT Exhibition and Convention Center, Hall 7, Bangkok, Thailand, during September 8-10, 2016.

ประวัติส่วนตัวผู้ร่วมโครงการวิจัย

1.ชื่อ - นามสกุล (ภาษาไทย) นางสาววันพุทธ แซ่ฉั่ว

ชื่อ - นามสกุล (ภาษาอังกฤษ) Ms. Wanphut Saechua

2.เลขหมายบัตรประจำตัวประชาชน 3839900366767

3.ตำแหน่งปัจจุบัน อาจารย์

เงินเดือน 37,480 (บาท)

เวลาที่ใช้ทำวิจัย (20 ชั่วโมง : สัปดาห์)

4.หน่วยงานและสถานที่อยู่ที่ติดต่อได้สะดวก พร้อมหมายเลขโทรศัพท์ โทรสาร และไปรษณีย์อิเล็กทรอนิกส์ (e-mail)

หลักสูตรวิศวกรรมเกษตร สาขาวิชาวิศวกรรมเครื่องกล คณะวิศวกรรมศาสตร์

สถาบันเทคโนโลยีพระจอมเกล้าเจ้าคุณทหารลาดกระบัง ถนนฉลองกรุง ลาดกระบัง

กรุงเทพฯ 10520

โทรศัพท์ 02-3298000 ต่อ 5010, 5008

โทรสาร 02-3298336

e-mail: wanphut.sa@kmitl.ac.th

5.ประวัติการศึกษา

ปริญญาตรี (พ.ศ.2538 - พ.ศ.2542) วศ.บ. (วิศวกรรมเครื่องกล) สถาบันเทคโนโลยีพระจอมเกล้าธนบุรี

ปริญญาโท (พ.ศ.2542 - พ.ศ. 2544) วศ.ม. (เทคโนโลยีพลังงาน) มหาวิทยาลัยเทคโนโลยีพระจอมเกล้าธนบุรี

ปริญญาโท (พ.ศ.2549 - พ.ศ. 2550) MSc (Manufacturing engineering), The University of Nottingham (UK)

ปริญญาเอก (พ.ศ.2551 - พ.ศ.2557) Ph.D. (Manufacturing engineering and operations management) The University of Nottingham (UK)

6.สาขาวิชาการที่มีความชำนาญพิเศษ (แตกต่างจากวุฒิการศึกษา) ระบุสาขาวิชาการ

- การใช้ Thermal spray ในการเคลือบผิววัสดุ (base materials) เพื่อปรับปรุงคุณสมบัติทางด้านการต้านทานการกัดกร่อนและการป้องกันการเกิดออกซิเดชั่นเพื่อยืดอายุการใช้งานของ base materials และช่วยในการปรับปรุงคุณสมบัติของ base materials ให้เหมาะสมกับสภาวะในการใช้งาน
- การใช้เทคนิคNIRs ในการวิเคราะห์ด้านพลังงานของวัสดุทางการเกษตร
- ระบบปรับอากาศโดยการใช้สารดูดความชื้นร่วมเพื่อการประหยัดพลังงานในอาคาร
- การใช้โปรแกรมMicrosoft Access มาใช้ในการจัดระบบฐานข้อมูลเพื่อใช้ในTechnology Road Mapping และ การทำ Benchmarking

7.ประสบการณ์ที่เกี่ยวข้องกับการบริหารงานวิจัยทั้งภายในและภายนอกประเทศ โดยระบุสถานภาพในการทำการวิจัยว่าเป็นผู้อำนวยการแผนงานวิจัยหัวหน้าโครงการวิจัย หรือผู้ร่วมวิจัยในแต่ละผลงานวิจัย

7.1 ผู้อำนวยการแผนงานวิจัย : ชื่อแผนงานวิจัย (ไม่มี)

7.2 หัวหน้าโครงการวิจัย : ชื่อโครงการวิจัย

โครงการวิจัย:การประเมินศักยภาพในการอนุรักษ์พลังงานในภาคอุตสาหกรรมของประเทศไทย

หัวหน้าโครงการวิจัย: นางสาววันพุทธ แซ่ฉั่ว

แหล่งทุน: เงินรายได้คณะวิศวกรรมศาสตร์ประจำปี 2547 สจล.(70,000)

7.3 งานวิจัยที่ทำเสร็จแล้ว : ชื่อผลงานวิจัย ปีที่พิมพ์ การเผยแพร่ และแหล่งทุน (อาจมากกว่า 1 เรื่อง)

1) A. Shrestha, W. Saechua, and P. Sirisomboon, 'Some Physical and Combustion Characteristic of Leucaeha leucocephala Pellet', 8th TSAE International conference,17-19 Mar. 2015, Bangkok, Thailand

2) J. Posom, W. Saechua and P. Sirisomboon (2015). "Evaluation of the moisture content of Jatropha curcas kernels and the heating value of the oil-extracted residue using near-infrared spectroscopy." Biosystems Engineering 130: 52-59.

3) J. Posom, A. Shrestha, W. Saechua, and P. Sirisomboon (2016). "Rapid non-destructive evaluation of moisture content and higher heating value of Leucaena leucocephala pellets using near infrared spectroscopy." Energy 107: 464-472.

4) W. Saechua, D.Z., K. T. Voisey and D. G. McCartney. Investigation of in-flight particle characteristics of HVOF sprayed MCrAlY coatings. in International Thermal Spray Conference. 2011. Hamburg, Germany Curran Associates, Inc.

5) W. Permchart, W. Sae-chua and S. Tanatvanit, 2005. 'Potential for Energy Conservation in the Industrial Sector of Thailand', Proceedings of World Renewable Energy.

6) W. Saechua, J. Hirunlabh and J. Khedari, 2003. 'Field performance of a new desiccant-based air condition, proceedings of 1st international conference on sustainable energy and green architecture, Bangkok, Thailand

7.4 งานวิจัยที่กำลังทำ :

ชื่อข้อเสนอการวิจัย แหล่งทุน และสถานภาพในการทำวิจัยว่าได้ทำการวิจัยลุล่วงแล้วประมาณร้อยละเท่าใด

ชื่อโครงการวิจัย:โรงเรือนเพาะเลี้ยงเห็ดระบบปิดควบคุมด้วยไมโครคอนโทรลเลอร์

ผู้ร่วมโครงการวิจัย: นางสาววันพุทธ แซ่ฉั่ว

แหล่งทุน สำนักงานคณะกรรมการวิจัยแห่งชาติ ปี 2558 (500,000 บาท)

ดำเนินการแล้วประมาณ 80%